

Photocatalytic Fluorination of Benzylic C-H Bonds and Studies Towards the Synthesis of Salinosporamide C

by

Abhimanyu Bagai

B.Sc., University of British Columbia, 2012

Thesis Submitted in Partial Fulfillment of the
Requirements for the Degree of
Master of Science

in the
Department of Chemistry
Faculty of Science

© Abhimanyu Bagai 2018

SIMON FRASER UNIVERSITY

Spring 2018

All rights reserved.

However, in accordance with the *Copyright Act of Canada*, this work may be reproduced, without authorization, under the conditions for Fair Dealing. Therefore, limited reproduction of this work for the purposes of private study, research, education, satire, parody, criticism, review and news reporting is likely to be in accordance with the law, particularly if cited appropriately.

Approval

Name: Abhimanyu Bagai
Degree: Master of Science (Chemistry)
Title: *Photocatalytic Fluorination of Benzylic C-H Bonds and Studies Towards the Synthesis of Salinosporamide C*

Examining Committee: **Chair:** Dr. Corina Andreoiu
Associate Professor

Dr. Robert A. Britton
Senior Supervisor
Professor

Dr Peter D. Wilson
Supervisor
Associate Professor

Dr. Erika Plettner
Supervisor
Professor

Dr. Robert Young
Internal Examiner
Professor

Date Defended/Approved: April 18th, 2018

Abstract

Fluorinated pharmaceuticals comprise nearly a quarter of the total pharmaceutical market. However, current fluorination methods and reagents lack a certain range particularly in the fluorination of C-H bonds. The first part of this thesis describes the fluorination of benzylic C-H bonds utilizing the hydrogen abstracting ability of a classic photocatalyst and a bench stable fluorine atom transfer reagent. The simple and straightforward reaction demonstrates a wide range of tolerance to functionalities and provides access to fluorinated compounds in moderate to good yield.

The second part of this thesis consists of research towards the synthesis of a marine natural product, salinosporamide C, which was discovered in 2002 and has yet to be synthesized. The true activity of the compound is unknown, however its biogenetically related counterpart salinosporamide A is considered a potent 20S proteasome inhibitor. Though the total synthesis of salinosporamide C was not accomplished, an advanced intermediate was successfully synthesized and the groundwork for a successful synthesis of this natural product was completed.

Keywords: photocatalysis; tetrabutylammonium decatungstate; *N*-fluorobenzenesulfonimide; marine natural products; salinosporamide

*To my parents, Sanjiv and Minakshi and to my wife,
Melissa for their constant support and obviously
apparent pleasure in seeing me succeed.*

Acknowledgements

First of all, I would like to thank and acknowledge my senior supervisor Dr. Robert Britton for his support, mentorship and willingness to take me on under his tutelage, without whom I would not be here. His optimistic and enthusiastic attitude towards chemistry was a beacon when my frustrations with failed reactions were high. I am grateful for the patience he has shown me during my time at SFU especially near the end of my degree.

I would also like to thank the members of my supervisory committee, Professors Peter Wilson and Erica Plettner for their helpful suggestions throughout my graduate studies. Dr. Wilson, on many occasions has steered me in the right direction in the lab and provided insightful instruction.

I would like to acknowledge the assistance of the staff within the chemistry department. Dr. Andrew Lewis and Colin Zhang have helped me many times to set up complex NMR experiments. Also, Nathalie Fournier and Evon Khor for their assistance in all of the clerical work that is involved.

I would also like to thank the graduate students and post doctoral fellows that I have had the pleasure of working with over that last few years. In no particular order, I would like to thank Dr. Matt Nodwell, Dr. Vimal Varghese, Dr. Ajay Naidu, Dr. Robbie Zhai, Dr. Jake Goodwin-Tindall, Dr. Stanley Chang, Dr. Shira Halperin, Dr. Milan Bergeron-Brlek, Jason Draper, Michael Holmes, Soo Hur (Steve), Matt Taron, Chris Adamson, Daniel Kwon, Mike Meanwell and Venugopal Rao Challa for all their help in the laboratory. I am truly fortunate as I have made some good friends during my time and that I got to work with such an easy going and friendly group of people.

I would also like to thank my parents, Sanjiv and Minakshi Bagai, and my wonderful wife, Melissa, who have supported me throughout this program, and have had to put up with some late nights and weekends spent apart. I am thankful that she had dinner prepared for me on multiple occasions when I returned home late. I would also like to thank my friends who pushed me to pursue graduate studies.

Table of Contents

Approval.....	ii
Abstract.....	iii
Dedication.....	iv
Acknowledgements.....	v
Table of Contents.....	vi
List of Tables.....	viii
List of Figures.....	ix
List of Schemes.....	x
List of Abbreviations.....	xii

1. Introduction	1
1.1. Medicinal Chemistry	1
1.2. Thesis overview.....	5

2. Photocatalytic Fluorination of Benzylic C-H Bonds'	6
2.1. Introduction.....	6
2.1.1. Fluorination in Medicinal Chemistry	6
2.1.2. Positron Emission Tomography and ¹⁸ F.....	9
2.2. C-F Bond Forming Methods.....	10
2.2.1. Nucleophilic Sources (F ⁻).....	11
2.2.2. Electrophilic (F ⁺) and Radical (F [•]) Sources of Fluorine	13
2.2.3. C-H abstraction using a decatungstate photocatalyst	16
2.3. Results and Discussion	20
2.4. Conclusion and Future Work	30
2.5. Experimental	30
2.5.1. General	30
2.5.2. General Methods.....	31
Procedure for Photochemical Fluorination with TBADT	31
2.5.3. Preparation and Experimental Data	32
Preparation of Acetamide 85	32
Preparation of Acetamide 86	32
Synthesis of p-Acetoxy(1-Fluoroethyl)benzene (88)	33
Synthesis of p-Acetyl(1-fluoroethyl)benzene (96)	33
Synthesis of Methyl 4-(1-Fluoroethyl)benzoate (98)	34
Synthesis of Fluoro-Ibuprofen Methyl Ester (100).....	35
Synthesis of 4-Fluoro-4-Phenylbutanenitrile (101)	35
Synthesis of γ-Fluorotetralone 105	36
Synthesis of Methyl 3-Fluoro-3-Phenylpropanoate (106).....	37
Synthesis of β-Fluoroindanone 107	37
Synthesis of β-Fluoroindanone 109	38
Synthesis of 1-Fluoro-1,2-Diphenylethane (110).....	39

3. Studies Towards the Synthesis of Salinosporamide C.....	40
3.1. Pyrrolidine Containing Natural Products	40
3.2. Application of α-Chloroaldehydes To the Synthesis of Pyrrolidines.....	41

3.2.1.	Introduction to α -Chloroaldehydes	41
3.2.2.	Nucleophilic Additions to α -Chloroaldehydes	43
3.2.3.	Formation of Pyrrolidines with α -Chloroaldehydes	44
3.3.	Introduction to Salinosporamides.....	45
3.3.1.	Previous Synthesis of Salinosporamide A.....	46
3.4.	Previous Work in the Britton group	49
3.4.1.	Initial Studies towards the Synthesis of Salinosporamide C.....	49
3.4.2.	Synthesis of Advanced Intermediate 191	51
3.4.3.	Synthesis of Enone 191	51
3.5.	Revised Strategy to Salinosporamide C	53
3.5.1.	Revised Route for Closing the Pyrrolidine Ring	59
3.6.	Future Work and Conclusions.....	64
3.7.	Experimental	65
3.7.1.	Preparation and Experimental Data	65
	Preparation of Dioxane 205	65
	Preparation of Dioxolane 184	65
	Preparation of Alcohol 206	66
	Preparation of Alcohol 185	67
	Preparation of Aldehyde 207	67
	Preparation of Aldehyde 186	68
	Preparation of α -Chloroaldehyde 204	69
	Preparation of α -Chloroaldehyde 187	69
	Preparation of β -Keto Enol Ether 183	70
	Preparation of Chlorohydrin 208	71
	Preparation of Chlorohydrin 190	72
	Preparation of Enone 209	72
	Preparation of Enone 191	73
	Preparation of Carbamate 212	74
	Preparation of Ketone 220	74
	Preparation of Carbamate 193	75
	Preparation of Carbamate 230 and Oxazinanone 231	76
References		77

List of Tables

Table 2.1	Bond Dissociation Energies of Fluorine Transfer Reagents ⁶⁰	14
Table 2.2	Applications of TBADT in Organic Synthesis	17
Table 2.3	Optimization of Benzyl Fluorination with TBADT	23
Table 2.4	TBADT Photocatalyzed Fluorination.....	25
Table 2.5	Scope of AIBN Initiated Benzylic C-H Fluorination	27
Table 2.6	Benefits of Fluorination of Ibuprofen ⁸⁶	29
Table 3.1	Cyclization Attempts with Varying Bases and Solvents	58
Table 3.2	Cyclization Attempts on Ketone 220	59
Table 3.3	Conditions for the Cyclization of Carbamate 231	62
Table 3.4	Opening the Oxazinanone Ring	63

List of Figures

Figure 1.1	Examples of biologically-active natural products.	1
Figure 1.2	New chemical entities by source, 1981 to 2014 ²	3
Figure 1.3	Examples of marine-derived natural products used as drugs.	4
Figure 1.4	Salinosporamide C.....	5
Figure 2.1	Examples of Fluorine Containing Pharmaceuticals.....	8
Figure 2.2	Beneficial properties of benzylfluorides in lead optimization. ^{27,28}	9
Figure 2.3	¹⁸ F Radiotracers for PET Imaging.....	10
Figure 2.4	Nucleophilic sources of fluoride (F ⁻).....	12
Figure 2.5	Electrophilic fluorinating reagents (F ⁺ sources).....	13
Figure 2.6	Structure of TBADT	17
Figure 3.1	Natural products containing pyrrolidine rings.	40
Figure 3.2	Cornforth model for rationalizing the nucleophilic addition to α -chloroaldehydes.	44
Figure 3.3	Natural products isolated from the genus Salinispora.....	46

List of Schemes

Scheme 1.1	Historical Synthesis of Aspirin from Salicin.....	2
Scheme 1.2	Novartis Synthesis of (+)-Discodermolide.....	4
Scheme 1.3	General Transformation Outlined in Chapter 2	5
Scheme 2.1	Fluorination of Cortisone	7
Scheme 2.2	Fluorination of Ezetimibe to Prolong Half-Life.....	9
Scheme 2.3	Aryl Fluorination	11
Scheme 2.4	Proposed Mechanism for Fluorination with DAST	13
Scheme 2.5	Fluorination with NFSI as an Electrophilic Fluorinating Agent ⁵⁸	13
Scheme 2.6	Mechanism Proposed by Sammis and Coworkers for Fluorodecarboxylation	14
Scheme 2.7	Fluorination of Unactivated C-H Bonds by Grooves and Lectka	15
Scheme 2.8	Proposed Mechanism for Fluorination with Selectfluor ⁶⁵	16
Scheme 2.9	Mechanism of Decatungstate Catalyzed Reactions for Carbon- Carbon Bond Formation	18
Scheme 2.10	Proposed Mechanism for TBADT Photocatalyzed for C-F Bond Formation.....	19
Scheme 2.11	Previous Photocatalytic Fluorinations of Unactivated C-H Bonds	19
Scheme 2.12	Fluorination of Ethyl Benzene (25) and 4-(Ethyl)phenyl Acetate (23)	21
Scheme 2.13	Brønsted Acid Catalyzed C–F Activation and Transformation to Acetamide	22
Scheme 2.14	AIBN Initiated Benzylic C-H Fluorination	26
Scheme 2.15	Differing Selectivities in the Fluorination of p-Ethyltoluenes.....	28
Scheme 2.16	Fluorination of Ibuprofen in Flow	29
Scheme 3.1	General Organocatalytic Cycle for α -Functionalization of Aldehydes	42
Scheme 3.2	Example of α -Chlorination of Aldehydes.....	43
Scheme 3.3	Synthesis of (+)-Preussin (120).....	45
Scheme 3.4	Corey's Synthesis of Salinosporamide A.....	48
Scheme 3.5	Romo's Synthesis of Salinosporamide A.....	49
Scheme 3.6	Original Retrosynthesis of Salinosporamide C	50
Scheme 3.7	Synthesis of α -Chloroaldehyde 187	51
Scheme 3.8	Synthesis of Enone 191	52

Scheme 3.9	Formation of the Pyrrolidine Ring	53
Scheme 3.10	Revised Retrosynthesis.....	54
Scheme 3.11	Synthesis of Chlorohydrin 209	55
Scheme 3.12	Synthesis of Carbamate 212	56
Scheme 3.13	Attempted Formation of Pyrrolidine 215	56
Scheme 3.14	Formation of Phenol 219	57
Scheme 3.15	Deprotection of the Dioxane to form Ketone 220	58
Scheme 3.16	Revised Retrosynthesis of salinosporamide C	60
Scheme 3.17	Oxazinanone Formation	61
Scheme 3.18	Reduction of the Ketone in Order to Prevent the Reverse Aza-Michael	63
Scheme 3.19	Future Work	64

List of Abbreviations

°C	Degrees Celsius
4-PPY	4-pyrrolidinopyridine
6-MSA	6-methylsalicylic acid
Ac	Acetyl
ACP	Acyl carrier protein
aq	Aqueous
AIBN	Azobisisobutyronitrile
AT	Acyltransferase
BAIB	(Diacetoxyiodo)benzene
BOPCI	<i>Bis</i> (2-oxo-3-oxazolidinyl)phosphinic chloride
Bn	Benzyl
Bu	Butyl
Bz	Benzoyl
CAN	Ammonium cerium (IV) nitrate
CBS	Corey-Bakshi-Shibata reduction
CoA	Coenzyme A
COSY	Correlated spectroscopy
Cp	Cyclopentadienyl
CSA	10-Camphorsulfonic acid
Cy	Cyclohexyl
D	Dextrorotatory
dba	Dibenzylideneacetone
DCE	Dichloroethane
DDQ	2,3-Dichloro-5,6-dicyano-1,4-benzoquinone
DH	Dehydratase
DIAD	Diisopropyl azodicarboxylate
DIBAL	Diisobutylaluminium hydride
DIC	Diisopropylcarbodiimide
DMAP	<i>N,N</i> -Dimethyl-4-aminopyridine
DMF	<i>N,N</i> -Dimethylformamide
DMP	Dess-Martin periodinane

DMSO	Dimethylsulfoxide
dr	Diastereomeric ratio
<i>E</i>	<i>entgegen</i>
ECD	Electronic circular dichromism
ee	Enantiomeric excess
Enz	Enzyme
ER	Enoyl reductase
Et	Ethyl
HMBC	Heteronuclear multiple bond correlation
HMDS	Hexamethyldisilazane
HPLC	High-performance liquid chromatography
HRMS	High resolution mass spectrometry
HSQC	Heteronuclear single quantum coherence
<i>i</i> Pr	<i>iso</i> -propyl
KR	Ketoreductase
KS	Ketosynthase
LA	Lewis Acid
LDA	Lithium diisopropylamide
Me	Methyl
MeCN	Acetonitrile
Mes	Mesityl
MOM	Methoxymethyl
MoOPh	Oxodiperoxymolybdenum(pyridine)(hexamethylphosphoramidate)
Ms	Mesyl
MTPA	α -Methoxy- α -trifluoromethylphenylacetic acid
NBS	<i>N</i> -bromosuccinimide
NCS	<i>N</i> -chlorosuccinimide
NHSI	Dibenzene-sulfonamide
NIS	<i>N</i> -iodosuccinimide
NMO	<i>N</i> -methylmorpholine- <i>N</i> -oxide
NMP	<i>N</i> -methyl-2-pyrrolidine
NMR	Nuclear magnetic resonance
Nuc	Nucleophile

PBB	<i>para</i> -Bromobenzyl
Ph	Phenyl
PMB	<i>para</i> -Methoxybenzyl
PMP	<i>para</i> -Methoxyphenyl
PNB	<i>para</i> -Nitrobenzoyl
R	Substituent
rt	Room temperature
S _N 2	Bimolecular nucleophilic substitution
SOMO	Singly occupied molecular orbital
TBADT	Tetrabutylammonium decatungstate
TBAF	Tetrabutylammonium fluoride
TBAB	Tetrabutylammonium bromide
TBDPS	<i>tert</i> -Butyldiphenylsilyl
TBS	<i>tert</i> -Butyldimethylsilyl
<i>t</i> Bu	<i>tert</i> -Butyl
TC	2-Thiophene carboxylate
TREAT·HF	Triethylamine trihydrofluoride
Tf	Trifyl
TFA	Trifluoroacetate
TFAA	Trifluoroacetic anhydride
THF	Tetrahydrofuran
TIPS	Triisopropylsilyl
TMS	Trimethylsilyl
Ts	Tosyl
TS	Transition state
TTMSS	Tris(trimethylsilyl)silane
XPhos	2-Dicyclohexylphosphino-2',4',6'-triisopropylbiphenyl
Z	<i>zusammen</i>

1. Introduction

1.1. Medicinal Chemistry

Humans have come to rely on medicinal substances for the treatment of illnesses and diseases. The practice of using natural product extracts derived mainly from botanical species for medicinal purposes dates back many centuries. In the mid to late nineteenth century relatively pure biologically-active organic compounds were isolated for medicinal use. The dangers of an unsuspecting public ingesting unknown and possibly toxic compounds led the American government to form the Food and Drug administration (FDA) responsible for protecting and promoting public health and for the regulation of pharmaceutical drugs. Due to the strict control of regulated drug administrative practices alongside the monumental advancements in science, the current methods for drug discovery and development have evolved greatly. Many natural products have now been structurally characterized and their biological targets identified. Some of these compounds have also been approved by the FDA and are manufactured on scale for the treatment of various ailments. Examples of natural products used as drugs are shown in Figure 1.1. For example morphine **1**, classified as an alkaloid was isolated from the opium poppy and was first marketed commercially by Merck as a potent pain killer.¹ Similarly penicillin (**2**), a known antibiotic, and paclitaxel (Taxol[®] **3**) an anticancer agent, are natural products that are commonly used as drugs.

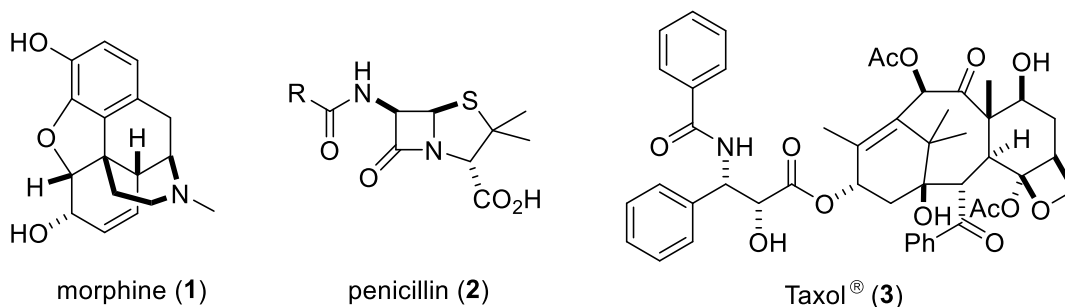
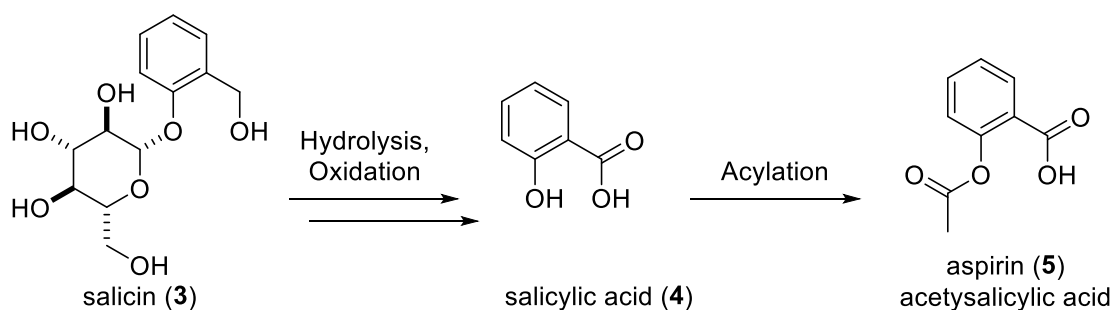


Figure 1.1 Examples of biologically-active natural products.

Through synthetic organic chemistry efforts, the pharmacological profiles of many natural products have been improved.^{2,3} One of the earliest examples is the development of aspirin (Scheme 1.1).⁴ Salicylic acid (**4**), isolated from the bark of the willow tree, was well known in herbal medicine to have an analgesic effect but also had undesirable side effects such as stomach pain.⁴ Chemists at Bayer AG discovered that acetylation of salicylic acid afforded aspirin (**5**), which retained the analgesic activity without the unwanted side effects. Aspirin has since gone on to become one of the most widely used pharmaceuticals in the world and is an excellent reminder of the impact that a comparatively small change to a molecule can have on its biological properties.

Scheme 1.1 Historical Synthesis of Aspirin from Salicin



Recently, Newman and Cragg reported their analysis of all drugs approved by the FDA during the period 1981 to 2014.² This survey shows that of the 1562 new chemical entities (NCEs) in that time period 5% are unaltered natural products while 21% are directly derived from natural products. A further 14% are synthetic analogues that contain the natural product pharmacophore. Including the 11% of synthetic drugs that mimic the biological activity of a natural product, this data shows that ~50% (Figure 1.2) of all drugs are natural products or natural product-inspired. As a result, the discovery and synthesis of new natural products remains a worthy endeavor especially as there is a need for new drugs to fight bacterial resistance and the spread of rapidly evolving diseases.

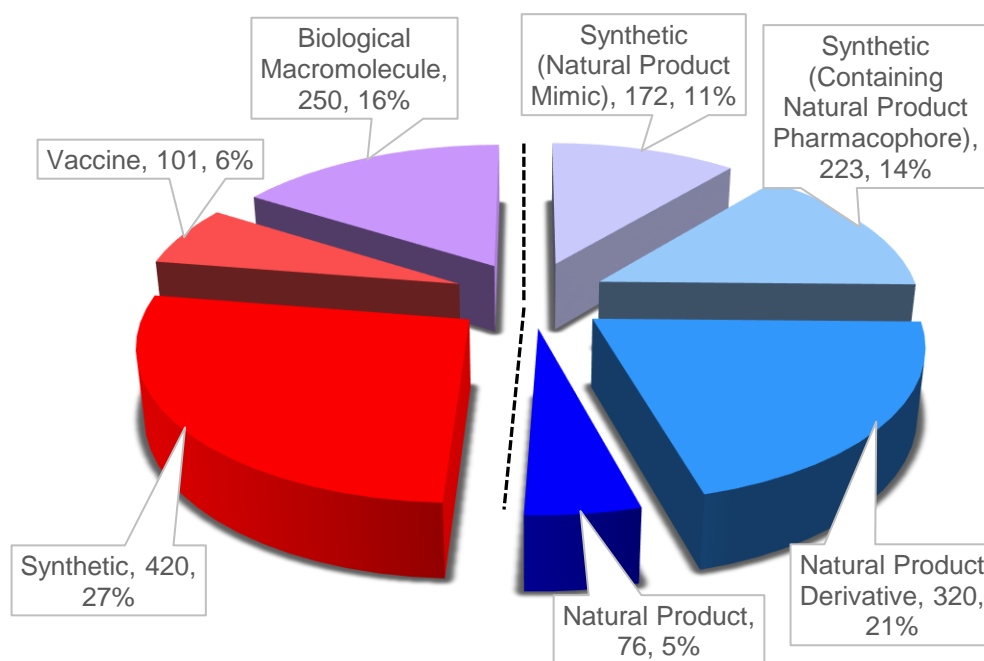


Figure 1.2 New chemical entities by source, 1981 to 2014²

One of the most common sources of biologically-active natural products is the marine environment. The World Register of Marine Species has named and identified over 226,000 marine species, however, it is hypothesized that greater than two thirds of marine species are not yet discovered and as a consequence, new natural products will continue to be reported. In particular, marine bacteria are expected to be a rich source of natural products.^{5,6} Two examples of marine derived natural products that serve as drugs today are bryostatin (**6**), currently in phase II for the treatment of Alzheimer's disease, and eribulin mesylate (**7**), an anticancer agent (Figure 1.3).

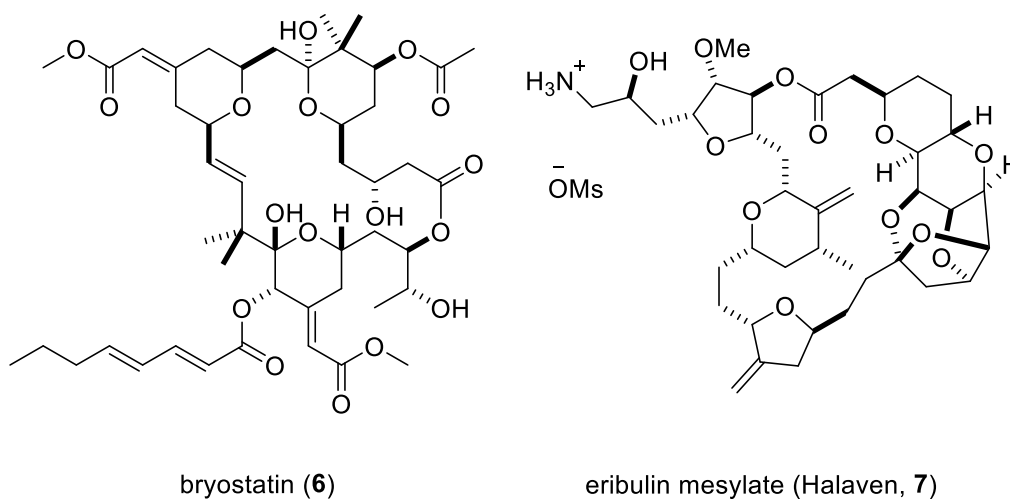
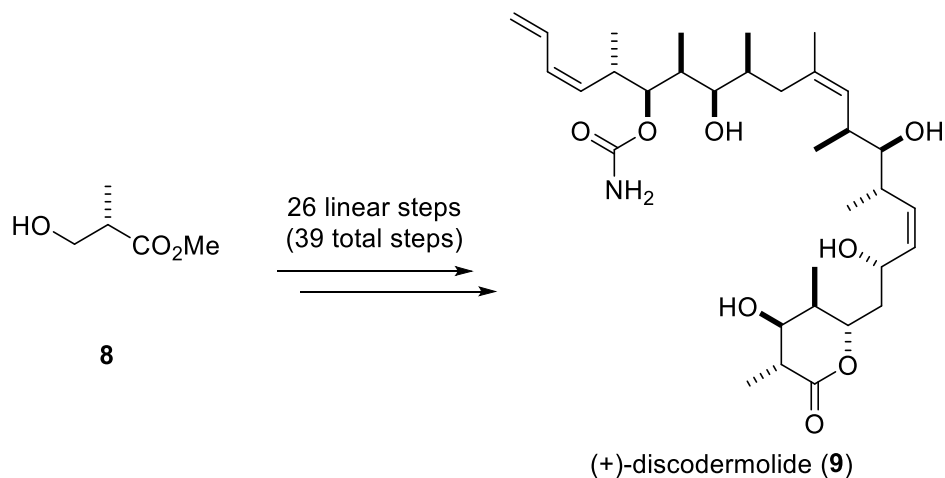


Figure 1.3 Examples of marine-derived natural products used as drugs.

Biologically active natural products can be widespread in nature or unique to a single organism. In many cases only a very limited amount of the compound of interest is stored by the producing organism, which means the isolation process requires the extraction of a large amount of biomass. Since obtaining sufficient quantities of some organisms is unfeasible due to environmental and practical concerns, natural product chemists often rely on total synthesis to access sufficient material for further biological studies. One impressive example is the total synthesis of the natural product (+)-discodermolide (9). In 2004, synthetic chemists at Novartis Pharma AG synthesized 60 g of compound (9) in 26 linear steps with 0.65% total overall yield (Scheme 1.2).⁷

Scheme 1.2 Novartis Synthesis of (+)-Discodermolide

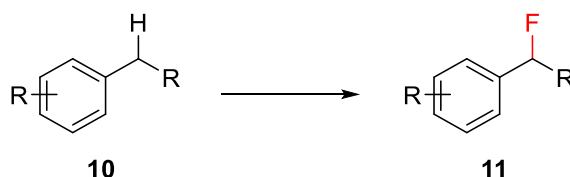


1.2. Thesis overview

The focus of this thesis is on the development of new synthetic methods that enable medicinal chemistry efforts and on the synthesis of biologically-interesting natural products.

In chapter 2, the development of a unique radical fluorination reaction that is capable of effecting benzylic C(sp³)-H fluorination is described. The development and optimization of this reaction enabled the synthesis of a number of benzylic fluorides and the exploration of the new mechanistic aspects of this reaction. The general transformation is shown in Scheme 1.3.

Scheme 1.3 General Transformation Outlined in Chapter 2



In chapter 3, we describe our efforts towards the first total synthesis of salinosporamide C (Figure 1.4, *i.e.* compound **12**). Salinosporamide C, isolated from a marine actinomycete bacteria *Salinispora tropica*, is the only member of the salinosporamide family that contains a pyrrolidine core. While the full biological profile of this molecule has not yet been reported, the potent anticancer activity of other members of this family indicated that this compound may well display some useful biological activity. Our efforts towards the synthesis of this natural product include an unusual aldol reaction involving an α -chloroaldehyde that forms a key C-C bond and simultaneously establishes the relative configuration of two new stereogenic centres.

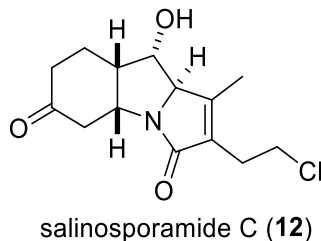


Figure 1.4 Salinosporamide C

2. Photocatalytic Fluorination of Benzylic C-H Bonds^{a,b}

2.1. Introduction

Fluorine is the most electronegative element in the periodic table, and as a result, has a significant effect on the properties of molecules in which is incorporated. For example, substituting a hydrogen atom for a fluorine atom in organic molecules can greatly alter the physical properties of the molecule due in part to the increased dipole of the newly-formed C-F bond relative to the original C-H bond.^{8,9} Furthermore, while fluorine has approximately twice the covalent radii compared to hydrogen (58 pm versus 32 pm)¹⁰, fluorine is still the second smallest atom after hydrogen, causing a minimal change in molecular size. Finally, the strength of an aliphatic C-F bond (463-481 kJ/mol) compared to that of an aliphatic C-H bond (413-439 kJ/mol) can also impart a greater degree of metabolic stability to a molecule.¹¹

2.1.1. Fluorination in Medicinal Chemistry

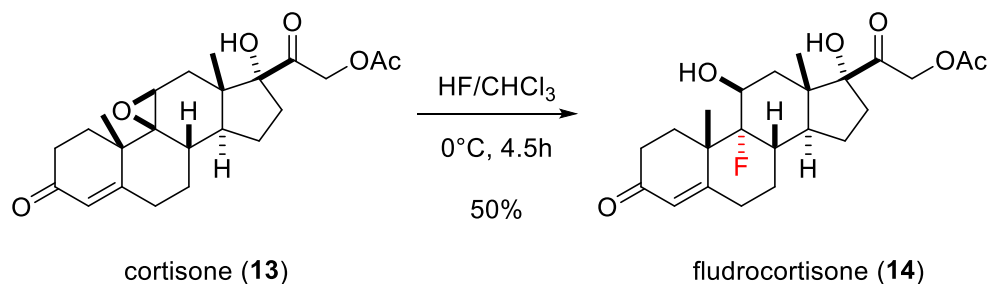
Incorporating a fluorine atom into organic compounds is of great interest in medicinal chemistry, as substituting a hydrogen atom or a hydroxyl function with a fluorine atom can improve several important pharmacokinetic properties including lipophilicity, binding affinity, distribution, permeation, and susceptibility to metabolism due to the aforementioned properties of fluorine.¹²⁻¹⁴ As a result, fluorinated pharmaceutical compounds constitute approximately 20-30% of current blockbuster drugs with an expected increase in that percentage over the next decade.¹⁵

a The results described in Chapter 2 have been reported in part, see: Nodwell, M. B.; Bagai, A.; Halperin, S. D.; Martin, R. E.; Knust, H.; Britton, R. *Chem. Commun.* **2015**, 51 (59), 11783–11786.⁸⁶

b Dr. Matthew Nodwell assisted in the fluorination, characterization and NMR spectroscopic analysis of some compounds described in this chapter. He was also as responsible for the development of the AIBN benzylic fluorination reaction.

The earliest example of the use of fluorination in medicinal chemistry appears in the fluorination of cortisone (**13**) in 1954, which led to an 11-fold increase in its potency as a glucocorticoid receptor agonist (Scheme 2.1).¹⁶

Scheme 2.1 Fluorination of Cortisone



In 1957 Heidelberger and coworkers reported one of the earliest studies of the positive effects of fluorination of a bioactive molecule when they synthesized 5-fluorouracil (Figure 2.1, **15**).¹⁷ They demonstrated that 5-fluorouracil inhibited the growth of tumors in mice¹⁸, and as a result compound **15** has been widely used as an anticancer therapeutic. It is now known that 5-fluorouracil is a suicide inhibitor of thymidylate synthase and that the fluorine plays a key role in the irreversible inhibition of the enzyme.¹⁹ Since this discovery, site-specific incorporation of fluorine in order to block metabolism, improve permeability and achieve physiochemical properties that are more favorable has been widely studied.^{13,14,20} Several examples where fluorination led to improved physiochemical properties are depicted in Figure 2.1. Norfloxacin (**16**) was shown to have significantly increased antibacterial activity after incorporation of a fluorine atom, which effected an approximate 63-fold improvement in the activity in the MIC against *E. coli* H560.²¹ This discovery led to further research into the application of fluoroquinolone as an antibacterial agent and the eventual discovery of ciprofloxacin (Figure 2.1, *i.e.* compound **17**), which showed a 2-10 fold increase in potency.²² The best selling drug of all time, atorvastatin (Figure 2.1, compound **18**), is an inhibitor of HMG-CoA reductase with over \$140 billion USD in sales between 1996 to 2012.²³ Atorvastatin is a LDL (low-density lipoprotein) lowering drug and during lead optimization it was found that the presence of an aryl fluoride resulted in a 5-fold increase in potency.²⁴ The importance of the 4-fluorophenyl substituent is highlighted by the subsequent incorporation of this structural feature in many other statin drugs.

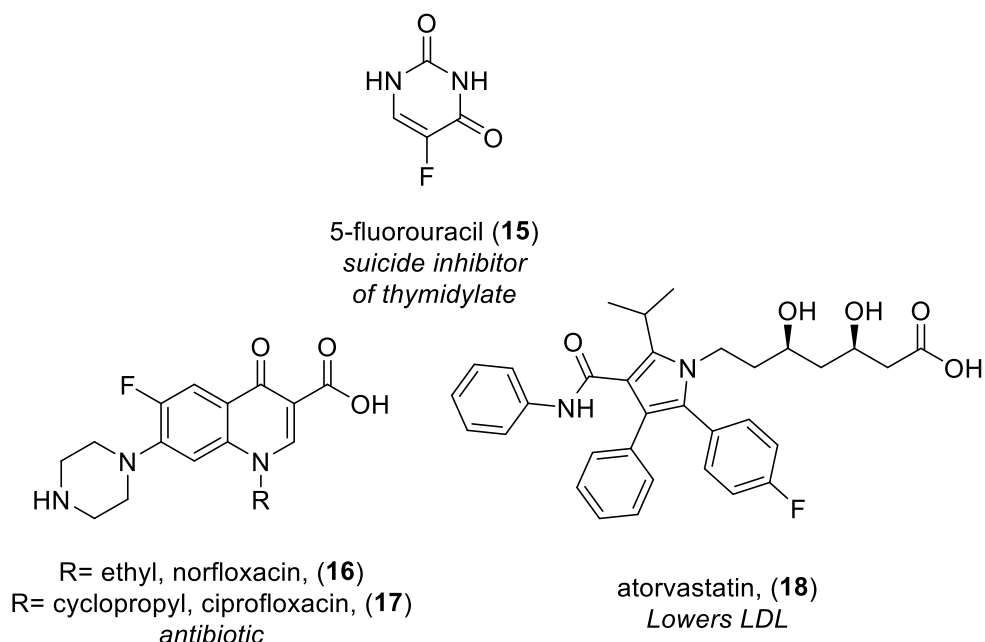
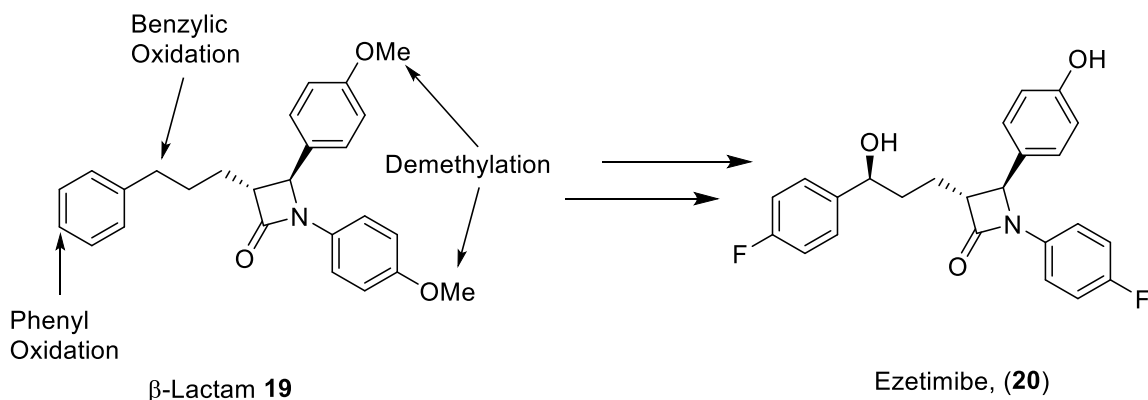


Figure 2.1 Examples of Fluorine Containing Pharmaceuticals

The addition of a highly electronegative fluorine atom may also allow medicinal chemists to tune the pharmacokinetic and pharmacodynamic properties of a drug. The improved metabolic profile following fluorination is highlighted in development of ezetimibe (Scheme 2.2), a drug that is currently used as an alternative to statins to lower cholesterol levels. Researchers at Schering-Plough had shown that the β -lactam (**19**) was an excellent candidate for lowering cholesterol levels in plasma. However, the molecule was easily metabolized by P450-mediated aromatic hydroxylation at the position indicated in Scheme 2.2²⁵ and the resultant phenol was rapidly excreted, resulting in a short drug half-life. During lead optimization studies, fluorination at the sites of metabolism along with other oxidative transformations led to an improved ED₅₀ for the drug (from 2.2 to 0.04 mg/kg/day). These transformations also improved other key properties including potency, which improved by ~50-fold.^{12,20,26}

Scheme 2.2 Fluorination of Ezetimibe to Prolong Half-Life



In the field of medicinal chemistry, the most common site of fluorine incorporation is on the aryl ring (e.g. compounds **15-18**, **20**). This is largely a result of the current challenges in incorporating fluorine in molecules in other positions at an advanced stage in the synthesis. Shown in Figure 2.2^{27,28} are two examples where fluorination in the benzylic position resulted in an overall improvement in the properties of the drug. The development of new late stage fluorination strategies is therefore especially attractive to drug discovery programs, where the direct fluorination of metabolically labile C–H bonds would obviate extensive re-synthesis campaigns. In particular, the fluorination of benzylic C–H^{29–36} bonds provides a means to attenuate metabolic degradation at these so-called “hot spots”.^{26,37}

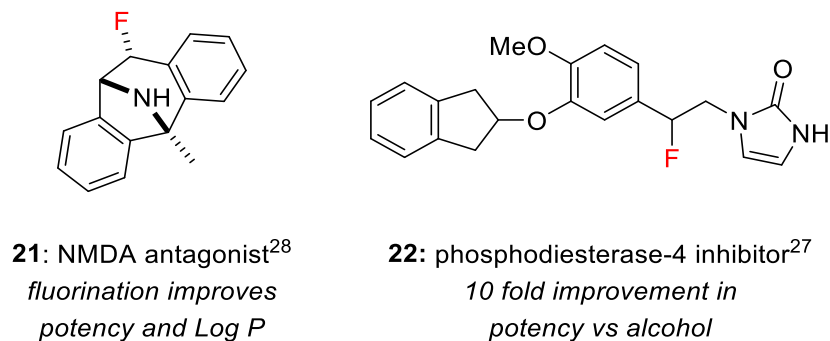


Figure 2.2 Beneficial properties of benzyldfluorides in lead optimization.^{27,28}

2.1.2. Positron Emission Tomography and ¹⁸F

In addition to the uses of fluorine in medicinal chemistry, ¹⁸F labeled compounds can be used in positron emission tomography (PET) to obtain *in vivo* images of organisms

and gain insight into the pharmacokinetic properties and location of the radionuclide and its metabolites.³⁸ PET imaging is a commonly utilized tool for the detection of positrons emitted by radiolabeled molecules. The radiotracer emits positrons (β), which undergo annihilation upon collision with an electron producing two gamma ray photons. The detection of these gamma rays gives an approximate location of the radionuclide.^{38,39} Positron-emitting radioisotopes most commonly used for PET imaging include ^{11}C , and ^{18}F . However, compared to ^{11}C , which has a half life of ~20 min, ^{18}F has a half life of ~110 min and a shorter positron range which correlates with higher resolution PET images and allows for more manageable times for radiosynthesis and transport.^{38,39} This makes fluorine a clinically relevant and often optimal radionuclide for PET imaging.⁴⁰

Two widely used radiolabeled imaging agents are [^{18}F] fluorodeoxyglucose ([^{18}F]-FDG, **23**), an analogue of glucose and 3,4-dihydroxy-6-[^{18}F]fluorophenylalanine ([^{18}F]-FDOPA, **24**), an amino acid analogue (Figure 2.3). [^{18}F]-FDG is used for the detection of tumor cells by quickly entering the glycolysis pathway as glucose metabolism is increased in cancerous cells versus noncancerous cells.⁴¹ This is possible because, [^{18}F]-FDG is structurally similar to glucose, and therefore accumulates in tumor cells. [^{18}F]-FDOPA is an analogue of L-3,4-dihydroxyphenylalanine and was one of the first ^{18}F radiolabeled substrates developed for studying the degeneration of dopaminergic pathways implicated in diseases such as Parkinson's.^{42,43}

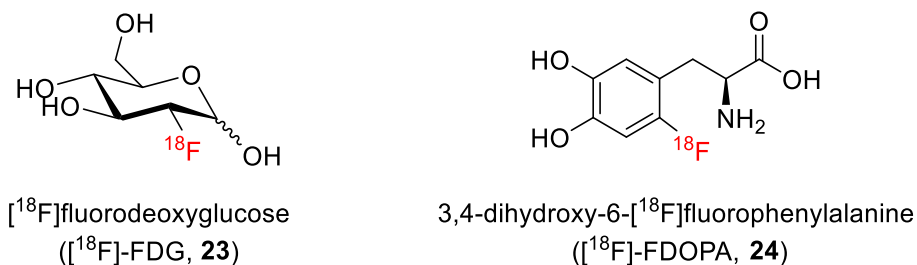


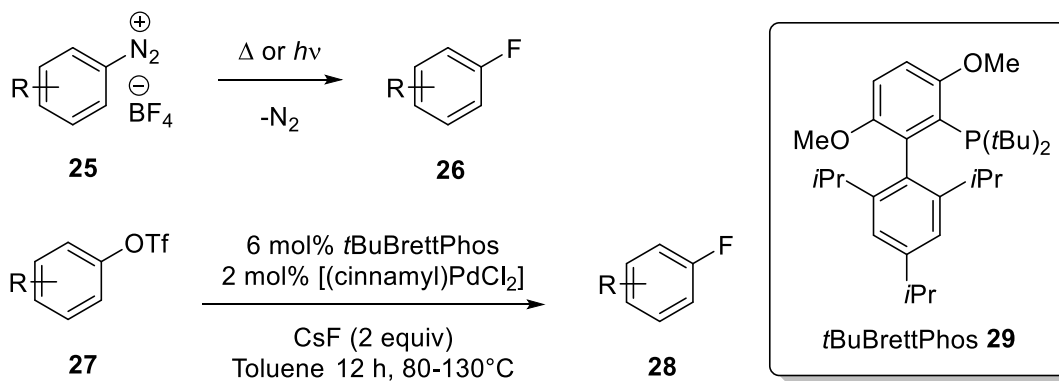
Figure 2.3 ^{18}F Radiotracers for PET Imaging

2.2. C-F Bond Forming Methods

Because of the significant utility of the fluorine atoms in drug discovery and PET imaging, there is a demand for fluorinating reagents that are easy to handle. For this reason many fluorine containing drugs (*vide supra*) are fluorinated in the aryl positions as

these are well studied and widely known transformations.⁴⁴ Examples of aryl fluorination reactions are depicted in Scheme 2.3.⁴⁴

Scheme 2.3 Aryl Fluorination



Fluorine gas and hydrogen fluoride were the first reagents used for the fluorination of non-aryl positions. However, these reagents are extremely toxic and corrosive and require specialized equipment and techniques for handling. Hydrofluoric acid reacts with water, glass, ceramics, concrete, rubber, certain plastics and most coatings.⁴⁵ Fluorine gas is also extremely toxic and can cause severe damage to the liver and kidney at concentrations as low as 25 ppm.⁴⁶ Furthermore, reactions with fluorine gas are vigorous and exothermic which makes them difficult to control and they are not suitable for site selective fluorination. These reagents are still commonly used in several industrial processes, however, they are not well suited for laboratory use. Owing to their unfavorable properties, there has been significant attention directed towards the development of new fluorination reagents and reactions.^{13,44,47–52}

2.2.1. Nucleophilic Sources (F⁻)

Fluoride salts are the simplest sources of nucleophilic F⁻ and can be paired with counterions such as lithium, sodium, potassium and cesium. However, the poor solubility of these inorganic fluorides in nonpolar solvents significantly reduces their utility.⁵³ Furthermore, elimination reactions are often competitive with displacement processes due to the relative basicity of the F⁻ ion (pK_a HF = 3.17 (15), H₂O (DMSO)). Although these

fluoride salts are soluble in polar solvents, they have a tendency to form hydrogen bonds and large solvation shells, due to the high electronegativity of fluorine, which results in a significant decrease in nucleophilicity as the fluoride anion becomes sterically shielded.^{53,54} For these reasons inorganic fluorides are rarely used as fluorinating reagents in organic synthesis.

These and other problems with inorganic fluorides and organic salts such as tetra-*n*-butylammonium fluoride (TBAF) has spurred the development of several activating nucleophilic fluorinating reagents of which the most commonly utilized are the aminosulfuranes (Figure 2.4). (Diethylamino)sulfur trifluoride (DAST, **30**) is one of the most widely used nucleophilic source of fluorine, though its drawbacks include sensitivity to moisture and its explosive potential when heated.⁵⁵ More thermally stable and safer to handle analogues have been developed (X-Tal Fluor, **31**, and Deoxofluor, **32**) in order to avoid these drawbacks.⁵³

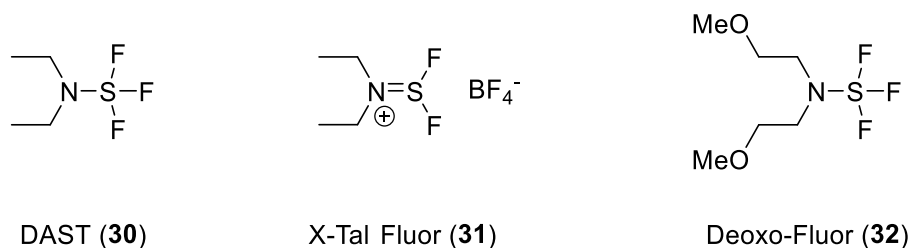
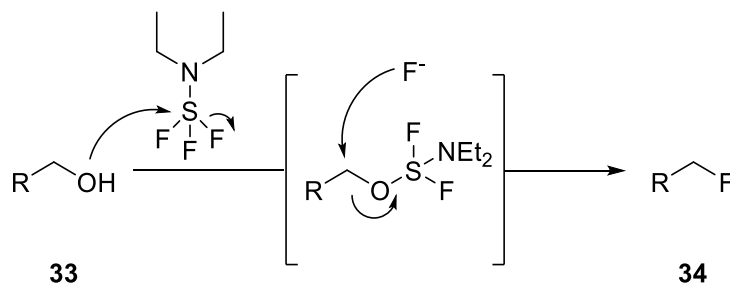


Figure 2.4 Nucleophilic sources of fluoride (F⁻)

The mechanism for fluorination using DAST is outlined in Scheme 2.4. Although this reaction works well for many substrates, it is important to note that this method requires a hydroxyl function to be present on the target molecule, which often requires prior functionalization and decreases the efficiency of the process. The efficiency of the process is further compromised as selective fluorination with DAST is difficult with multiple hydroxyl or ketone functions present on the target molecule. Therefore, fluorination utilizing DAST may not be ideal at a later stage in organic synthesis.

Scheme 2.4 Proposed Mechanism for Fluorination with DAST



2.2.2. Electrophilic (F⁺) and Radical (F[•]) Sources of Fluorine

In 1986 the first bench stable electrophilic fluorine sources were developed in order to avoid the use of fluorine gas. These are the *N*-fluoropyridinium salts (Figure 2.5),⁵⁶ which react with a variety of carbon nucleophiles to form new carbon-fluorine bonds.⁵⁷ In 1990 Ofner developed another electrophilic fluorinating agent *N*-fluorobenzenesulfonimide (NFSI, **36**, Figure 2.5) which was synthesised from benzenesulfonimide and F₂/N₂.⁵⁸ In 1992, Banks introduced Selectfluor® (**37**, Figure 2.5), which he demonstrated to be an effective electrophilic fluorinating agent.⁵⁹ An example of the use of NFSI as an electrophilic fluorinating reagent is depicted in Scheme 2.5.

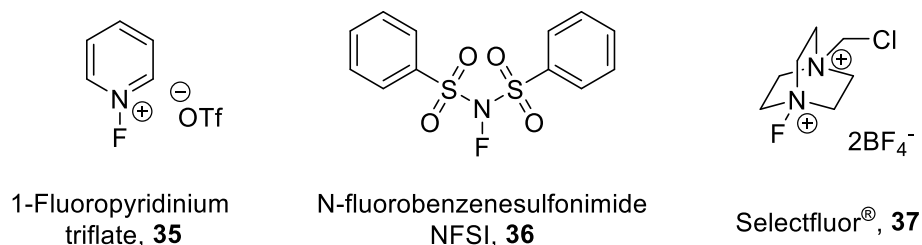
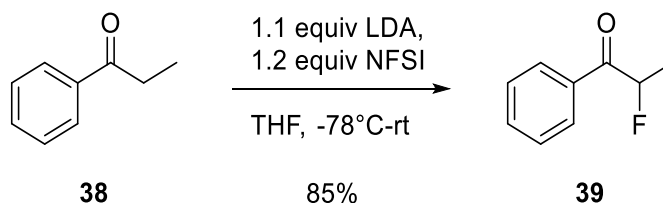


Figure 2.5 Electrophilic fluorinating reagents (F⁺ sources)

Scheme 2.5 Fluorination with NFSI as an Electrophilic Fluorinating Agent⁵⁸

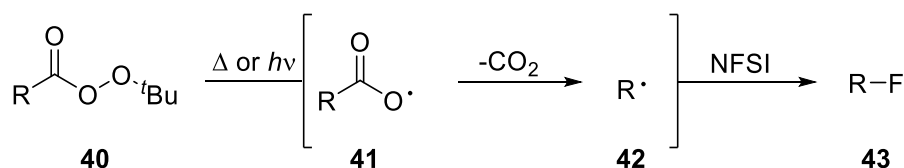


While the vast majority of fluorination reactions involve these electrophilic or nucleophilic fluorinating agents, in 2012 Sammis, Paquin and Kennepohl described the use of electrophilic fluorinating reagents as fluorine atom transfer reagents.⁶⁰ Sammis and coworkers compared the DFT calculations of the bond dissociation energies (Table 2.1) of *N*-fluoropyridinium triflate (**35**), *N*-fluorobenzenesulfonimide (**36**), and Selectfluor (**37**), and concluded that due to their relatively low bond dissociation energies they could undergo a homolytic cleavage and transfer a fluorine atom to an alkyl radical.⁶⁰ They further demonstrated this process by forming an alkyl radical through decarboxylation of a peroxyester using either heat or light and subsequently trapped the alkyl radical with NFSI or Selectfluor to form a new carbon-fluorine bond (Scheme 2.6). This discovery has led to many new methods for C-F bond formation using either NFSI or Selectfluor as fluorine transfer reagents. One drawback of this fluorinating technique is that it again requires the prior introduction of a peroxyester.

Table 2.1 Bond Dissociation Energies of Fluorine Transfer Reagents⁶⁰

Fluorinating Agents	DFT Calculated BDE kJ/mol
<i>N</i> -fluoropyridinium triflate	314
NFSI	264
Selectfluor	255

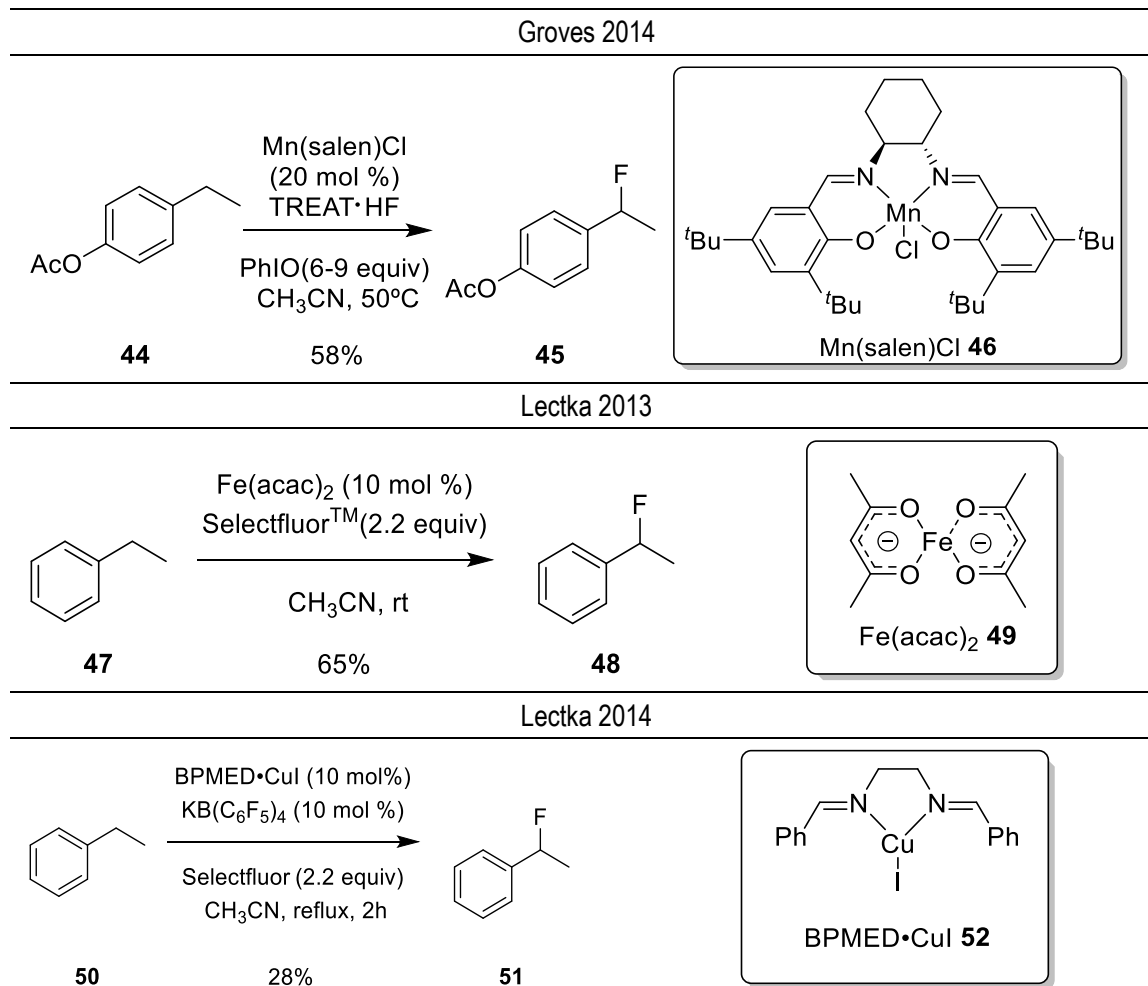
Scheme 2.6 Mechanism Proposed by Sammis and Coworkers for Fluorodecarboxylation



With this seminal publication from Sammis and coworkers, several methods have been reported that utilize either Selectfluor or NFSI to transfer a fluorine atom to a variety of substrates. Of particular interest have been the development of methodologies that rely on C-H activation rather than prior functionalization (e.g., peroxyesters) to generate the carbon radical, possibly paving the way for late-stage fluorination, which would have significant impact in medicinal chemistry efforts. To compliment these processes, there has been considerable interest in the direct fluorination of unactivated C-H bonds.^{61–64}

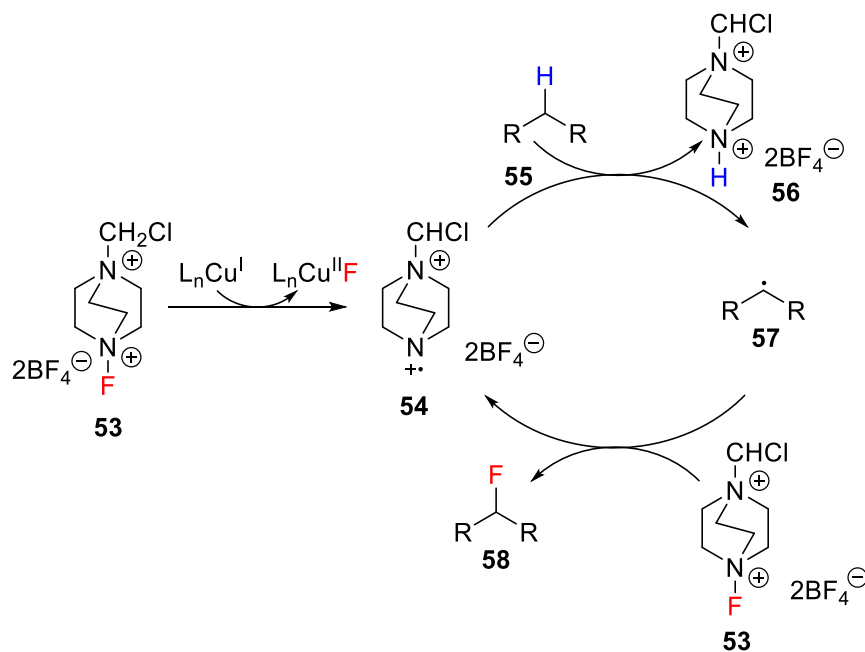
In recent years Groves³⁰ and Lectka^{33,36,65,66} have demonstrated mild methods for fluorinating benzylic C(sp³)-H bonds that utilize a metal-based catalyst of either manganese, iron or copper (Scheme 2.7).

Scheme 2.7 Fluorination of Unactivated C-H Bonds by Grooves and Lectka



Recently, Lectka described the mechanism of C–H fluorination with Selectfluor and proposed that fluorine transfer from Selectfluor ($\text{BDE}_{\text{NF}} \sim 255 \text{ kJ mol}^{-1}$) to a carbon radical generates a cationic nitrogen-centered radical that is responsible for further hydrogen atom abstraction (Scheme 2.1Scheme 2.8).⁶⁵ Curiously, the related fluorine transfer reagent NFSI (**36**, $\text{BDE}_{\text{NF}} \sim 264 \text{ kJ mol}^{-1}$) was shown to be unable to propagate aliphatic C–H fluorination.

Scheme 2.8 Proposed Mechanism for Fluorination with Selectfluor⁶⁵



2.2.3. C-H abstraction using a decatungstate photocatalyst

Polyoxometalates have been used for a variety of applications in organic synthesis.⁶⁷ In particular, interest has focused on the decatungstate ($\text{W}_{10}\text{O}_{32}^{4-}$) anion and its ability to photocatalytically abstract a hydrogen atom to form an alkyl radical that can be subsequently trapped with electron poor alkenes to form new C-C bonds.^{68,69} One of the earliest uses of decatungstate was to photocatalytically oxidize secondary alcohols to ketones in the presence of oxygen gas. Later Maldotti⁷⁰ and Giannotti^{71,72} showed that the decatungstate anion could abstract the hydrogen from a variety of aliphatic substrates to form a carbon centered radical that can be trapped by dioxygen to form the corresponding hydroperoxide and alcohol. They also demonstrated that under similar oxidative conditions aliphatic substrates can be oxidized to ketones by tuning the pressure of dioxygen. The utility of the decatungstate anion (TBADT (**59**), Figure 2.6) has been well studied for its ability to abstract C-H bonds^{68,73–78} and shown in Table 2.2 are some notable transformations involving photocatalysis with the use of TBADT.

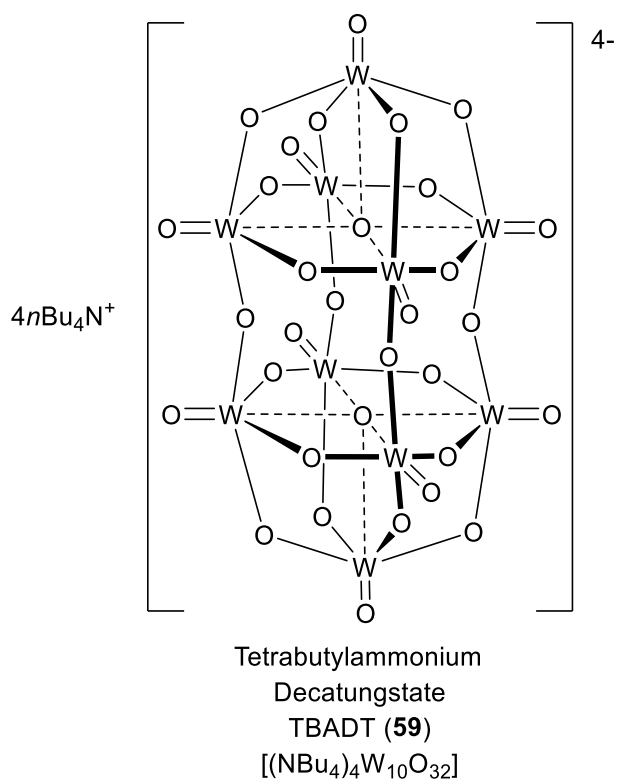


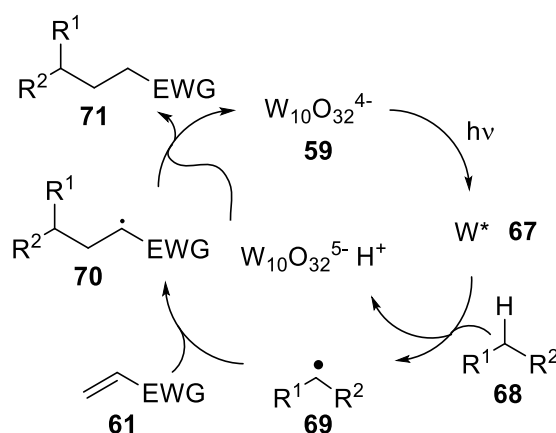
Figure 2.6 Structure of TBADT

Table 2.2 Applications of TBADT in Organic Synthesis

Hill ⁶⁹ 1995			
	+		
60		61	62
Maldotti ⁷⁰ and Giannotti ^{71,72} 1999			
60		63	64
63:64 controlled by O ₂ Pressure			
Fagnoni ⁷⁷ 2007			
	+		
65		61	66

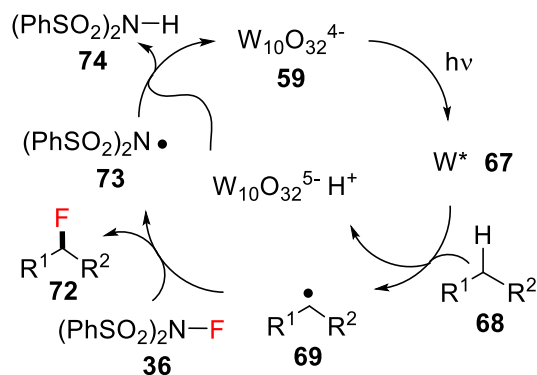
Described in Scheme 2.9 is the mechanism for the formation of a new C-C bond photocatalyzed by the decatungstate anion.⁷⁷ The first step involves the photoexcitation of decatungstate, which then abstracts a hydrogen atom from a C(sp³)-H bond to form a carbon centred radical and the reduced form of decatungstate. The carbon centred radical subsequently reacts with a radical acceptor (e.g., compound **61**) to form a new carbon-carbon bond and receives the hydrogen atom back from decatungstate to regenerate the catalyst.

Scheme 2.9 Mechanism of Decatungstate Catalyzed Reactions for Carbon-Carbon Bond Formation

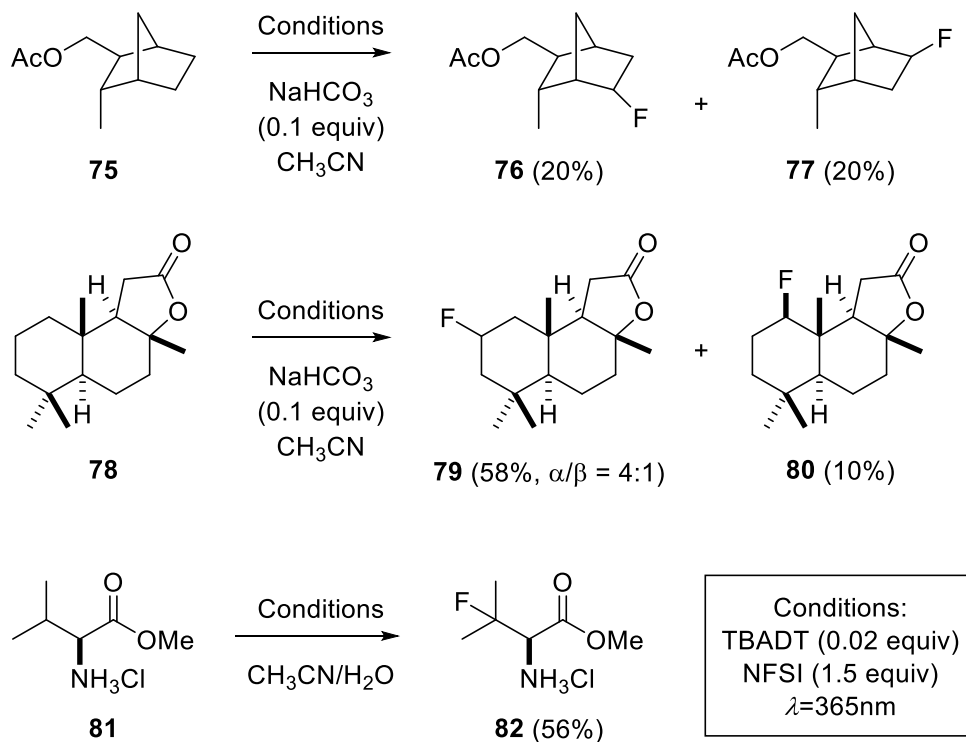


With the ability of TBADT to abstract a hydrogen atom from an unactivated C-H bond well established, it was hypothesized by the Britton group that this alkyl radical could instead react with a fluorine atom transfer reagent to form a new C-F bond (Scheme 2.10). This has led to a publication describing the fluorination of unactivated C-H bonds.⁷⁹ This method proved useful for the fluorination of a wide assortment of complex aliphatic substrates while tolerating a variety of functional groups. Some of the notable fluorination reactions are highlighted in Scheme 2.11.

Scheme 2.10 Proposed Mechanism for TBADT Photocatalyzed for C-F Bond Formation.



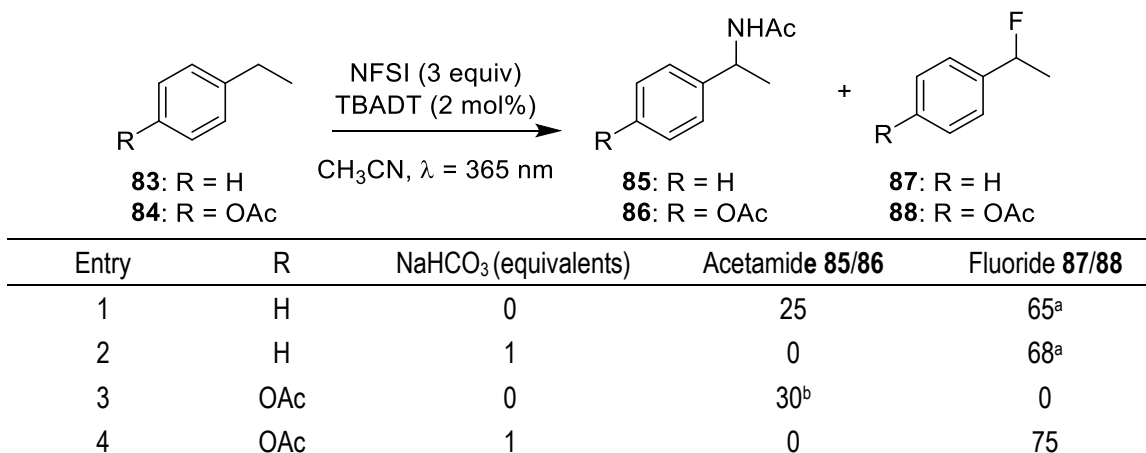
Scheme 2.11 Previous Photocatalytic Fluorinations of Unactivated C-H Bonds



2.3. Results and Discussion

While we had demonstrated the fluorination of unactivated aliphatic C-H bonds, the fluorination of benzylic C-H bonds had not yet been successful using this methodology. Accordingly, we initiated an investigation aimed towards extending this methodology to the selective synthesis of a wide range of benzylic fluorides. As depicted in Scheme 2.12, we first investigated the fluorination of ethylbenzene (**83**) and the *p*-acetoxy derivative (**84**) using conditions previously developed for aliphatic C-H fluorinations (*vide supra*).⁷⁹ We were surprised that a major product of both reactions were the acetamides **85** and **86**. While decatungstate oxidation of an intermediate benzylic radical to a carbocation⁸⁰ followed by reaction with acetonitrile would explain the formation of these Ritter-type products, Brønsted acid activation^{81,82} of initially formed benzylic C-F bonds by dibenzenesulfonamide (**74**, NHSI) may also be operative. Thus, we evaluated the effect of various bases as additives to the fluorination of **83**. Soluble amine bases such as pyridine and triethylamine were not compatible with this process, neither were a small collection of inorganic bases (*e.g.*, Cs₂CO₃, Na₂CO₃, K₂CO₃, LiOH). Fortunately, when either NaHCO₃ or Li₂CO₃ were added to the reaction mixture the desired benzyl fluoride **87** was formed as the exclusive product in good yield. Likewise, employing these reaction conditions with *p*-acetoxy ethylbenzene (**84**), *p*-acetoxy 1-fluoroethylbenzene (**88**) was produced in 75% yield.

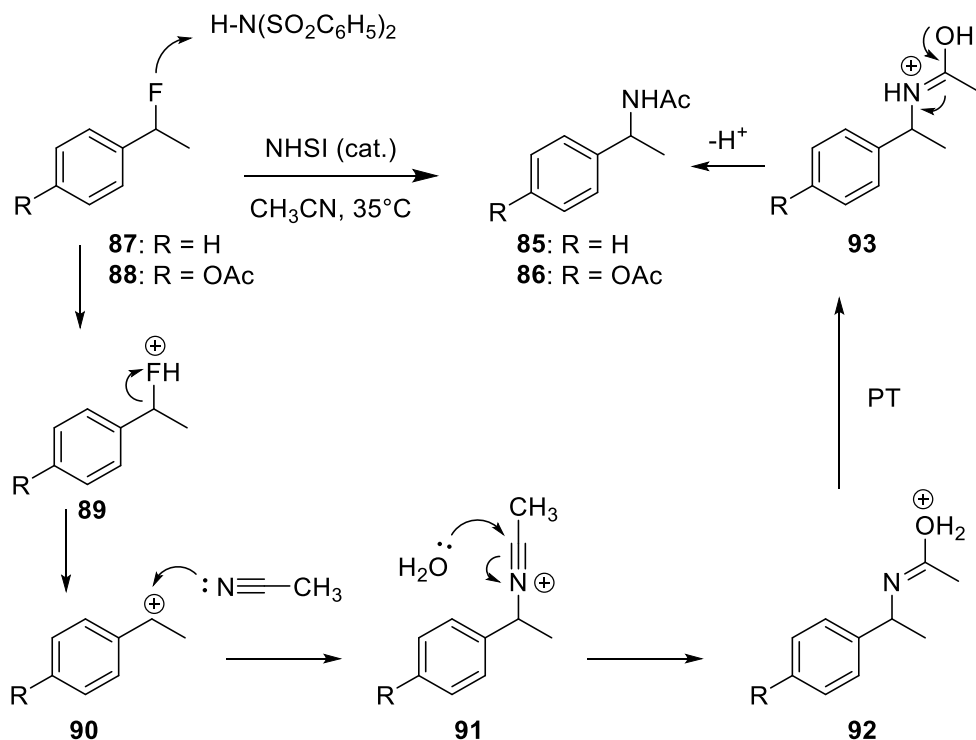
Scheme 2.12 Fluorination of Ethyl Benzene (25) and 4-(Ethyl)phenyl Acetate (23)



a) Yield of the volatile benzyl fluoride **85** based on analysis of ¹H NMR spectra with internal standard. b) Accompanied by 42% recovered **84**.

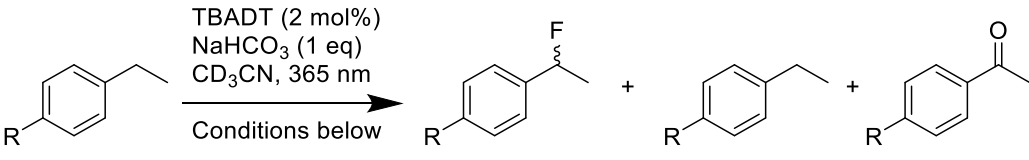
To further probe the formation of acetamides **85** and **86**, the benzyl fluorides **87** and **88** were treated independently with a catalytic amount of NHSI (**74**) in CH₃CN. This led to mixtures containing predominantly the acetamides **85** and **86** at temperatures as low as 35°C (Scheme 2.13). When these reactions were repeated without NHSI, the benzyl fluorides were recovered unreacted. This NHSI-promoted fluoride substitution reaction represents a unique example of Brønsted acid-catalyzed C–F activation.

Scheme 2.13 Brønsted Acid Catalyzed C–F Activation and Transformation to Acetamide



In order to optimize the fluorination process with TBADT multiple reaction conditions were screened including reaction time, additives and fluorinating agents. As a result it was discovered that NFSI is the preferred fluorinating agent over Selectfluor, which gave a lower yield under identical conditions (entry 4, Table 2.3). We discovered that oxidation by TBADT is a competing reaction and can be prevented by deoxygenation of the reaction mixture (entries 12-14, Table 2.3). Based on multiple substrates the conversion to the highest yielding fluorinated product (entry 2) and the least oxidized (entries 12 and 13) occurs between 24-48 hours with an increase in oxidation over longer time periods. We also envisioned lowering the reaction time by increasing the equivalents of NFSI from 2 to 3 equivalents and were pleased to discover an increase in the fluorinated product in a period of 24 hours of irradiation.

Table 2.3 Optimization of Benzyl Fluorination with TBADT

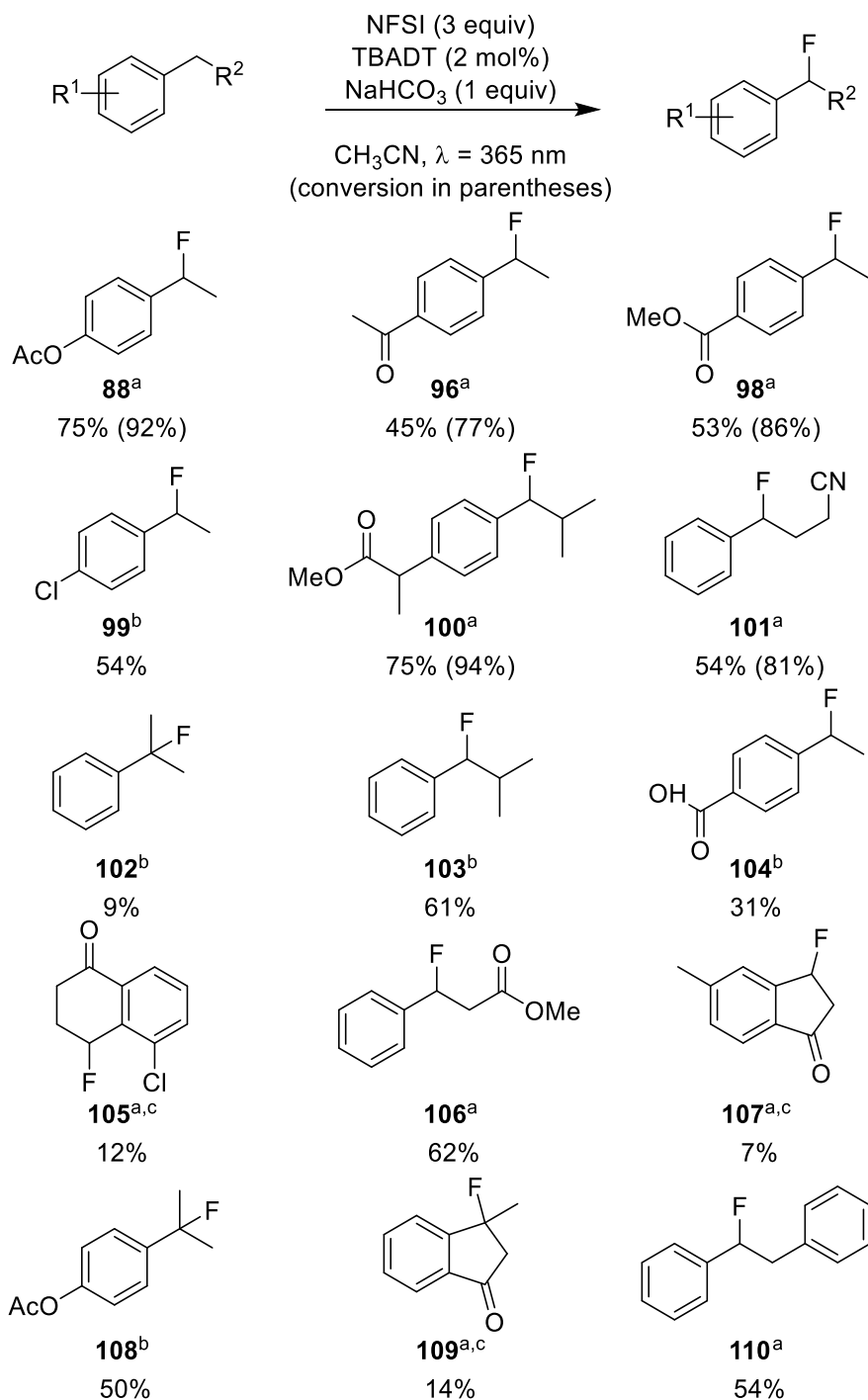
<div><div><div><div><div></div><div><div>95</div><div>96</div><div>95</div><div>97</div></div></div></div></div></div>					
Entry	R	Fluorinating agent	Equivalents	Time	96:95:97 ^a
1	H	NFSI	2	4	39:59:1
2	H	NFSI	2	24	76:19:5
3	H	NFSI	2	96	78:8:14
4	H	Selectfluor	2	24	33:66:1
5	C(O)CH ₃	NFSI	1	24	16:64:21
6	C(O)CH ₃	NFSI	2	24	22:56:22
7	C(O)CH ₃	NFSI	3	24	32:48:21
8	C(O)CH ₃	NFSI	4	24	31:47:22
9	C(O)CH ₃	NFSI	3	48	43:22:35
10	C(O)CH ₃	NFSI	3	72	47:16:37
11	C(O)CH ₃	NFSI	3	96	47:13:40
12	C(O)CH ₃ ^b	NFSI	3	24	47:40:12
13	C(O)CH ₃ ^b	NFSI	3	48	58:26:15
14	C(O)CH ₃ ^b	NFSI	3	120	60:20:20

a) Conversion based on analysis of ¹H NMR spectra. b) Deoxygenated reaction mixture.

In order to gain insight into the scope of the decatungstate-catalyzed benzylic C(sp³)-H fluorination reaction, we evaluated its effectiveness on a range of substrates with differing electronic and steric features. As summarized in Table 2.4, we were pleased to find that this reaction is general and cleanly provided access to a range of benzyl fluorides (**88**, **96**, **98–109**) in modest to good yield. It is notable that the discrepancies between conversion (in parentheses) and isolated yields reflect the difficulty in isolating and separating the benzyl fluoride products from the parent hydrocarbon, a challenge

common to late-stage C–H fluorination strategies.⁶¹ Importantly, both electron rich (e.g., compounds **88** and **108**) and electron poor (e.g., compounds **96**, **98** and **99**) alkylbenzenes are suitable substrates for this reaction. The fluorination of isobutylbenzenes proceeded smoothly (e.g., compounds **100** and **103**). Sterically encumbered isopropyl benzenes proved difficult to fluorinate (e.g., compound **102**) and proceeded in modest yield only with the electron rich *p*-acetoxy derivative where the desired fluoroisopropyl adduct (fluorinated *p*-acetoxyisopropylbenzene (**108**)) was produced in 50% yield. In all cases, deoxygenation of the acetonitrile solvent was critical to avoid competing decatungstate-catalyzed benzylic oxidation. In contrast to other benzylic C–H fluorination reactions,^{29,31,35} replacing NFSI with Selectfluor resulted in significantly lower yields. Interestingly, despite the necessary addition of base to these reactions (e.g., NaHCO₃), benzylic C–H fluorination is competitive with α -fluorination of ketone-containing substrates, and provides access to the unusual γ -fluorotetralone **105** and β -fluoroindanones **107** and **109**.

Table 2.4 TBADT Photocatalyzed Fluorination



a) Isolated yield. b) Yield based on analysis of ¹H NMR spectra recorded on the crude reaction mixture with an internal standard. c) Accompanied by the isomeric α -fluoroketone.

In an effort to gain further insight into the mechanism of decatungstate-catalyzed benzylic fluorination, we examined the fluorination of ethylbenzene derivatives (*i.e.*, **83**→**87**, Scheme 2.12) without the photocatalyst and observed no formation of the benzylfluoride **87**. However, when a catalytic amount of the radical initiator AIBN was added and the reaction mixture was heated (75 °C), we observed clean conversion to the benzylfluoride **87**, albeit in modest yield (~20%, Scheme 2.14). We were able to improve the yield of this AIBN-initiated reaction to 70% by simply replacing NaHCO₃ with Li₂CO₃. This dramatic base effect may be understood by considering that two equivalents of NaHCO₃ slowly decompose to H₂O, CO₂, Na₂CO₃⁸³ at the elevated temperatures required for the AIBN-initiated reaction, and that Na₂CO₃ is incompatible with the NFSI fluorination reaction (*vide supra*). It is notable that several aliphatic substrates failed to fluorinate using these reaction conditions (*i.e.*, AIBN, NFSI, Li₂CO₃) suggesting that unlike Selectfluor, NFSI is only capable of propagating the radical fluorination of relatively weak C–H bonds (BDE_{CH} benzylic ~377 kJ mol⁻¹ vs BDE_{CH} aliphatic ~404-439 kJ mol⁻¹). As summarized in Table 2.5, these reaction conditions proved to be less optimal and general than the decatungstate-catalyzed fluorination, and several substrates containing benzylic C–H bonds failed to provide any fluorinated products (*e.g.*, compounds **102–104**).

Scheme 2.14 AIBN Initiated Benzylic C-H Fluorination

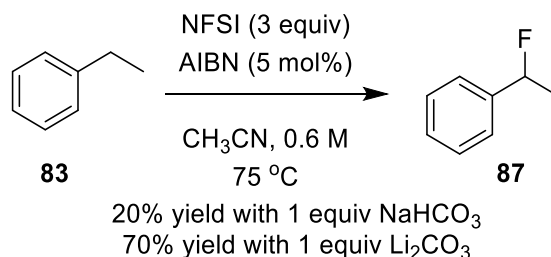
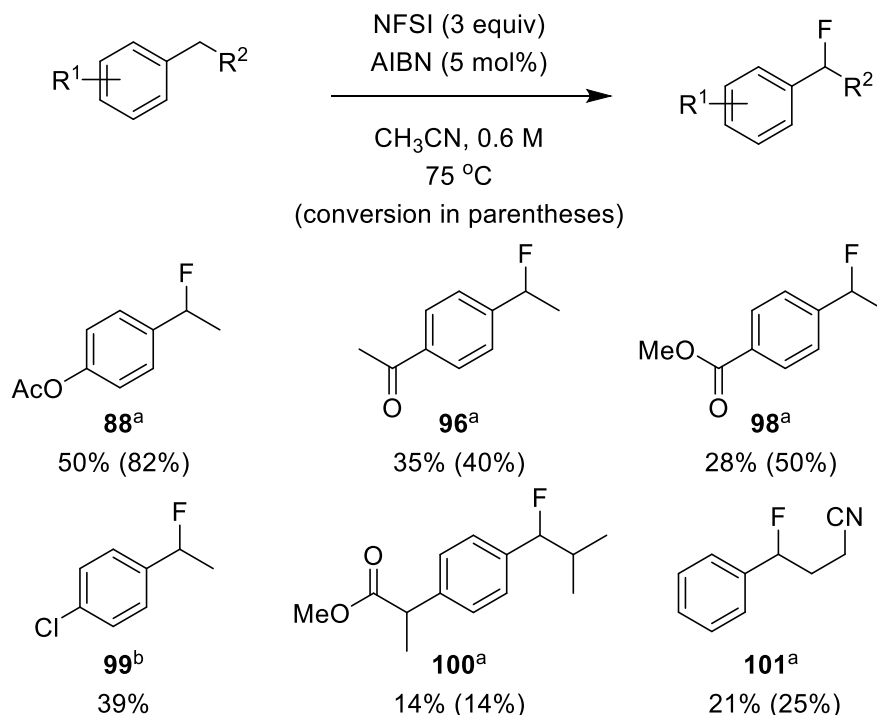


Table 2.5 Scope of AIBN Initiated Benzylic C-H Fluorination

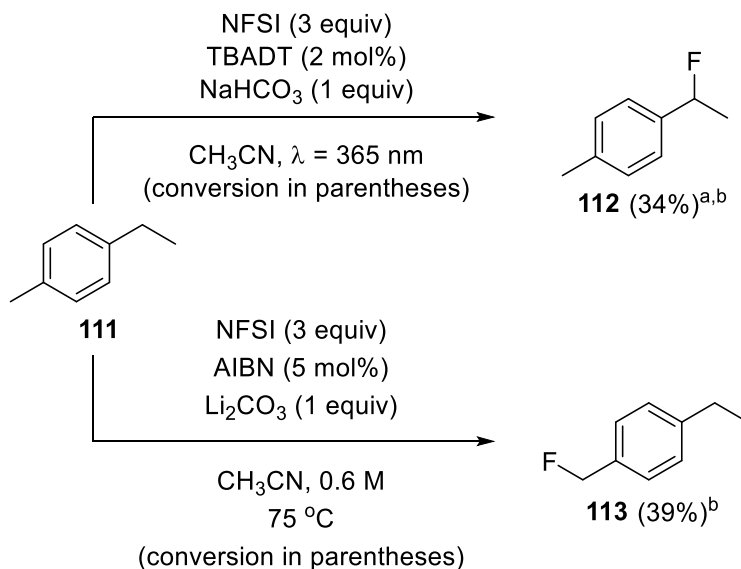


a) Isolated yield. b) Yield based on analysis of ¹H NMR spectra recorded on the crude reaction mixture with an internal standard.

During our examination of both the decatungstate-catalyzed and AIBN-initiated fluorination reactions, we evaluated the fluorination of *p*-ethyltoluene (**111**) (Scheme 2.15). Surprisingly, the decatungstate-catalyzed reaction selectively fluorinated the ethyl group in compound **111**, while the AIBN-initiated fluorination provided the fluoromethyl product **113** exclusively. Ni has reported analogous selectivity in the amination of *p*-ethyltoluene with NFSI, and suggested a preference for hydrogen abstraction from the methyl group in compound **111** based on steric considerations.⁸⁴ In the present case, it is important to note that NFSI is not completely dissolved in the decatungstate-catalyzed reactions at room temperature but is fully solubilized at 75 °C in the AIBN-initiated reactions. Thus, we speculated that the unique fluorination selectivities may in fact result from a higher concentration of NFSI in the heated reactions and the consequent trapping of an initially formed methyl radical. Conversely, at lower concentrations of NFSI (decatungstate-catalyzed reaction), equilibration between benzylic radicals may be responsible for the preferred formation of the fluoroethyl product **112**. To probe this hypothesis, the AIBN-

initiated fluorination of **111** was repeated with decreasing amounts of NFSI to assess the effect of NFSI concentration. When substoichiometric amounts (0.5 equiv.) of NFSI were added to this reaction, the fluoroethyl product **112** was also observed as a minor product (**113** : **112** = 1.4 : 1). This result indicates that the equilibration of benzylic radicals is likely responsible for the differing selectivities in the fluorination of ethyltoluenes, and provides a useful tool for imparting or attenuating selectivity in the fluorination of substrates with multiple benzylic C–H bonds.

Scheme 2.15 Differing Selectivities in the Fluorination of *p*-Ethyltoluenes

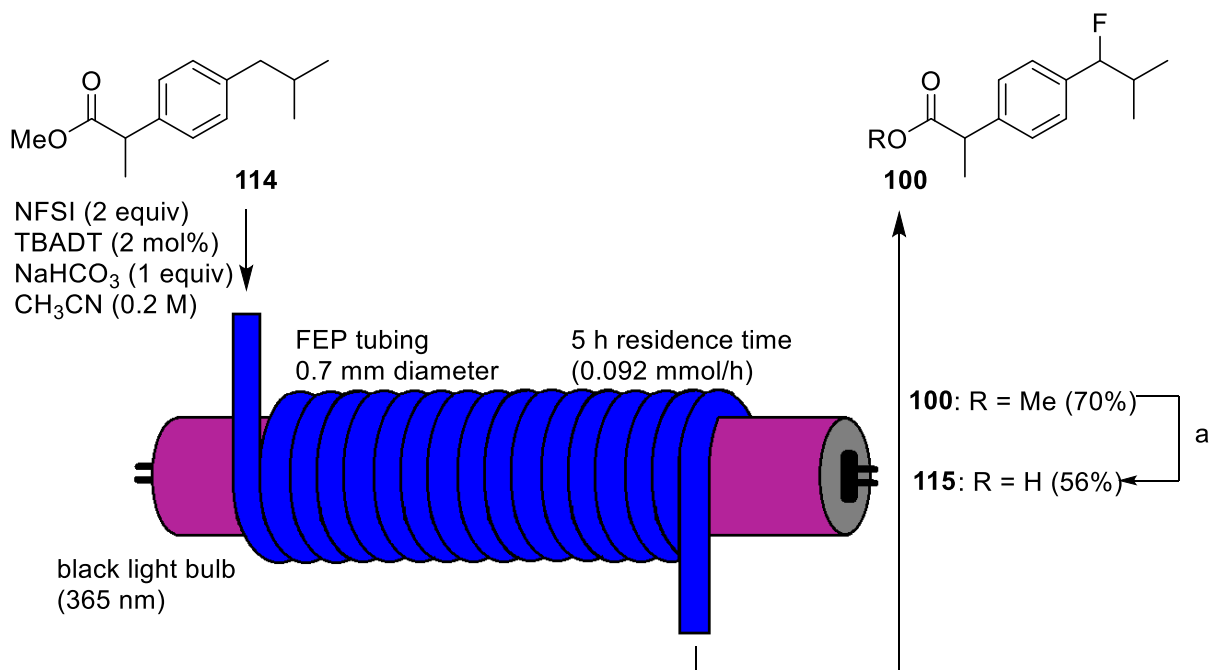


a) Accompanied by 7% of compound **113**. b) Yield based on analysis of ¹H NMR spectra with internal standard.

Finally, in an effort to decrease the reaction time for the decatungstate-catalyzed fluorination, we examined the fluorination of ibuprofen methyl ester (**114**) in flow.^{32,85} As depicted in Scheme 2.16 irradiation of the reaction mixture in FEP (Fluorinated Ethylene Propylene) tubing (3 m length, 1.4 mL total volume) wrapped around a blacklight blue lamp (BLB lamp, $\lambda = 365$ nm) reduced the reaction time from 24 h (batch) to 5 h (flow) without any significant impact to the yield (75% in batch vs 70% in flow). Considering the potential importance of late-stage fluorination to medicinal chemistry we were also interested in gauging the effect of benzylic fluorination on some of the basic pharmacokinetic properties of ibuprofen. Thus, the ester **100** was hydrolyzed to afford the fluoroibuprofen **115** (Scheme 2.16 Fluorination of Ibuprofen in Flow Scheme 2.16). Not

surprisingly, fluorination of ibuprofen resulted in a modest decrease in pK_a (from 4.35 (ibuprofen) to 4.23 (**115**)). Fluorination of ibuprofen also slightly improved metabolic stability in both human and rat microsomes, leading to a decrease in clearance from 19 to 12 $\mu\text{g min}^{-1} \text{mg}^{-1}$ protein in human microsomes and 71 to 39 $\mu\text{g min}^{-1} \text{mg}^{-1}$ protein in rat microsomes (Table 2.6).^{86, C}

Scheme 2.16 Fluorination of Ibuprofen in Flow



a) LiOH, MeOH, THF, H_2O , 24 h

Table 2.6 Benefits of Fluorination of Ibuprofen^{86, C}

	Human Cell Line ($\mu\text{g min}^{-1} \text{mg}^{-1}$)	Rat Cell Line ($\mu\text{g min}^{-1} \text{mg}^{-1}$)
Ibuprofen	19	71
Fluoroibuprofen	12	39

c Mrs. Isabelle Walter collected and analysed the microsomal stability data discussed above.⁸⁶

2.4. Conclusion and Future Work

In summary, we have developed two complimentary methods for benzylic fluorination that rely on the fluorine transfer agent NFSI in combination with either a decatungstate photocatalyst or the radical initiator (AIBN). These processes tolerate a range of functional groups in providing benzyl fluorides in modest to excellent yield. Furthermore, the photocatalytic fluorination can be adapted to continuous flow without compromising yield. In future studies involving photocatalytic fluorination with TBADT and NFSI the Britton group is looking to expand the scope of the reaction to include heterocycles as well as looking to adapt the reaction to use [^{18}F]-NFSI to incorporate radionuclides into agents for PET imaging.

2.5. Experimental

2.5.1. General

All reactions were carried out with commercial solvents and reagents that were used as received. For extended TBADT photochemical reactions, degassing of the solvent was carried out via several freeze/pump/thaw cycles. Flash chromatography was carried out with 230-400 mesh silica gel (SiliCycle, SiliaFlash® P60). Concentration and removal of trace solvents was done via a Büchi rotary evaporator using dry ice/acetone condenser, and vacuum applied from an aspirator or Büchi V-500 pump. All reagents and starting materials were purchased from Sigma Aldrich, Alfa Aesar, TCI America, and/or Strem, and were used without further purification. All solvents were purchased from Sigma Aldrich, EMD, Anachemia, Caledon, Fisher, or ACP and used without further purification, unless otherwise specified. Nuclear magnetic resonance (NMR) spectra were recorded using chloroform- d (CDCl_3) or acetonitrile- d_3 . Signal positions (δ) are given in parts per million from tetramethylsilane (δ 0) and were measured relative to the signal of the solvent (^1H NMR: CDCl_3 : δ 7.26, CD_3CN : δ 1.94; ^{13}C NMR: CDCl_3 : δ 77.16, CD_3CN : δ 118.26). Coupling constants (J values) are given in Hertz (Hz) and are reported to the nearest 0.1 Hz. ^1H NMR spectral data are tabulated in the order: multiplicity (s, singlet; d, doublet; t, triplet; q, quartet; quint, quintet; m, multiplet), coupling constants, number of protons. NMR spectra were recorded on a Bruker Avance 600 equipped with a QNP or TCI cryoprobe

(600 MHz), Bruker 500 (500 MHz), or Bruker 400 (400 MHz). Assignments of ^1H and ^{13}C NMR spectra are based on analysis of ^1H - ^1H COSY, HSQC, HMBC, TOCSY and 1D NOESY spectra, where applicable. Where necessary, 1,3,5-tris(trifluoromethyl)benzene was added to the crude reaction mixtures and used as an internal standard. Yields were then calculated following analysis of ^1H NMR spectra. Volatile substrates **x**, **y** and **z** were partially purified by extraction of the crude reaction mixtures with pentane. Removal of the solvent via careful air-drying yielded mixtures of these compounds. No further purification was carried out to separate isomers of these compounds or to remove unreacted starting materials. High-resolution mass spectra were performed on an Agilent 6210 TOF LC/MS, Bruker MaXis Impact TOF LC/MS, or Bruker micrOTOF-II LC mass spectrometer.

2.5.2. General Methods

Procedure for Photochemical Fluorination with TBADT

A suspension of substrate (1 eq), NFSI (3 eq), TBADT (2 mol %), and Li_2CO_3 or NaHCO_3 (1 eq) in CH_3CN (0.6-0.8 M substrate) was degassed via 3 x freeze/pump/thaw cycles. The reaction was irradiated with a black light (long-wave UV, ~ 365 nm) for 24-72 h, until reaction progress as analyzed by ^1H NMR spectroscopy indicated no additional reaction progress. The resulting suspension was concentrated to dryness, CH_2Cl_2 was added and the mixture was filtered through a pad of celite and the crude reaction product was concentrated then purified by column chromatography.

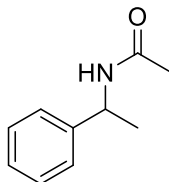
Procedure for Thermal AIBN-Initiated Fluorination

To a suspension of substrate (1 eq), NFSI (3 eq) and Li_2CO_3 (1 eq) was added AIBN (5 mol %, 250 mM solution in CH_3CN , 0.6-0.8 M substrate). The resulting reaction mixture was then heated to 75°C for 16-20 h, cooled and filtered through a pad of celite and the crude reaction product was concentrated then purified by column chromatography.

2.5.3. Preparation and Experimental Data

Preparation of Acetamide **85**

Acetamide **85** was formed as a side product during the fluorination of ethylbenzene and then further used to probe the reaction mechanism and optimize the fluorination process. (Scheme 2.12)



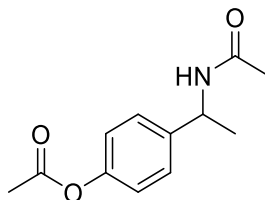
$^1\text{H-NMR}$ (400 MHz, CDCl_3): δ 7.30 (m, 5H), 5.86 (br s, 1H), 5.12 (m, 1H), 1.48 (d, $J = 6.9$, 3H) ppm

$^{13}\text{C-NMR}$ (100 MHz, CDCl_3): δ 169.3, 143.3, 128.8, 127.5, 126.3, 48.9, 23.6, 21.8 ppm

HRMS (EI^+) calculated for $\text{C}_{10}\text{H}_{13}\text{NO}^+$ 163.0997, found 163.0976

Preparation of Acetamide **86**

Acetamide **86** was formed as a side product during the fluorination of ethylbenzene and then further used to probe the reaction mechanism and optimize the fluorination process. (Scheme 2.12)

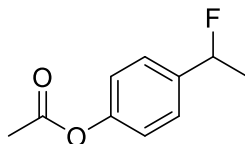


$^1\text{H-NMR}$ (500 MHz, CDCl_3): δ 7.33 (d, $J = 8.6$ Hz, 2H), 7.05 (d, $J = 8.6$ Hz, 2H), 5.69 (br s, 1H), 5.13 (m, 1H), 2.29 (s, 3H), 1.97 (s, 3H), 1.48 (d, $J = 6.9$ Hz, 3H) ppm

$^{13}\text{C-NMR}$ (125 MHz, CDCl_3): δ 169.7, 169.2, 150.0, 140.8, 127.6, 121.9, 48.4, 23.6, 21.6, 21.3 ppm

HRMS (ESI⁺) calculated for C₁₂H₁₅NO₃H⁺ 222.1125, found 222.1109

Synthesis of *p*-Acetoxy(1-Fluoroethyl)benzene (**88**)



The reaction was performed according to the general procedure using 4-ethylphenyl acetate as the substrate followed by purification by flash chromatography (5-10% EtOAc/Pentane). This afforded the fluorinated product 4-(1-fluoroethyl)phenyl acetate (**24**) in 75% yield as a pale yellow clear oil.

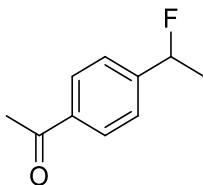
¹H-NMR (400 MHz, CDCl₃): δ 7.37 (d, *J* = 8.1 Hz, 2H), 7.10 (d, *J* = 8.2 Hz, 2H), 5.62 (dq, *J* = 47.6, 6.4 Hz, 1H), 2.31 (s, 3H), 1.64 (dd, *J* = 23.9, 6.5 Hz, 3H) ppm

¹³C-NMR (100 MHz, CDCl₃) δ 169.6, 150.6 (d, *J* = 2.3 Hz), 139.2 (d, *J* = 19.9 Hz), 126.6 (d, *J* = 6.7 Hz), 121.8, 90.6 (d, *J* = 168.1 Hz), 23.1 (d, *J* = 25.1 Hz), 21.3 ppm

¹⁹F-NMR (470 MHz, CDCl₃) δ -166.4 ppm

HRMS (ESI⁺) calculated. for C₁₀H₁₁FN₂O₂⁺ 205.0635, found 205.0609

Synthesis of *p*-Acetyl(1-fluoroethyl)benzene (**96**)



The reaction was performed according to the general procedure using 1-(4-ethylphenyl)ethan-1-one as the substrate followed by purification by flash chromatography (5-10% EtOAc/Pentane). This afforded the fluorinated product 1-(4-(1-fluoroethyl)phenyl)ethan-1-one (**96**) in 45% yield as a pale oil.

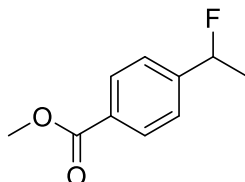
^1H -NMR (500 MHz, CDCl_3): δ 7.97 (d, J = 8.1 Hz, 2H), 7.43 (d, J = 8.1 Hz, 2H), 5.68 (dq, J = 47.6, 6.4 Hz, 1H), 2.60 (s, 3H), 1.64 (dd, J = 24.1, 6.5 Hz, 3H) ppm

^{13}C -NMR (125 MHz, CDCl_3): δ 197.8, 146.8 (d, J = 19.6 Hz), 137.0 (d, J = 1.8 Hz), 128.7, 125.2 (d, J = 7.3 Hz), 90.4 (d, J = 169.8 Hz), 26.8, 23.1 (d, J = 24.6 Hz) ppm

^{19}F -NMR (470 MHz, CDCl_3) δ -171.3 ppm

HRMS (EI^+) calculated for $\text{C}_{10}\text{H}_{11}\text{FO}_2^+$ 182.0743, found 182.0736

Synthesis of Methyl 4-(1-Fluoroethyl)benzoate (**98**)



The reaction was performed according to the general procedure using methyl 4-ethylbenzoate as the substrate followed by purification by flash chromatography (5-15% EtOAc/Pentane). This afforded the fluorinated product methyl 4-(1-fluoroethyl)benzoate (**98**) in 53% yield as a pale yellow oil.

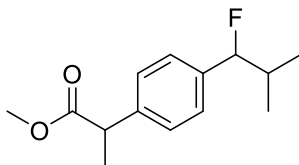
^1H -NMR (500 MHz, CDCl_3): δ 8.05 (d, J = 8.1 Hz, 2H), 7.41 (d, J = 8.1 Hz, 2H), 5.68 (dq, J = 47.6, 6.4 Hz, 1H), 3.92 (s, 3H), 1.65 (dd, J = 24.1, 6.5 Hz, 3H) ppm

^{13}C -NMR (125 MHz, CDCl_3): δ 166.9, 146.7 (d, J = 19.7 Hz), 130.6, 130.0, 125.1 (d, J = 7.2 Hz), 90.5 (d, J = 169.6 Hz), 52.3, 23.1 (d, J = 24.8 Hz) ppm

^{19}F -NMR (CDCl_3) δ -171.0 ppm

HRMS (EI^+) calculated for $\text{C}_{10}\text{H}_{11}\text{FO}_2^+$ 182.0743, found 182.0722

Synthesis of Fluoro-Ibuprofen Methyl Ester (**100**)



The reaction was performed according to the general procedure using ibuprofen methyl ester (**114**) as the substrate followed by purification by flash chromatography (10-15% EtOAc/Pentane). This afforded the fluorinated product **100** in 75% yield as a pale clear oil.

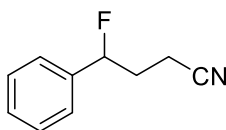
$^1\text{H-NMR}$ (500 MHz, CDCl_3): δ 7.30 (d, $J = 8.1$ Hz, 2H), 7.25 (d, $J = 8.1$ Hz, 2H), 5.08 (dd, $J = 46.9, 6.8$ Hz, 1H), 3.74 (q, $J = 7.1$ Hz, 1H), 3.66 (s, 3H), 2.10 (m, 1H), 1.50 (d, $J = 7.3$ Hz, 3H), 1.02 (d, $J = 6.78$ Hz, 3H), 0.85 (d, $J = 6.9$ Hz, 3H) ppm

$^{13}\text{C-NMR}$ (150 MHz, CDCl_3) δ 175.1, 140.5, 138.4 (d, $J = 20.8$ Hz), 127.5, 126.6 (d, $J = 7.1$ Hz), 99.2 (d, $J = 173.6$ Hz), 52.2, 45.3, 34.4 (d, $J = 22.7$ Hz), 18.7, 18.5 (d, $J = 5.8$ Hz), 17.7 (d, $J = 5.1$ Hz) ppm

$^{19}\text{F-NMR}$ (470 MHz, CD_3CN) δ -179.0 ppm

HRMS (EI^+) calculated for $\text{C}_{14}\text{H}_{19}\text{FO}_2\text{H}^+$ 239.1447, found 239.1454

Synthesis of 4-Fluoro-4-Phenylbutanenitrile (**101**)



The reaction was performed according to the general procedure using 4-phenylbutanenitrile as the substrate followed by purification by flash chromatography (5-10% EtOAc/Pentane). This afforded the fluorinated product 4-fluoro-4-phenylbutanenitrile (**101**) in 54% yield as a clear yellow oil.

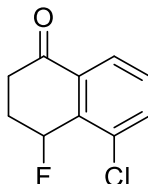
$^1\text{H-NMR}$ (400 MHz, CDCl_3): δ 7.38 (m, 5H), 5.58 (ddd, $J = 47.6, 8.5, 4.0$ Hz, 1H), 2.58 (dt, $J = 17.0, 7.93$ Hz, 1H), 2.48 (ddd, $J = 17.0, 7.7, 5.7$ Hz, 1H), 2.24 (m, 2H) ppm

^{13}C -NMR (150 MHz, CDCl_3) δ 138.4 (d, J = 19.7 Hz), 129.1 (d, J = 1.7 Hz), 129.0, 125.4 (d, J = 7.0 Hz), 118.9, 92.2 (d, J = 173.9 Hz), 33.1 (d, J = 24.8 Hz), 13.5 (d, J = 4.9 Hz) ppm

^{19}F -NMR (470 MHz, CD_3CN) δ -178.0 ppm

HRMS (EI^+) calculated for $\text{C}_{10}\text{H}_{10}\text{FN}^+$ 163.0797, found 163.0780

Synthesis of γ -Fluorotetralone **105**



The reaction was performed according to the general procedure using 5-chloro-3,4-dihydronaphthalen-1(2H)-one as the substrate followed by purification by flash chromatography (5-20% EtOAc/Pentane). This afforded the fluorinated product 5-chloro-4-fluoro-3,4-dihydronaphthalen-1(2H)-one (**105**) in 12%.

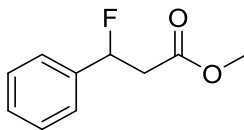
^1H -NMR (500 MHz, CDCl_3): δ 8.01 (d, J = 7.9 Hz, 1H), 7.67 (d, J = 7.9 Hz, 1H), 7.48 (dt, J = 7.9, 2.2 Hz, 1H), 6.11 (dt, J = 48.5, 2.6 Hz, 1H), 3.04 (m, 1H), 2.68 (m, 2H), 2.33 (m, 1H) ppm

^{13}C -NMR (125 MHz, CDCl_3) δ 196.0 (d, J = 1.8 Hz), 135.6 (d, J = 22.4 Hz), 135.5 (d, J = 10.2 Hz), 134.9 (d, J = 2.7 Hz), 133.9 (d, J = 2.4 Hz), 131.1 (d, J = 3.7 Hz), 125.8 (d, J = 2.7 Hz), 83.3 (d, J = 168.8 Hz), 32.1 (d, J = 2.7 Hz), 28.1 (d, J = 23.6 Hz)

^{19}F -NMR (CDCl_3) δ -175.1

HRMS (ESI^+) calculated for $\text{C}_{10}\text{H}_8\text{ClFONa}^+$ 221.0140, found 221.0126

Synthesis of Methyl 3-Fluoro-3-Phenylpropanoate (**106**)



The reaction was performed according to the general procedure using methyl 3-phenylpropanoate as the substrate followed by purification by flash chromatography (5-10% EtOAc/Pentane). This afforded the fluorinated product Methyl 3-fluoro-3-phenylpropanoate (**106**) in 62% yield as a pale yellow oil.

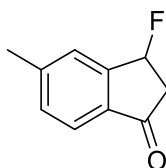
^1H -NMR (400 MHz, CDCl_3): δ 7.38 (m, 5H), 5.93 (ddd, J = 46.9, 9.1, 4.1 Hz, 1H), 3.74 (s, 3H), 3.04 (ddd, J = 16.0, 13.5, 9.1 Hz, 1H), 2.80 (ddd, J = 32.6, 16.0, 4.1 Hz, 1H) ppm

^{13}C -NMR (150 MHz, CDCl_3) δ 170.3 (d, J = 4.9 Hz), 138.8 (d, J = 19.5 Hz), 129.0 (d, J = 1.9 Hz), 128.8, 125.7 (d, J = 6.5 Hz), 90.8 (d, J = 172.6 Hz), 52.2, 42.4 (d, J = 27.2 Hz) ppm

^{19}F -NMR (470 MHz, CDCl_3) δ -173.2 ppm

HRMS (EI^+) calculated for $\text{C}_{10}\text{H}_{11}\text{FO}_2^+$ 182.0743, found 182.0756

Synthesis of β -Fluoroindanone **107**



The reaction was performed according to the general procedure using 5-methyl-2,3-dihydro-1H-inden-1-one as the substrate followed by purification by flash chromatography (5-10% EtOAc/Pentane). This afforded the fluorinated product 3-fluoro-5-methyl-2,3-dihydro-1H-inden-1-one (**107**) in 7% yield.

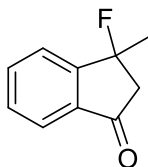
^1H -NMR (500 MHz, CDCl_3): δ 7.69 (d, J = 7.9 Hz, 1H), 7.54 (s, 1H), 7.39 (d, J = 7.9 Hz, 1H), 6.13 (ddd, J = 55.5, 6.6, 1.9 Hz, 1H), 3.11 (ddd, J = 19.0, 12.2, 6.6 Hz, 1H), 2.87 (ddd, J = 24.0, 19.0, 2.1, 1H), 2.50 (s, 3H)

^{13}C -NMR (125 MHz, CDCl_3) δ 200.9, 150.9 (d, J = 17.0 Hz), 147.0 (d, J = 2.7 Hz), 135.0, 132.2 (d, J = 3.4 Hz), 127.1 (d, J = 1.8 Hz), 123.5, 88.2 (d, J = 177.2 Hz), 44.4 (d, J = 20.8 Hz), 22.3 ppm

^{19}F -NMR (CDCl_3) δ -168.2 ppm

HRMS (ESI^+) calculated. for $\text{C}_{10}\text{H}_{10}\text{FO}^+$ 165.0710, found 165.0683

Synthesis of β -Fluoroindanone **109**



The reaction was performed according to the general procedure using 3-methyl-2,3-dihydro-1H-inden-1-one as the substrate followed by purification by flash chromatography (5-10% EtOAc/Pentane). This afforded the fluorinated product 3-fluoro-3-methyl-2,3-dihydro-1H-inden-1-one (**109**) in 14% yield

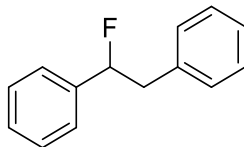
^1H -NMR (500 MHz, CDCl_3): δ 7.77 (d, J = 7.7 Hz, 1H), 7.73 (d, J = 4.1 Hz, 2H), 7.56 (m, 1H), 3.13 (dd, J = 20.5, 19.0 Hz, 1H), 2.88 (dd, J = 19.0, 11.7 Hz, 1H), 1.87 (d, J = 21.0 Hz, 3H)

^{13}C -NMR (125 MHz, CDCl_3) δ 201.4 (d, J = 2.7 Hz), 153.8 (d, J = 20.2 Hz), 136.3 (d, J = 1.8 Hz), 135.6 (d, J = 2.3 Hz), 130.6 (d, J = 2.7 Hz), 124.3, 123.4, 95.5 (d, J = 176.1 Hz), 50.7 (d, J = 23.7 Hz), 25.9 (d, J = 29.8 Hz) ppm

^{19}F -NMR (CDCl_3) δ -127.3 ppm

HRMS (EI^+) calculated for $\text{C}_{10}\text{H}_9\text{FO}^+$ 164.0637, found 164.0616

Synthesis of 1-Fluoro-1,2-Diphenylethane (**110**)



The reaction was performed according to the general procedure using 1,2-diphenylethane as the substrate followed by purification by flash chromatography (5% EtOAc/Pentane). This afforded the fluorinated product (1-fluoroethane-1,2-diyl)dibenzene (**110**) in 54% yield as pale white solid. This compound was isolated as an inseparable mixture with the parent compound 1,2-diphenylethane.

$^1\text{H-NMR}$ (400 MHz, CDCl_3): δ 7.32 (m, 10H), 5.61 (ddd, $J = 47.4, 8.1, 4.9$ Hz, 1H), 3.27 (ddd, $J = 17.4, 14.3, 8.1$ Hz, 1H), 3.11 (ddd, $J = 28.7, 14.3, 4.9$ Hz, 1H)) ppm

$^{13}\text{C-NMR}$ (150 MHz, CDCl_3) δ 139.9 (d, $J = 19.9$ Hz), 136.8 (d, $J = 3.9$ Hz), 129.7, 128.5, 128.5, 128.5, 126.9, 125.8 (d, $J = 6.6$ Hz), 95.0 (d, $J = 174.1$ Hz), 44.1(d, $J = 24.6$ Hz) ppm

$^{19}\text{F-NMR}$ (470 MHz, CDCl_3) δ -173.2ppm

HRMS (EI^+) calculated for $\text{C}_{14}\text{H}_{13}\text{F}^+$ 200.1001, found 200.1008

3. Studies Towards the Synthesis of Salinosporamide C

3.1. Pyrrolidine Containing Natural Products

There are a number of biologically active natural products that contain a pyrrolidine ring as part of their structural motif. For example, iminosugars and dihydroxypyrrolidine containing natural products [e.g., hyacinthacine A₄ (**121**) and swainsonine (**122**)] have been shown to exhibit inhibitory activity toward various carbohydrate processing enzymes and as such are considered an attractive class of carbohydrate mimetics.^{87–89} Broussonetine B (**123**) was isolated from the branches of *Broussonetia kazinoki* in Japan and was found to inhibit the activity of glucosidase, galactosidase and mannosidase enzymes.⁹⁰ Preussin (**120**), originally isolated from *Aspergillus ochraceus* has been shown to have antifungal activity and it also displays cytotoxic effects towards human cancer cells. Trandolapril (**124**) is marketed as Mavik an angiotensin-converting-enzyme (ACE) inhibitor used to treat high blood pressure.^{91,92}

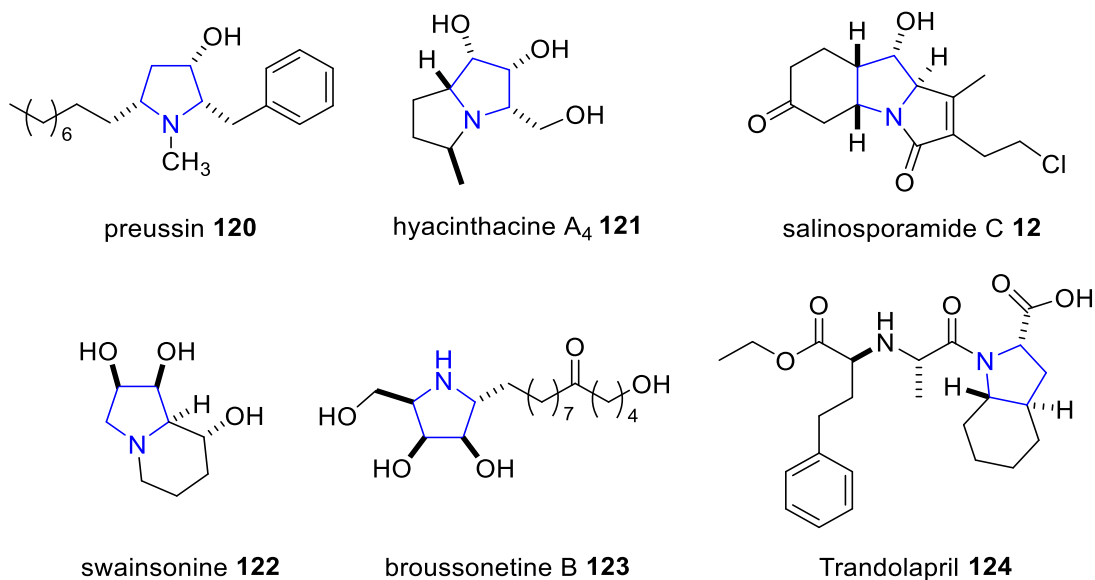


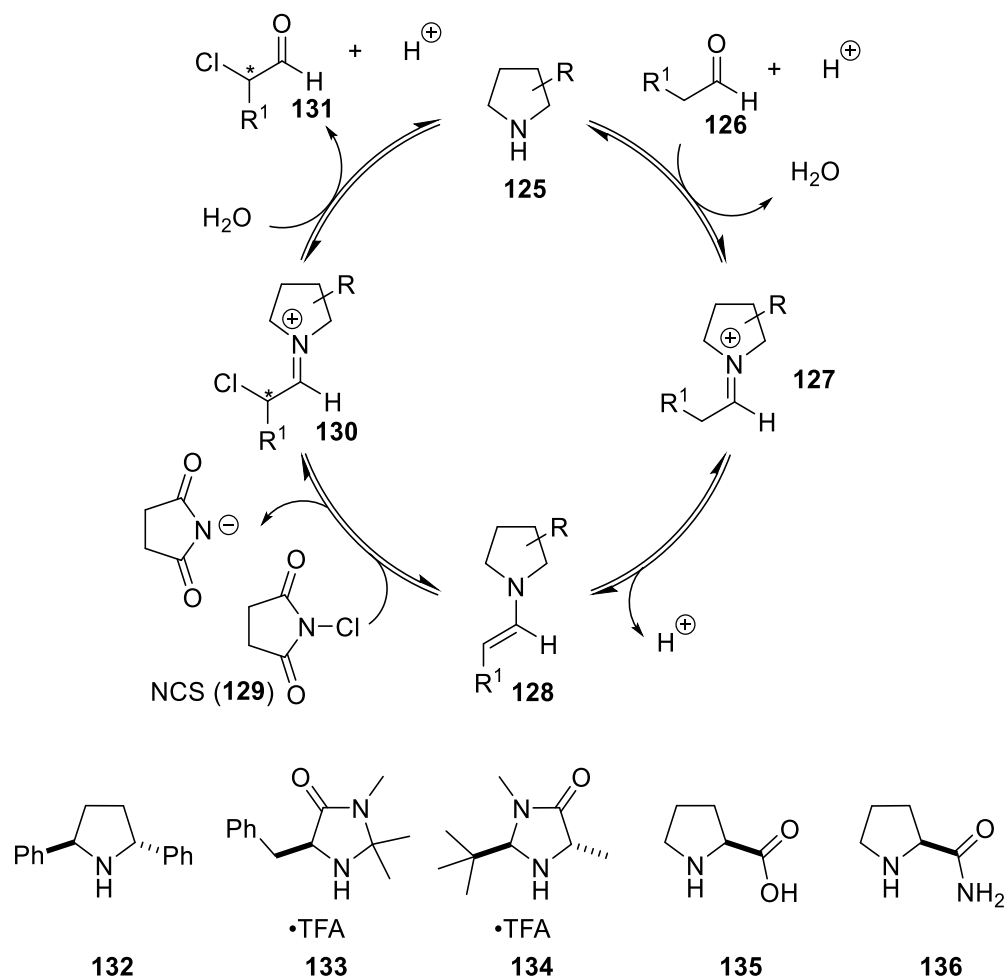
Figure 3.1 Natural products containing pyrrolidine rings.

3.2. Application of α -Chloroaldehydes To the Synthesis of Pyrrolidines

3.2.1. Introduction to α -Chloroaldehydes

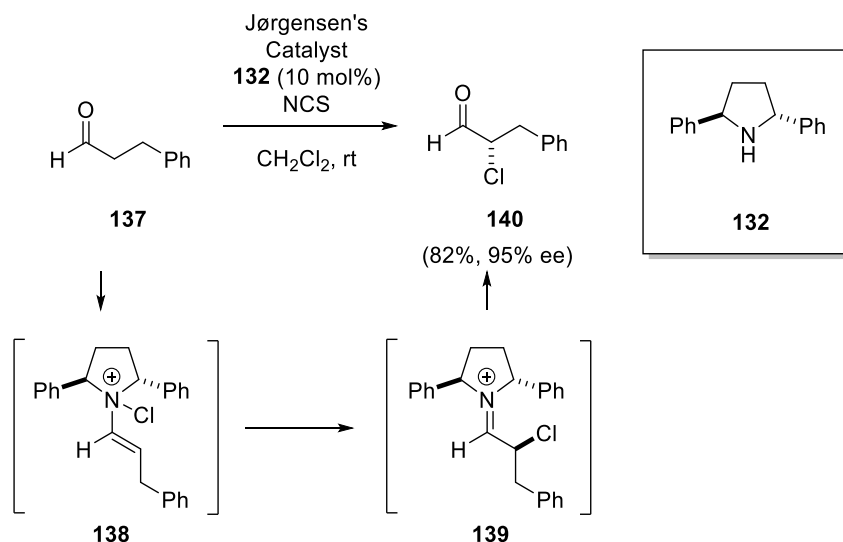
Due to the wide range of biological activities found in pyrrolidine-containing natural products, there has been considerable efforts devoted to the development of new methodologies to access this scaffold. However, most methods require lengthy synthetic sequences and expensive chiral starting materials, which has limited potential uses in large scale synthesis. Therefore, there remains room for improving overall efficiency of these methods and extending their utility in pyrrolidine synthesis. Work in the Britton group has focused on utilizing enantiomerically-enriched α -chloroaldehydes to access this important scaffold. These chiral starting materials are synthesized through an enantioselective organocatalytic α -chlorination reaction of an aldehyde as shown in Scheme 3.1. Initially, a condensation of chiral pyrrolidine catalyst (e.g., compound **132**) with aldehyde **126** forms the iminium ion **127**, which subsequently tautomerizes to the enamine **128**. The enamine (**128**) can then react with an electrophilic source of chlorine (e.g., *N*-chlorosuccinimide NCS) to add a chlorine atom at the α position and reform the iminium ion. The iminium ion (**130**) is then hydrolyzed to release the organocatalyst and afford the α -chloroaldehyde **131**. It is important to note that the R-group of the organocatalyst is able to direct the approach of the chlorine source and control the enantioselectivity. R-group characteristics that control such factors include a hydrogen bond attraction with the approaching electrophile or reversely, repulsion due to steric hindrance.^{93–95}

Scheme 3.1 General Organocatalytic Cycle for α -Functionalization of Aldehydes



An alternate method utilizing the organocatalyst 2,5-diphenylpyrrolidine (**132**) was reported by Jørgensen.⁹⁶ Jørgensen suggested that initial *N*-chlorination of the intermediate enamine (**138**) occurs followed by a 1,3 sigmatropic rearrangement resulting in the chlorination of the α carbon.⁹⁶ An example of an α -chlorination using Jørgensen's method is shown in Scheme 3.2. This reaction affords α -chloroaldehydes in high yield and enantiomeric excess across a range of substrates.^{95,96}

Scheme 3.2 Example of α -Chlorination of Aldehydes



3.2.2. Nucleophilic Additions to α -Chloroaldehydes

A powerful tool for the formation of C-C bonds is the addition of nucleophiles to aldehydes. In general, the addition occurs via approach of the nucleophile from a trajectory known as the Bürgi-Dunitz trajectory ($\sim 107^\circ$) which allows for maximum optimal overlap with the π^* orbital of the carbonyl. When reacting with α -chloroaldehydes the nucleophile can form both 1,2-*syn* (**145**) and 1,2-*anti* (**146**) (Figure 3.2) chlorohydrins. The 1,2-*anti* chlorohydrin **146** has been shown to be the major product of this addition reaction in contrast to addition reactions involving α -alkylaldehydes, which predominantly favour formation of the 1,2-*syn* product. This is best explained by the Evans-Cornforth model whereby the C-Cl bond and the carbonyl are oriented *anti*-periplanar in the lowest energy transition structure, which minimizes the net dipole of the molecule (e.g., aldehydes **143**, **144**). The nucleophile then approaches from the least sterically-hindered face of the aldehyde (*i.e.* aldehyde **144**) leading to the formation of 1,2-*anti*-chlorohydrins as the major product.

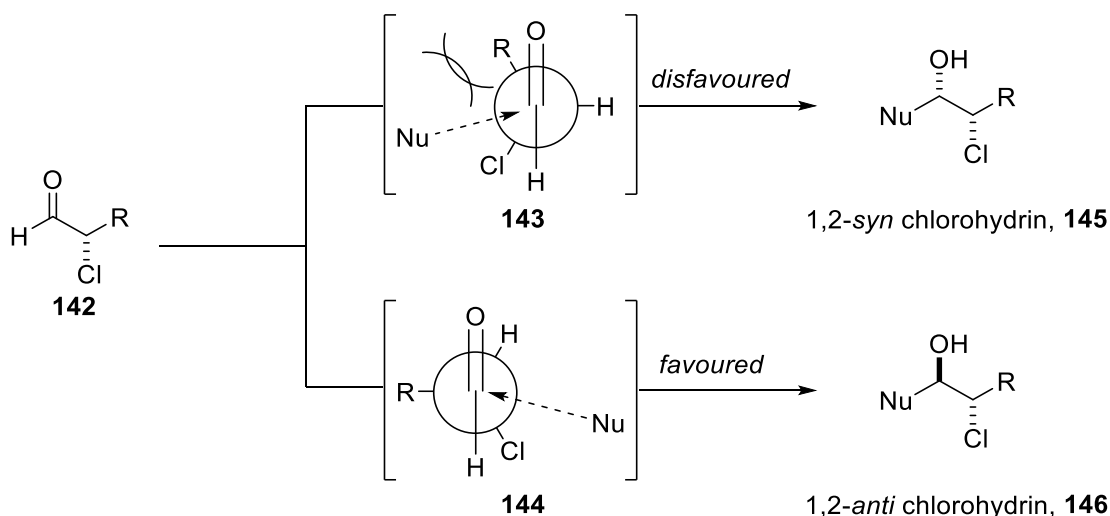
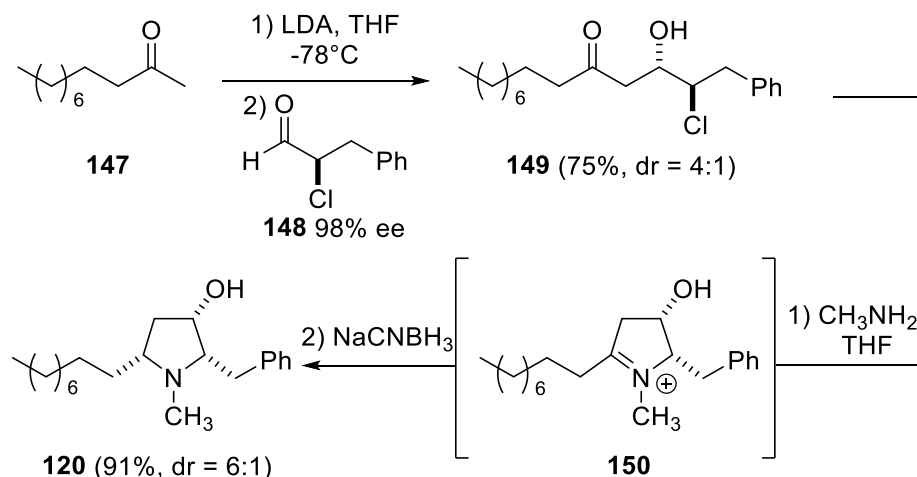


Figure 3.2 Cornforth model for rationalizing the nucleophilic addition to α -chloroaldehydes.

3.2.3. Formation of Pyrrolidines with α -Chloroaldehydes

Previous work in the Britton lab has exploited α -chloroaldehydes in the synthesis of the natural product (+)-preussin (**120**, Scheme 3.3). α -Chloroaldehyde **148** was reacted with the lithium enolate derived from ketone **147** to afford the 1,2-*anti* chlorohydrin **149** in a reasonable yield (75%) and moderate dr (4:1). Treatment with methylamine, followed by spontaneous cyclization, afforded intermediate compound **150**. Subsequent in situ addition of sodium cyanoborohydride reduced the intermediate iminium ion to the corresponding pyrrolidine. This sequence afforded (+)-preussin (**120**) in only three steps from hydrocinnamaldehyde and represents the shortest synthesis of preussin to date of over 25 reported syntheses.^{97–104}

Scheme 3.3 Synthesis of (+)-Preussin (120)



With this successful synthesis of a pyrrolidine-containing natural product complete, we were interested in expanding the utility of this reaction and examining its use in the synthesis of more structurally-complicated natural products. As a result, we decided to investigate the synthesis of salinosporamide C, a member of a class of compounds that have shown applications in anticancer therapy.

3.3. Introduction to Salinosporamides

Discovered in 2002, *Salinispora tropica* is a species of marine actinobacteria responsible for the production of salinosporamides A-K (e.g., compounds **151-154**, Figure 3.3).^{105,106} Most salinosporamides in the series share a γ -lactam- β -lactone bicyclic core that is common in compounds isolated from terrestrial *Streptomyces* such as omuralide (**155**). An exception to this is salinosporamide C (**12**), which contains a pyrrolidine ring at the core of the molecule.

Salinosporamide A has been shown to have potent cytotoxic activity against a wide range of human cancer cell lines.¹⁰⁶ As a result, salinosporamide A is currently under investigation in several phase I trials for the treatment of different cancers and has demonstrated early potential as a drug candidate.¹⁰⁸ Other salinosporamides, such as salinosporamide C, may also possess useful biological activity. Unfortunately, only limited

amount of the natural product can be isolated from the producing organism and the lack of a synthetic route to salinosporamide C has thus far prevented the full evaluation of its biological potential.

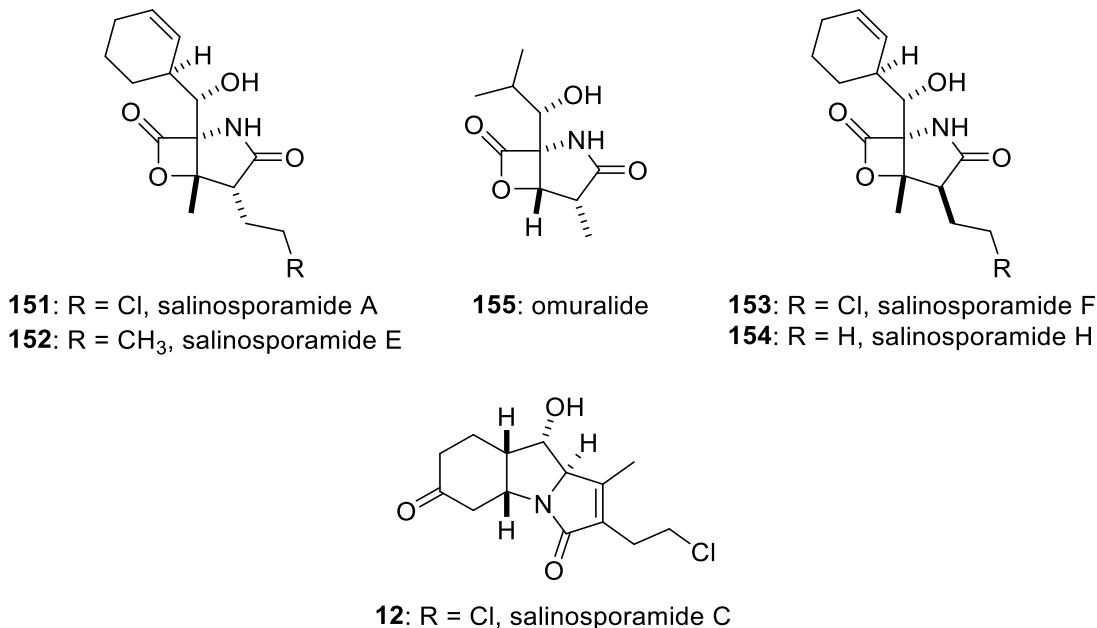


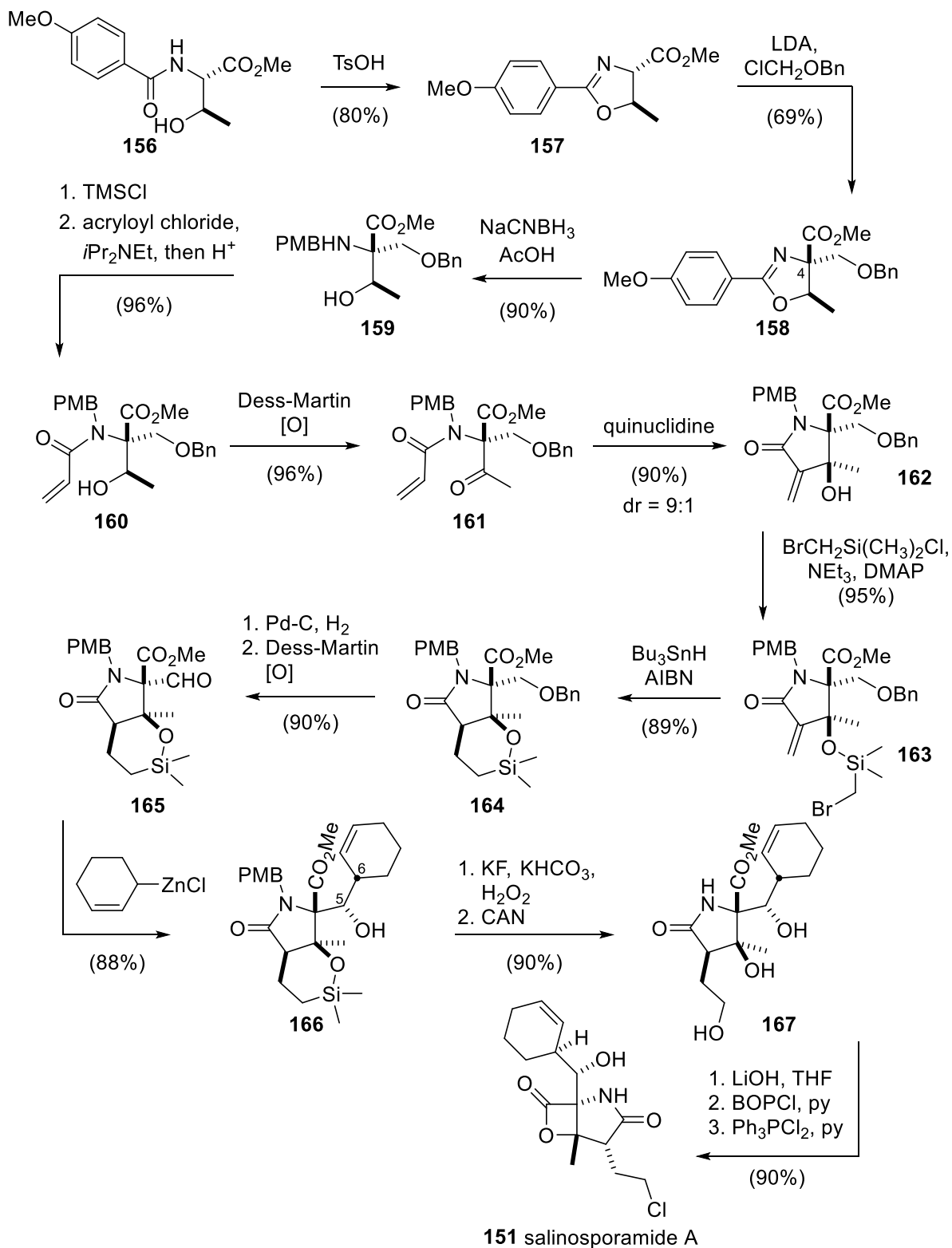
Figure 3.3 Natural products isolated from the genus *Salinispora*.

3.3.1. Previous Synthesis of Salinosporamide A

There have been several successful syntheses of salinosporamide A.^{105,109–115} The first total synthesis of salinosporamide A (**151**) was reported in 2004 by Corey and co-workers (Scheme 3.4).¹⁰⁵ This is the shortest stereoselective synthesis and required 17 linear steps from compound **156** and proceeded in 13.6% overall yield. The synthesis begins with an (S)-threonine derivative **156**, which was cyclized under acidic conditions to produce oxazoline **157**. Alkylation of compound **157** with chloromethyl benzyl ether (BOMCl) installs the quaternary centre at C4 to give oxazoline **158**. A reductive opening of the oxazoline ring then affords the free alcohol in compound **159**, which was protected directly as a silyl ether allowing the amine function to be selectively acylated with acryloyl chloride to give alcohol **160**. A Dess-Martin oxidation then afforded ketone **161**, which proceeded to the γ -lactam **162** via a Baylis–Hillman reaction in the presence of quinuclidine with 9:1 dr for the desired lactam. Lactam **162** was silylated with bromomethyldimethylsilyl chloride to give silyl ether **163** that subsequently underwent

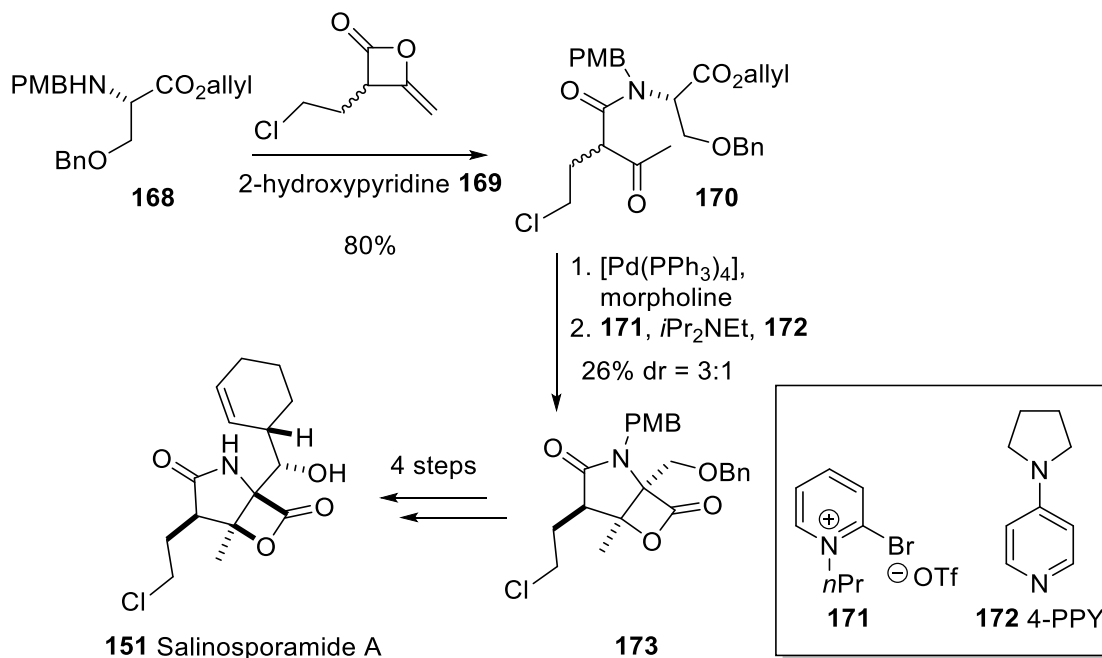
radical cyclization by treatment with tributyltin hydride and AIBN to afford *cis*-fused lactam **164**. A reductive deprotection of the benzyl ether followed by Dess-Martin oxidation led to aldehyde **165** which was treated with 2-cyclohexenylzinc chloride to install the cyclohexenyl function and install the new stereogenic centres at C5 and C6 (**166**). A Tamao-Fleming oxidation followed by CAN-mediated *N*-PMB deprotection gave access to triol **167**. Saponification of the methyl ester followed by lactonization with BOPCl and finally an Arbuzov reaction was used to install the aliphatic chlorine atom and complete the synthesis of salinosporamide A (**151**).

Scheme 3.4 Corey's Synthesis of Salinosporamide A



In 2007 Romo and co-workers completed a short racemic synthesis that represents the shortest synthesis to date (Scheme 3.5).¹⁰⁹ Treating serine derivative **168** with racemic chloroethylene substituted ketene dimer **169** afforded amide **170**. Palladium-catalyzed allyl deprotection followed by a biomimetic *bis*-cyclization led to the formation of the γ -lactam- β -lactone bicyclic core **173** in 26% yield and 3:1 diastereoselectivity, favoring the relative stereoisomer found in salinosporamide A. A further four steps including the addition of the 2-cyclohexenyl moiety gave racemic salinosporamide A (**151**).

Scheme 3.5 Romo's Synthesis of Salinosporamide A



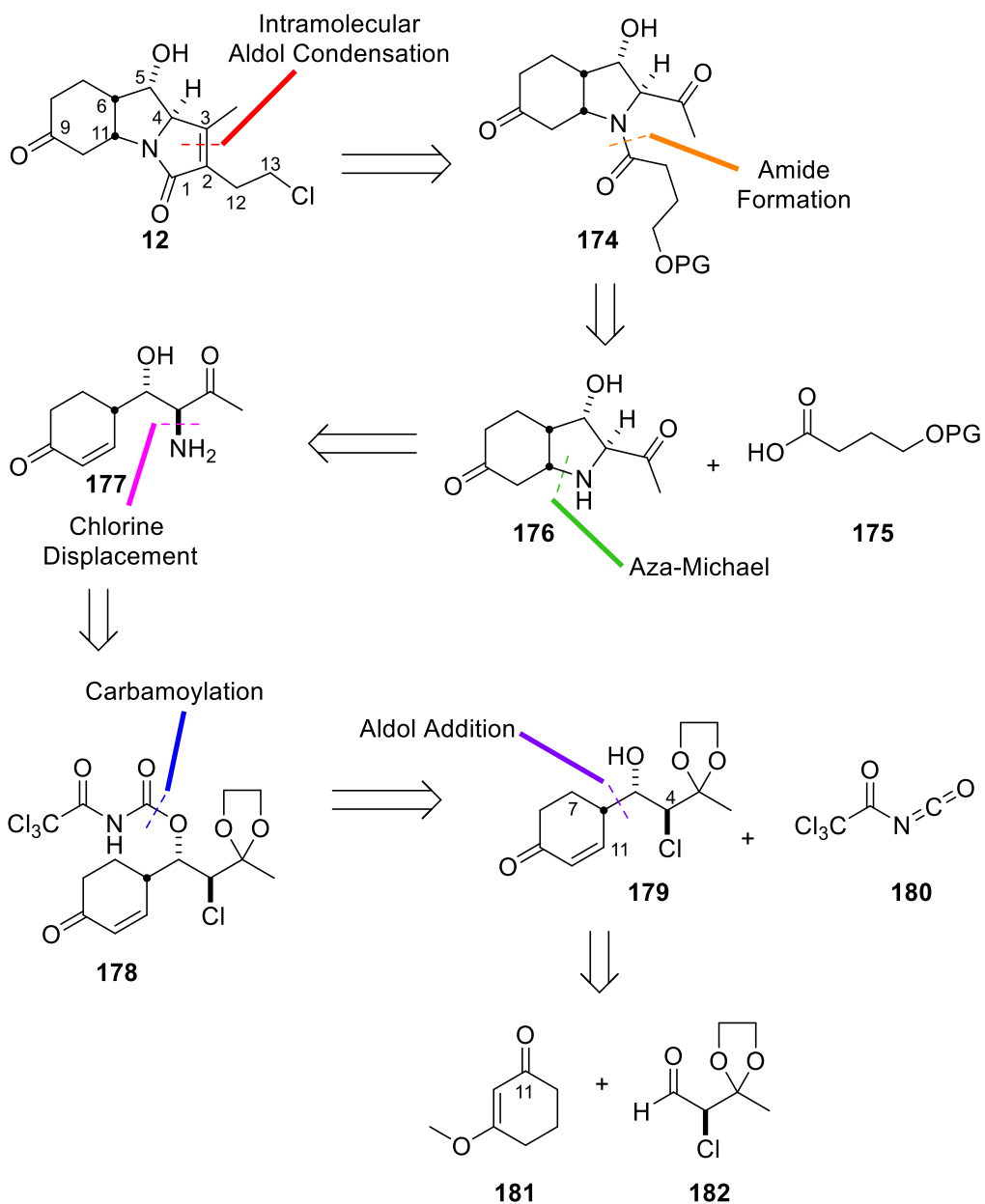
3.4. Previous Work in the Britton group

3.4.1. Initial Studies towards the Synthesis of Salinosporamide C

The original strategy designed to access salinosporamide C in the Britton lab was carried out by Jason Draper. His retrosynthetic analysis is outlined in Scheme 3.6. Installation of the chlorine could be achieved by an Arbuzov reaction similar to that employed by Corey in his synthesis of salinosporamide A (Scheme 3.4). He proposed that the γ -lactam could then be accessed through an intramolecular aldol condensation on amide **174**. The amide could be installed via an amide coupling reaction using *N,N*-

dicyclohexylcarbodiimide (DCC) and carboxylic acid **175**. Pyrrolidine **176** could then be introduced through an aza-Michael addition involving enone **177**. The nitrogen at C4 could be installed via intramolecular displacement of a chlorine by carbamate **178**. Carbamate **178** could then be accessed from a carbamoylation between alcohol **179** and isocyanate **180**. The enone of **179** could be produced from an aldol reaction between ketone **181** and chloroaldehyde **182** followed by a reduction of the carbonyl at C11.

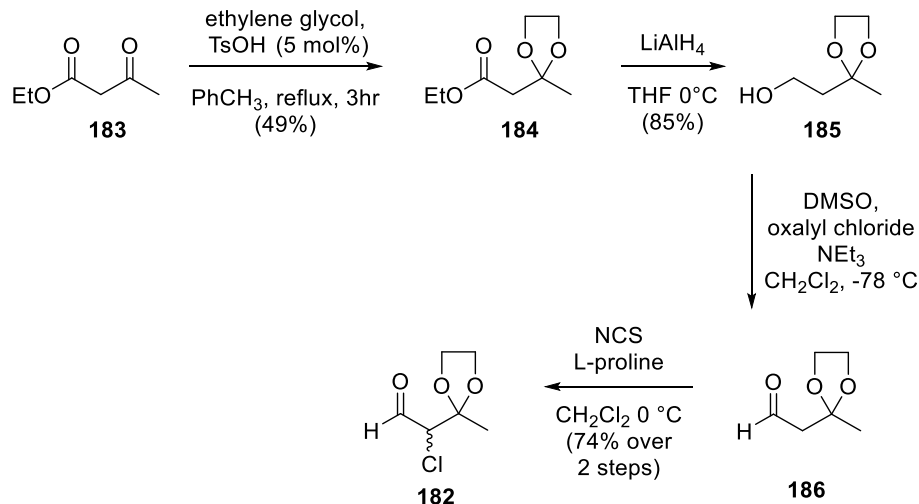
Scheme 3.6 Original Retrosynthesis of Salinosporamide C



3.4.2. Synthesis of Advanced Intermediate 191

Efforts to access pyrrolidine **174** began with the synthesis of dioxolane **187** by heating ethyl acetoacetate (**183**) with ethylene glycol and catalytic acid (Scheme 3.7). The reduction of the ester moiety on dioxolane **184** with lithium aluminum hydride gave alcohol **185** in good yield without the need for further purification. Alcohol **185** was transformed into aldehyde **186** by a Swern oxidation. Purification of compound **186** by flash chromatography resulted in the migration of the dioxolane onto the aldehyde and therefore crude aldehyde **186** was used directly in the α -chlorination reaction with L-proline and *N*-chlorosuccinimide to afford racemic α -chloroaldehyde **187**.

Scheme 3.7 Synthesis of α -Chloroaldehyde 187

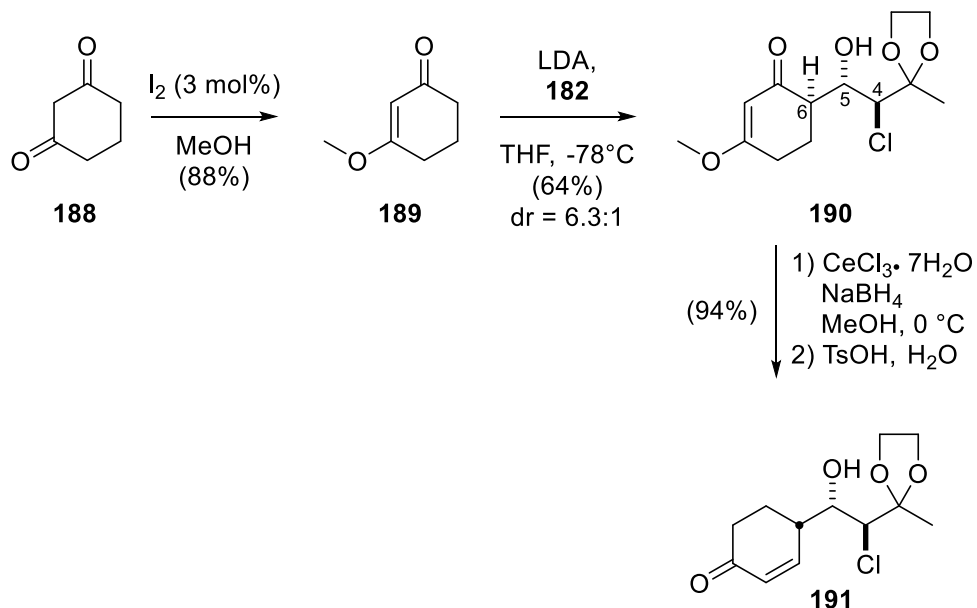


3.4.3. Synthesis of Enone 191

The other partner for the aldol reaction, ketone **181**, was accessed by dissolving 1,3-cyclohexanedione **188** in methanol and treating this reaction mixture with a catalytic amount of iodine (Scheme 3.8). The formation of the lithium enolate using LDA followed by addition of α -chloroaldehyde **182** gave the chlorohydrin **190** in 6.3:1 d.r., favouring the 1,2-*anti*-chlorohydrin. The stereochemical outcome of this reaction can be rationalized by the Evans-Cornforth model as discussed earlier. In addition, the *anti*-relative stereochemistry between carbons 5 and 6 in the aldol adduct **190** is expected based on the formation of a *trans*-enolate and subsequent reaction with aldehyde **182** via a

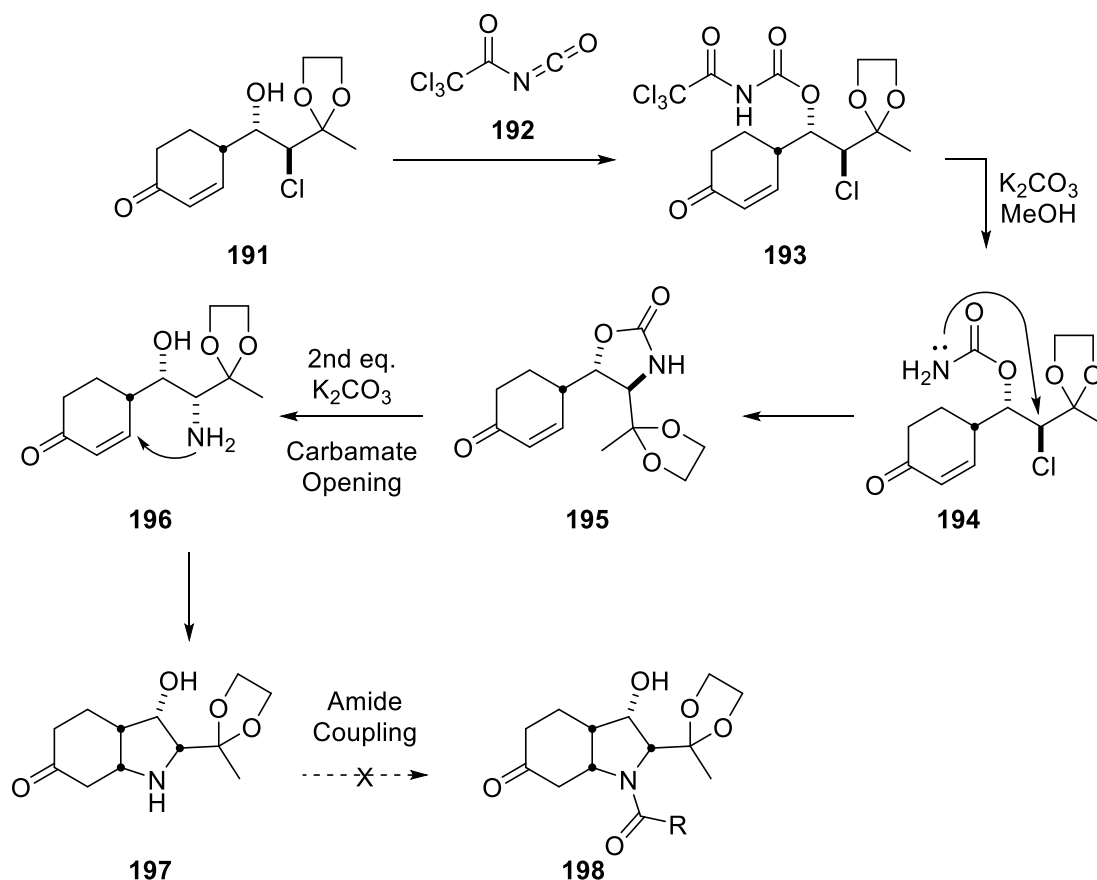
Zimmermann-Traxler transition state.¹¹⁶ A subsequent Luche reduction produced enone **191** in good yield.

Scheme 3.8 Synthesis of Enone 191



Enone **191** was treated with trichloroacetyl isocyanate (**192**) which gave carbamate **193**. A subsequent reaction with potassium carbonate in MeOH effected hydrolysis of the trichloroacetyl group to give carbamate **194**, which then underwent intramolecular displacement of the chloride to afford oxazolidinone **195** (Scheme 3.9). A second equivalent of base then effects ring opening of the oxazolidinone and the free amine undergoes an aza-Michael addition into enone **196** to afford pyrrolidine **197** in 60% yield.

Scheme 3.9 Formation of the Pyrrolidine Ring



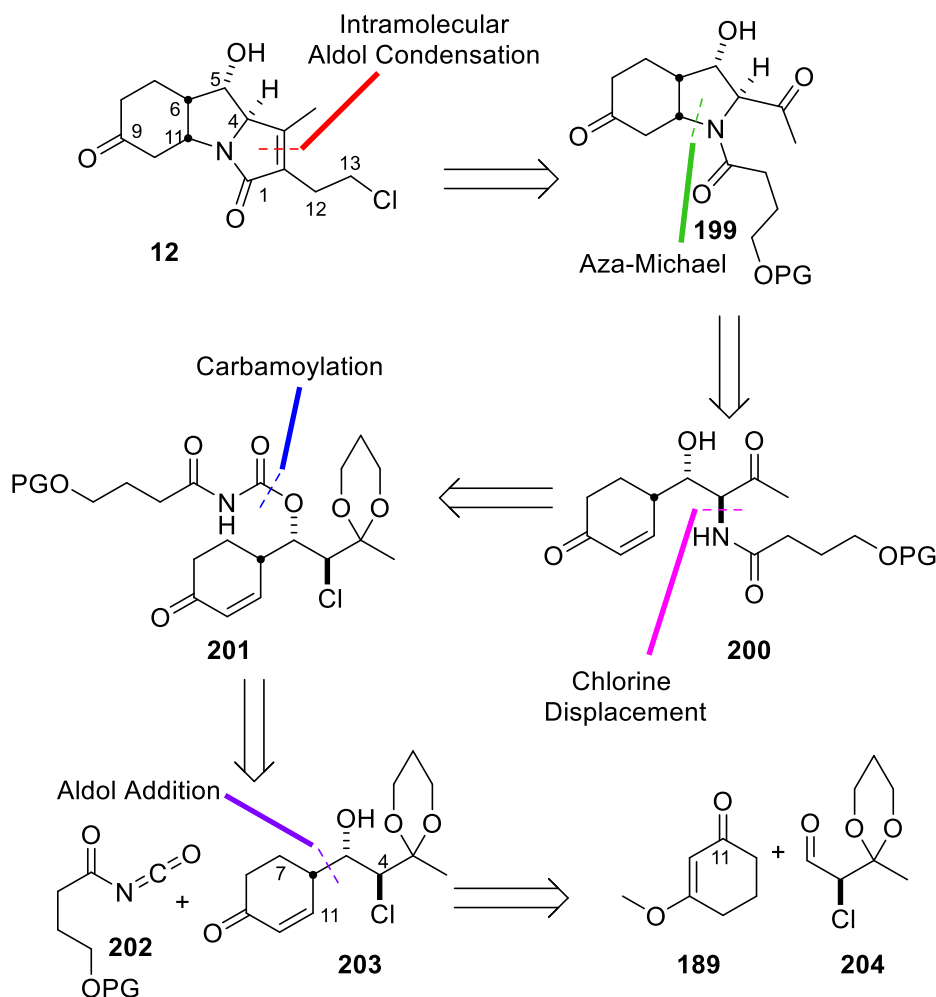
Unfortunately, further efforts by Jason Draper to derivatize pyrrolidine **197** via amide couplings were unsuccessful. However, the synthesis of pyrrolidine **197** was an important breakthrough and we considered that similar chemistry could be used to access salinosporamide C.

3.5. Revised Strategy to Salinosporamide C

As described above, attempts to exploit the pyrrolidine **197** scaffold in a synthesis of salinosporamide C were unsuccessful. Thus, we devised a new strategy that would install the amide functionality earlier in the synthesis. The retrosynthesis (Scheme 3.10) is similar to that shown earlier (Scheme 3.6) with the modification of the carbamoylation step where the desired group would be incorporated prior to pyrrolidine formation.

Furthermore, we decided to replace the 1,3-dioxolane function with a 1,3-dioxane group due to the comparative ease in removal of this protecting group.¹¹⁷

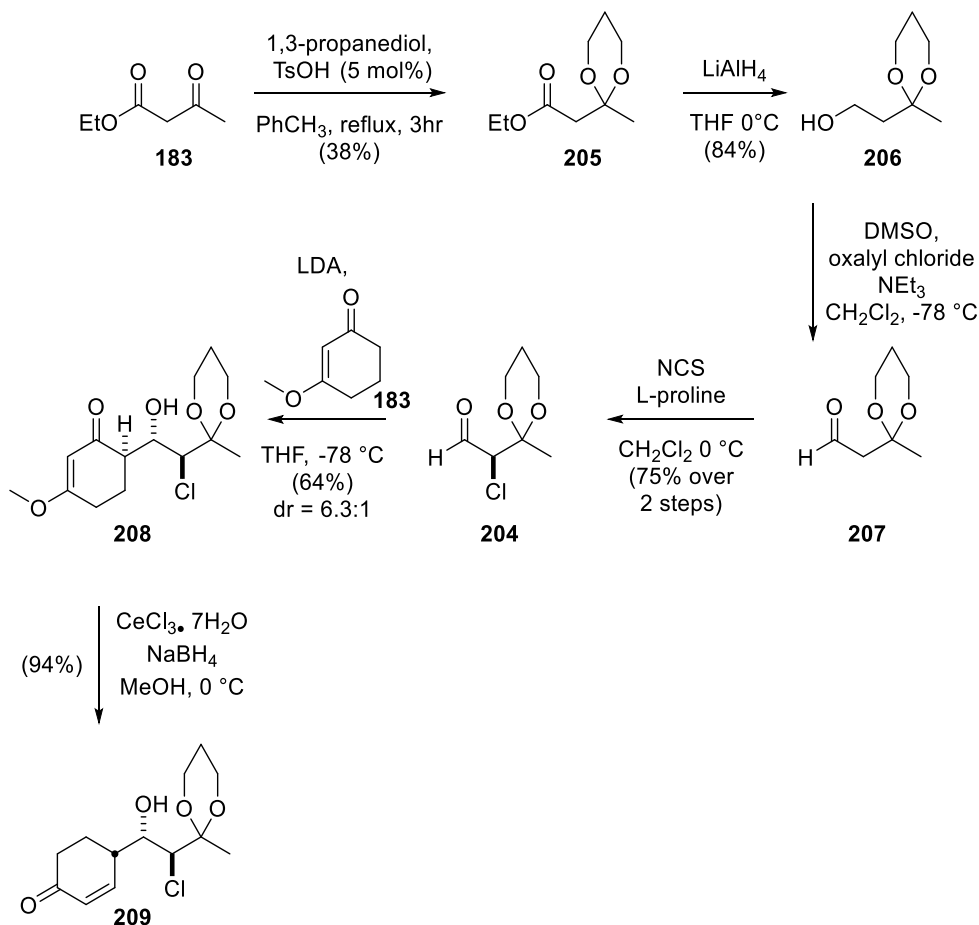
Scheme 3.10 Revised Retrosynthesis



The synthesis of enone **203** was repeated as described above with use of a 1,3 propanediol protecting group instead of ethylene glycol in the first step. Thus, heating a solution of ethyl acetoacetate (**183**) with 1,3 propanediol and catalytic amount of acid gave dioxane **205**. The formation of alcohol **206** from dioxane **205** was accomplished using lithium aluminum hydride in good yield. Alcohol **206** was then transformed into racemic α -chloroaldehyde **204** over two steps. The first step was a Swern oxidation to access aldehyde **207** and the second a α -chlorination reaction with L-proline and *N*-chlorosuccinimide. The lithium enolate of enone **183** was formed using LDA and subsequent addition of α -chloroaldehyde **204** gave the α -chlorohydrin **208** in 6.3:1 dr

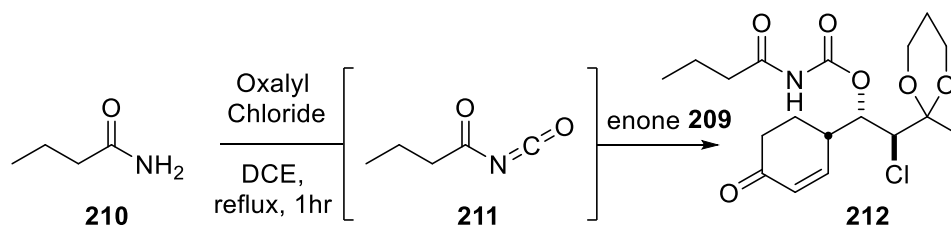
favouring the 1,2-*anti*-product. A Luche reduction of chlorohydrin **208** gave enone **209** in good yield.

Scheme 3.11 Synthesis of Chlorohydrin **209**



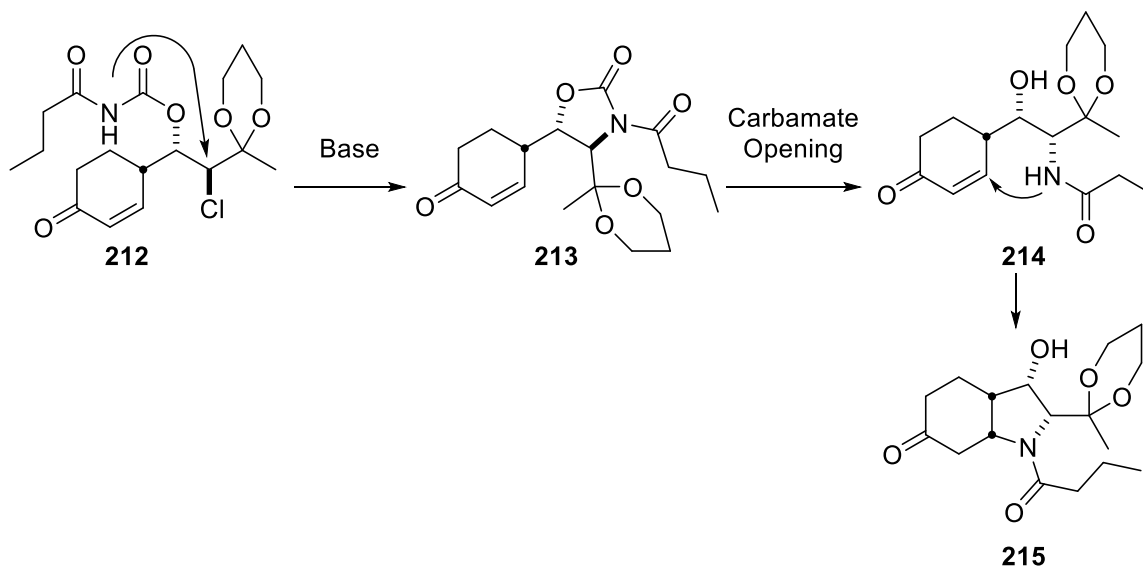
To examine whether chlorine displacement would be compatible with a carbamate on the nitrogen, we chose to pursue the use of test substrate (butanamide, *i.e.*, compound **210**). Accordingly, we accessed carbamate **212** by reacting butanamide (**210**) with oxalyl chloride to form isocyanate **211** *in situ*, which was directly reacted with enone **209** to afford the desired carbamate (Scheme 3.12).

Scheme 3.12 Synthesis of Carbamate 212



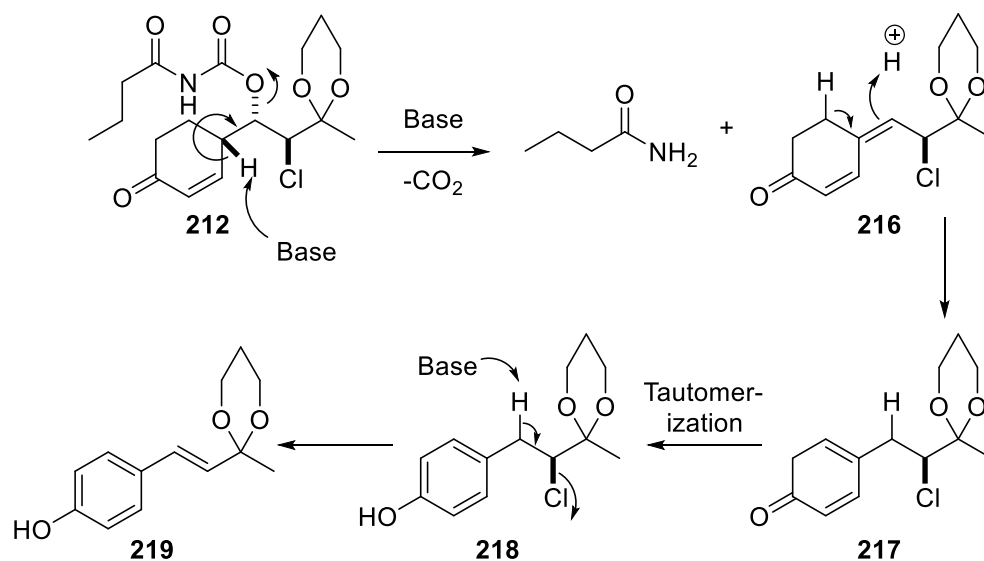
We then investigated the intramolecular chloride displacement by the amide function to form oxazolidinone **213**, which would expectedly be converted into pyrrolidine **215** after carbamate opening and an aza-Michael addition into the enone functionality (See Scheme 3.13).

Scheme 3.13 Attempted Formation of Pyrrolidine 215



Unfortunately efforts to replicate the cyclization described above (Scheme 3.9) for the amide derived from trichloro isocyanate (**192**) did not afford any of the desired pyrrolidine and instead gave clean access to phenol **219**. The formation of phenol **219** is consistent with the mechanism depicted in Scheme 3.14. It is proposed that elimination of the carbamate group followed by isomerization and tautomerization results in the formation of phenol **218**. Finally, elimination of the chloride leads to the styrene derivative **219**.

Scheme 3.14 Formation of Phenol 219



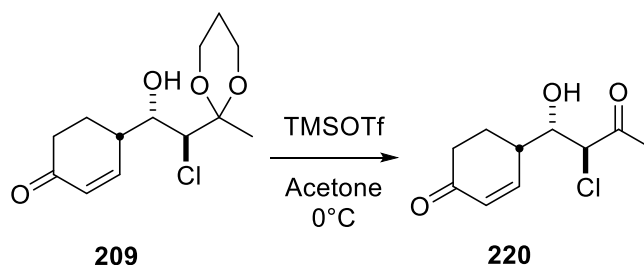
Considering the above, we screened reaction conditions in an effort to identify a suitable reagent combination to effect cyclization of compound **212** to **215** (Table 3.1). Unfortunately, no conditions were effective for the formation of the pyrrolidine ring and we proposed that the increased steric bulk of the 1,3-dioxane function in **212** was impeding the cyclization event. The cyclization of carbamate **212** using mild bases (entries 1,2,9,10) resulted in no reaction and some decomposition to phenol **219**. Progressively, the use of stronger bases was also explored, which resulted in near complete decomposition (entries 3-6). Given that a key difference between the chlorohydrin/enone **209**, which did not lead to the cyclized product, and the previously reported chlorohydrin/enone **191**, which led to the cyclized product smoothly, was the change in ring size of the carbonyl protecting group, we proposed that the increased steric bulk of the 1,3-dioxane function was impeding the cyclization event.

Table 3.1 Cyclization Attempts with Varying Bases and Solvents

Entry	Solvent	Base	Product(s)
1	MeOH	Li ₂ CO ₃	SM + trace 219
2	MeOH	Na ₂ CO ₃	SM + trace 219
3	MeOH	K ₂ CO ₃	219
4	MeOH	LDA	219
5	MeOH	KHMDS	219
6	MeOH	NEt ₃	219
7	MeOH	DBU	SM + 219
8	MeOH	NaH	219
9	THF	Li ₂ CO ₃	SM
10	THF	Na ₂ CO ₃	SM + 219
11	THF	K ₂ CO ₃	219

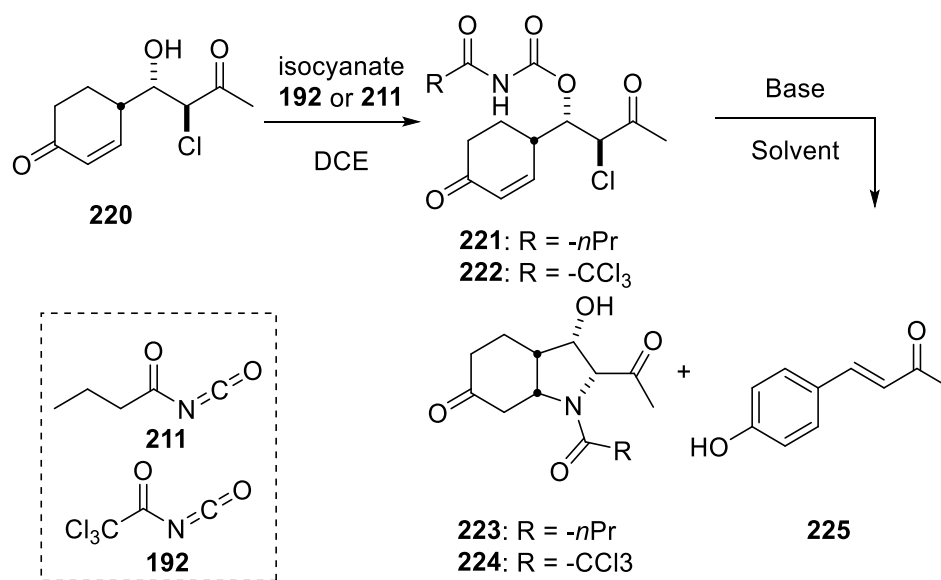
Accordingly, we attempted to remove the carbonyl protecting group to reduce or remove any steric impediments to cyclization and at the same time further activate the chloromethine function for the desired displacement reaction. Attempts to effect the carbonyl deprotection proved to be challenging and several experiments led to the formation of phenol **219**. We eventually found that treatment of dioxolane (**209**) with trimethylsilyl trifluoromethanesulfonate (TMSOTf) in acetone afforded ketone **220** in >95% yield.

Scheme 3.15 Deprotection of the Dioxane to form Ketone 220



All attempts to affect the desired sequence of reactions (Table 3.2) involving reactions of compound **220** with the isocyanate **192** or **211**, followed by chloride displacement and hetero-Michael addition led to elimination and aromatization to form phenol **219**. In fact, this process proved to be much more facile with the ketone **220**. It is likely that the formation of phenol **219** is a facile and unavoidable process due the stability of the extended pi system.

Table 3.2 Cyclization Attempts on Ketone 220



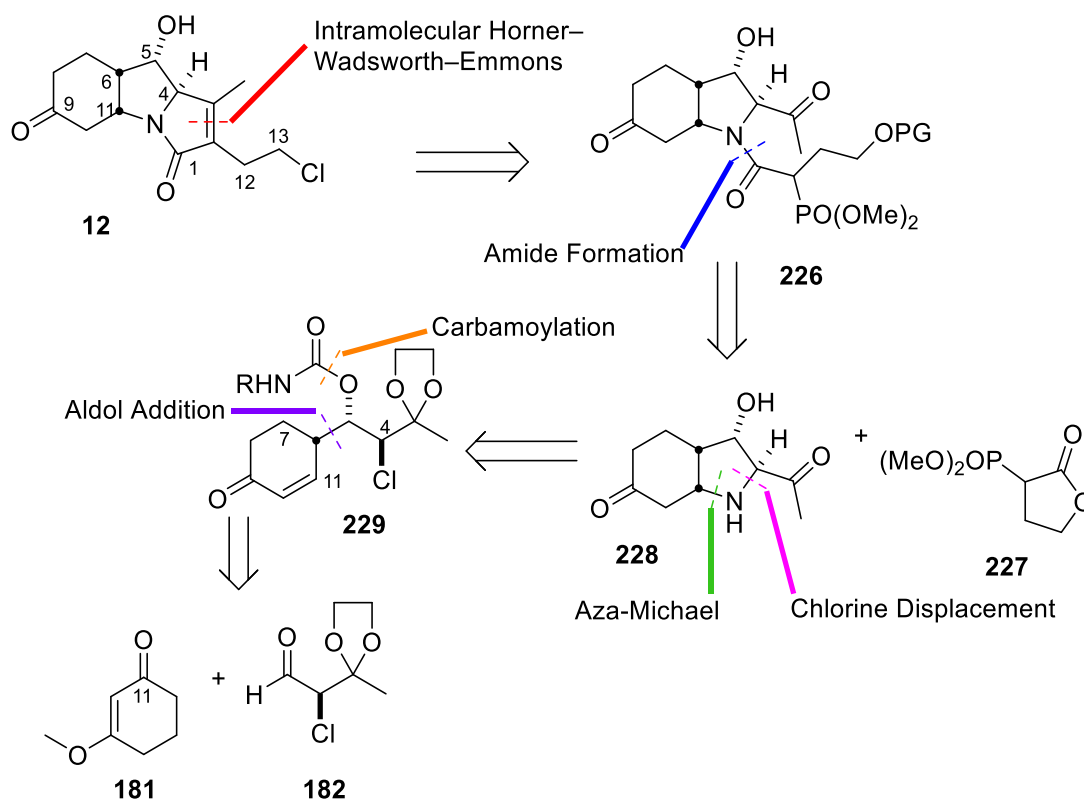
Entry	Isocyanate R	Solvent	Base	Product
1	<i>n</i> Pr	DCE/MeOH	K ₂ CO ₃	225
2	<i>n</i> Pr	EtOH	Cs ₂ CO ₃	225
3	-CCl ₃	CH ₂ Cl ₂ /MeOH	K ₂ CO ₃	225
4	-CCl ₃	CH ₂ Cl ₂ /MeOH	DBU	225

3.5.1. Revised Route for Closing the Pyrrolidine Ring

Having realized that it was unlikely that the sequence of reactions depicted in Scheme 3.13 would provide access to the pyrrolidine **215**, we decided to return to the original route developed by Draper, who had reported successful access to pyrrolidine **197**. As depicted in Scheme 3.9, the synthetic route was further revised and it was

imagined that the γ -lactam of the final target could be accessed via an intramolecular Horner-Wadsworth-Emmons reaction from phosphonate **226**. The amide bond of **226** would be formed via nucleophilic attack of amine **228** onto lactone **227**. The two C-N bonds of the pyrrolidine **228** can arise from a chlorine displacement at C4 and an aza-Michael addition to C11 on enone **229**. Enone **229** is the aldol adduct of ketone **181** and chloroaldehyde **182** followed by a reduction of the carbonyl at C11.

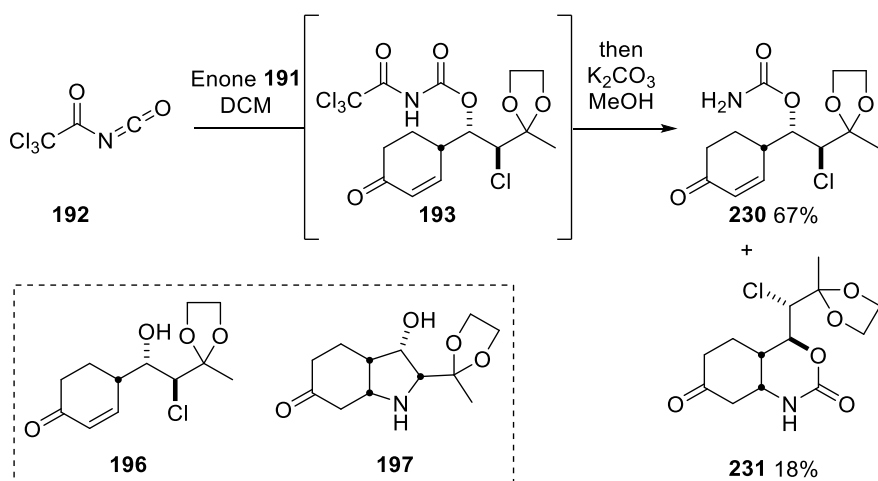
Scheme 3.16 Revised Retrosynthesis of salinosporamide C



While we were able to reproduce the work reported by Draper and access enone **191**, when we subjected enone **191** to conditions reported earlier (isocyanate **192** and base) we isolated a compound whose ^1H and ^{13}C NMR spectra were analyzed and the product was characterized as oxazinanone **231**. However, these spectra were in agreement with those of the compound previously assigned as pyrrolidine **197**, suggesting that the structure of pyrrolidine **197** was previously misassigned. Mass spectroscopic analysis was consistent with the expected mass of oxazinanone **231**, $m/z = 304.0940$, and no sign of the mass ($m/z = 242.1387$) corresponding to pyrrolidine **197** was found. Further

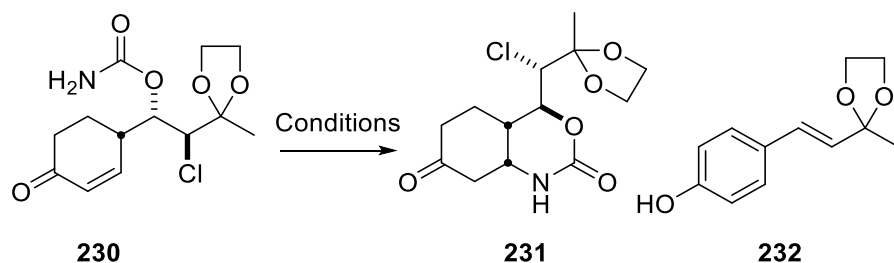
analysis of the ^{13}C NMR spectrum revealed a resonance at 152.2 ppm, which is characteristic of the carbon belonging to the carbonyl in a carbamate group.¹¹⁸ Based upon there data, it was clear that the compound previously assigned as pyrrolidine **197** was in fact oxazinanone **231** (Scheme 3.17). Further investigations have determined the mechanism by which this compound is produced and it first involves the formation of the carbamate **193** which upon addition of potassium carbonate in methanol undergoes methanolysis of the trichloroacetyl group to rapidly afford carbamate **230**. This compound then undergoes an aza-Michael reaction to form carbamate **231** in 18% yield with carbamate **230** (67%) as the major product.

Scheme 3.17 Oxazinanone Formation



Conditions to improve the yield of oxazinanone **231** were screened (Table 3.3).

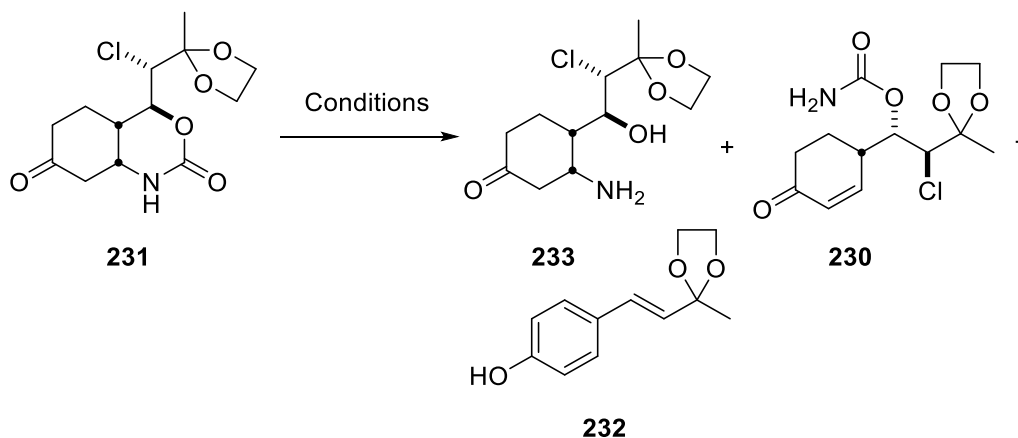
Table 3.3 Conditions for the Cyclization of Carbamate 231



Entry	Conditions	Products
1	NaH, MeOH	232
2	Cs ₂ CO ₃ , Ethanol	SM + 232
3	DBU, CH ₂ Cl ₂ /MeOH	232
4	K ₂ CO ₃ , MeOH, rt 3hr	34% 231 with 45% recovered SM and trace 232

With oxazinanone **231** in hand, we attempted to open the oxazinanone group in order to form the free amine and alcohol which we had hoped would provide access to the pyrrolidine through an intramolecular S_N2 reaction. Attempts to cleave the oxazinanone **231** are described in Table 3.4. Unfortunately, the most common product following several attempted cleavage reactions (Table 3.4) was the phenol **232**. Thus, under the basic reaction conditions the retro-aza-Michael reaction proceeds smoothly and subsequent aromatization occurred rapidly.

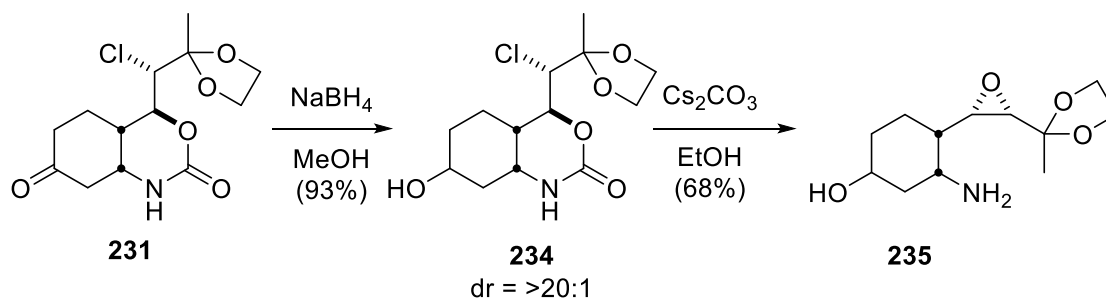
Table 3.4 Opening the Oxazinanone Ring



Entry	Solvent	Base	Product
1	EtOH	Cs ₂ CO ₃	230 / 232
2	EtOH	NaOH	232
3	EtOH	LiOH	232
4	1,4-dioxane, H ₂ O	CsOH	232
5	1,4-dioxane, H ₂ O	Ba(OH) ₂ 8H ₂ O	SM / 232

To reduce the propensity of the substrate to aromatize, we reduced the ketone using sodium borohydride, which gave alcohol **234** cleanly and in high diastereoselectivity (d.r. >20:1) (Scheme 3.18). Treatment of the alcohol (**234**) with cesium carbonate in ethanol removed the carbamate and lead to the formation of epoxide **235** in 68% yield. Unfortunately, at this point, we were not able to access sufficient material to further explore opening of the epoxide ring to form the pyrrolidine core of salinosporamide C, however, this may prove to be a viable route to the natural product with further experimentation.

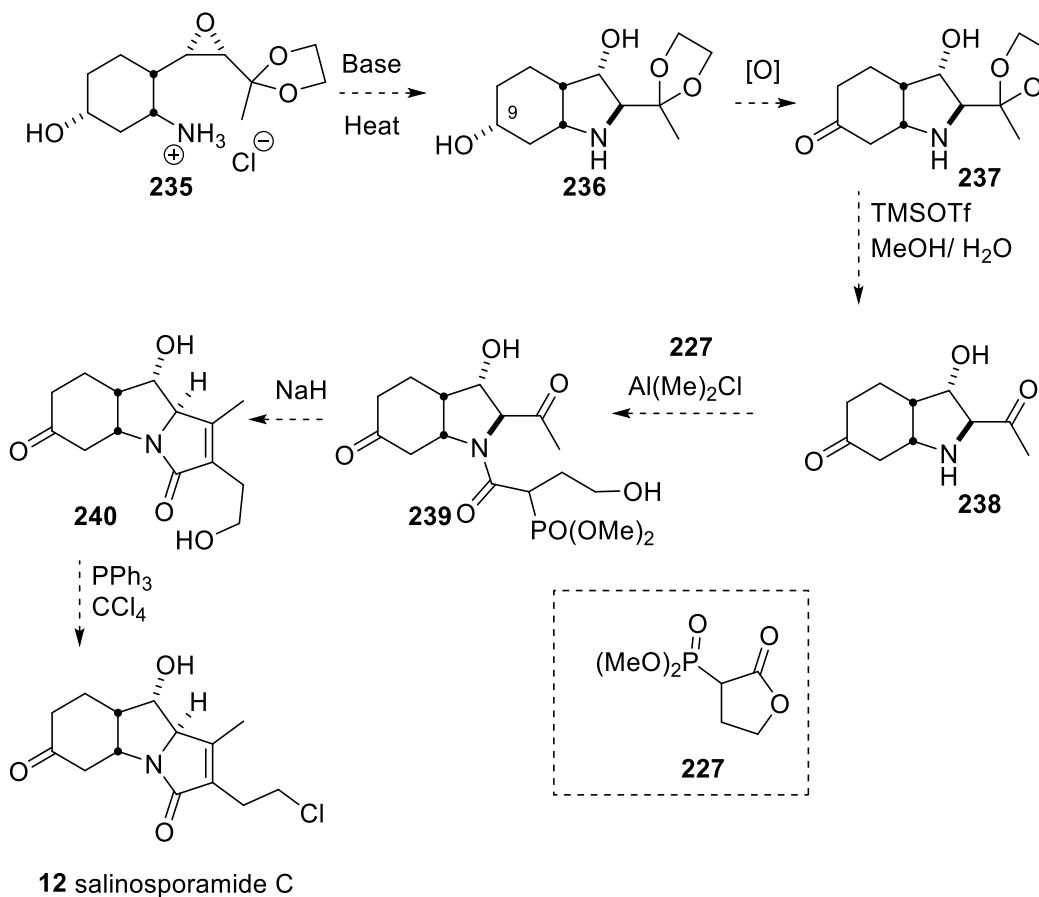
Scheme 3.18 Reduction of the Ketone in Order to Prevent the Reverse Aza-Michael



3.6. Future Work and Conclusions

The synthesis of key intermediate oxazinanone **231** is necessary to continue further experimentation and synthesis of salinosporamide C. To accomplish this synthesis and optimization of the oxazinanone deprotection is required to free the amine and the alcohol functionalities followed by closing the pyrrolidine ring, possibly by simply heating a solution of epoxide **235**. Then a selective oxidation of the alcohol at C9 followed by deprotection of the dioxalane group will expose the ketone. Amide formation of the pyrrolidine nitrogen with ring opening of lactone **227** would allow for an intramolecular Horner-Wadsworth-Emmons reaction to give γ -lactam **240**. Finally, an Appel reaction will replace the primary alcohol with a chlorine group to complete the racemic synthesis of salinosporamide C

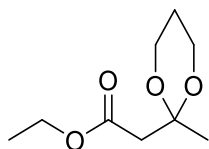
Scheme 3.19 Future Work



3.7. Experimental

3.7.1. Preparation and Experimental Data

Preparation of Dioxane 205

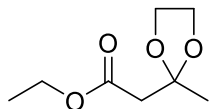


A round bottom flask was charged with a mixture of ethyl acetoacetate (**183**, 13.0 g, 100 mmol), 1,3-propanediol (13.7 g, 180 mmol), *p*-toluenesulfonic acid monohydrate (*p*-TsOH) (0.95 g, 5 mmol), toluene (200 ml) and fitted with a Dean Stark trap and heated to reflux. The solution was refluxed for 2.5 hours and then cooled to rt. The resulting solution was washed with saturated aqueous sodium bicarbonate (2 x 150 mL), deionized water (2 x 150 mL) and brine (1 x 150 ml). The aqueous mixture was back extracted with dichloromethane (3 x 100 mL) and the organic layers were combined. The mixture was dried with MgSO₄ (anhydrous), filtered, and concentrated in vacuo to give a crude mixture, which was purified by flash chromatography (10-25% ethyl acetate/pentane) resulting in a pale yellow oil of pure ethyl 2-(2-methyl-1,3-dioxan-2-yl)acetate (**205**, 7.21 g, 38% yield).

¹H NMR (600 MHz, CDCl₃) δ: 4.16 (q, *J* = 7.1 Hz, 2H), 3.94 (m, 4H), 2.80 (s, 2H), 1.72 (m, 2H), 1.56 (s, 3H), 1.27 (t, *J* = 7.1 Hz, 3H),

¹³C NMR (150 MHz, CDCl₃) δ: 169.7, 97.7, 60.7, 60.1, 42.3, 25.2, 23.2, 14.3

Preparation of Dioxolane 184



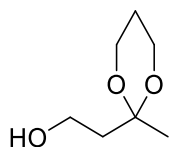
A round bottom flask was charged with a mixture of ethyl acetoacetate (**183**, 13.0 g, 100 mmol), ethylene glycol (11.2 mL, 200 mmol), *p*-toluenesulfonic acid (*p*-TsOH) (0.95 g, 5 mmol), toluene (200 ml) and fitted with a Dean Stark trap and heated to reflux. The solution was refluxed for 2.5 hours and then cooled to rt. The resulting solution was washed with saturated

aqueous sodium bicarbonate (2 x 150 mL), deionized water (2 x 150 mL) and brine (1 x 150 mL). The aqueous mixture was washed with dichloromethane (3 x 100 mL) and the organic layers were combined. The mixture was dried with MgSO_4 (anhydrous), filtered, and concentrated *in vacuo* to give a crude mixture, which was purified by flash chromatography (10-25% ethyl acetate/pentane) resulting in a pale yellow oil of pure ethyl 2-(2-methyl-1,3-dioxan-2-yl)acetate (**184**, 8.57 g, 49% yield).

^1H NMR (400 MHz, CDCl_3) δ : 4.16 (q, $J = 7.2$ Hz, 2H), 3.98 (s, 4H), 2.67 (s, 2H), 1.51 (s, 3H), 1.27 (t, $J = 7.2$ Hz, 3H),

^{13}C NMR (100 MHz, CDCl_3) δ : 14.2, 24.5, 44.3, 60.5, 64.7, 107.6, 169.5

Preparation of Alcohol 206

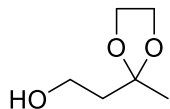


To a cold (0 °C), stirred solution of lithium aluminum hydride (2.617 g, 68.95 mmol) in THF (156 mL) was added dioxane **205** (7.21 g 38.3 mmol) as a solution in THF and the solution was stirred for 30 min and allowed to reach rt. The reaction mixture was diluted in ether (150 mL) and cooled to 0 °C then H_2O (3 mL) was added slowly followed by 15% aqueous sodium hydroxide (3 mL) followed by H_2O (8 mL) and stirred for 15 min while the reaction mixture reached rt. Anhydrous magnesium sulfate was added to the mixture and stirred for 15 min. The reaction mixture was filtered and the solvent was removed *in vacuo*. This afforded the product alcohol **206** in (4.77 g, 85%) as a pale colourless and transparent oil.

^1H NMR (400 MHz, CDCl_3) δ : 4.01 (m, 2H), 3.85 (m, 4H), 2.97 (t, $J = 5.7$ Hz, 1H), 1.98 (m, 1H), 1.91 (t, $J = 5.5$ Hz, 2H), 1.49 (s, 3H), 1.47 (m, 1H)

^{13}C NMR (100 MHz, CDCl_3) δ : 100.1, 59.8, 58.6, 41.9, 25.5, 19.5

Preparation of Alcohol 185

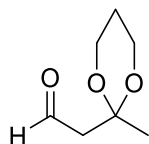


To a cold (0 °C), stirred solution of lithium aluminum hydride (4.10 g, 108 mmol) in THF (240 mL) was added dioxolane **184** (10.5 g, 60.0 mmol) as a solution in THF and the solution was stirred for 30 min and allowed to reach rt. The reaction mixture was diluted in ether (150 mL) and cooled to 0 °C then H₂O (3 mL) was added slowly followed by 15% aqueous sodium hydroxide (3 mL) followed by H₂O (8 mL) and stirred for 15 min while the reaction mixture reached rt. Anhydrous magnesium sulfate was added to the mixture and stirred for 15 min. The reaction mixture was filtered and the solvent was removed *in vacuo*. This afforded the product alcohol **185** in (7.0 g, 88%) as a pale colorless and transparent oil.

¹H NMR (400 MHz, CDCl₃) δ: 3.99 (s, 4H), 3.77 (dt, *J* = 5.5, 5.5 Hz, 2H), 2.77 (t, *J* = 5.5 Hz, 1H), 1.95 (t, *J* = 5.5 Hz, 2H), 1.37 (s, 3H)

¹³C NMR (100 MHz, CDCl₃) δ: 109.9, 64.5, 59.0, 40.2, 23.7

Preparation of Aldehyde 207



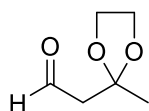
To a cold (-78 °C) solution of dimethylsulfoxide (6.90 mL, 97.5 mmol) in CH₂Cl₂ (325 mL, 0.1 M) oxalyl chloride (5.50 mL, 65.0 mmol) was added dropwise over 20 min. The reaction mixture was stirred for 30 min then alcohol **206** (4.75 g, 32.5 mmol) was added dropwise as a solution in CH₂Cl₂ over 10 min and stirred for an additional 20 min. Triethylamine (22.7 mL, 163 mmol) was added and the reaction was allowed to reach room temperature. The mixture was washed with H₂O (2 x 200 mL) and brine (1 x 250 mL) and the aqueous extracts were back extracted with CH₂Cl₂ (2 x 200 mL). The combined organics were dried with MgSO₄ and filtered, and solvent removed *in vacuo*.

The major component of the crude mixture was aldehyde **207**, which was carried to the next step without any further purification.

^1H NMR (400 MHz, CDCl_3) δ : 9.84 (t, $J = 2.9$ Hz, 1H), 4.00 (m, 2H), 3.98 (m, 2H), 2.67 (d, $J = 2.9$ Hz, 2H), 1.89 (m, 1H), 1.57 (m, 1H), 1.52 (s, 3H)

^{13}C NMR (100 MHz, CDCl_3) δ : 201.3, 103.5, 62.3, 49.9, 27.0, 23.9

Preparation of Aldehyde **186**

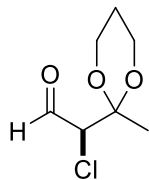


To a cold ($-78\text{ }^{\circ}\text{C}$) solution of dimethylsulfoxide (11.3 mL, 159 mmol) in CH_2Cl_2 (530 mL, 0.1 M) oxalyl chloride (9.00 mL, 106 mmol) was added dropwise over 20 min. The reaction mixture was stirred for 30 min then alcohol **185** (7.00 g, 53.0 mmol) was added dropwise as a solution in CH_2Cl_2 over 10 min and stirred for an additional 20 min. Triethylamine (35 mL, 250 mmol) was added and the reaction was allowed to reach room temperature. The mixture was washed with H_2O (2 x 250 mL) and brine (1 x 300 mL) and the aqueous extracts were washed with CH_2Cl_2 (2 x 200 mL). The combined organics were dried with MgSO_4 and filtered, and solvent removed *in vacuo*. The major component of the crude mixture was aldehyde **186**, which was carried to the next step without any further purification.

^1H NMR (400 MHz, CDCl_3) δ : 9.75 (t, $J = 2.9$ Hz, 1H), 4.01 (m, 4H), 2.71 (d, $J = 2.9$ Hz, 2H), 1.43 (s, 3H)

^{13}C NMR (100 MHz, CDCl_3) δ : 200.1, 101.4, 64.5, 50.9, 24.1

Preparation of α -Chloroaldehyde **204**

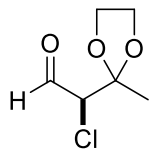


To a cold (0 °C) solution of *N*-chlorosuccinimide (4.60 g, 34.3 mmol) and proline (3.95 g, 34.3 mmol) in CH₂Cl₂ (100 mL, 0.3 M) a crude mixture of aldehyde **207** (4.51 g, 31.2 mmol) was added slowly over 10min. The solution was allowed to reach room temperature and stirred for 1 hr. The mixture was washed with H₂O (2 x 50 mL) and aqueous layers were washed with CH₂Cl₂ (2 x 50mL). The combined organics were dried over MgSO₄, filtered, and concentrated *in vacuo*. The crude material (6.75 g) was purified by a short flash chromatography column (1% triethylamine: 10% ethylacetate: 89% pentane). This resulted in the synthesis of 4.27 g (74% yield over two steps) of pure racemic α -chloroaldehyde **204**.

¹H NMR (500 MHz, CDCl₃) δ : 9.75 (d, *J* = 3.1 Hz, 1H), 4.28 (d, *J* = 3.1 Hz, 1H), 3.99 (m, 4H), 1.93 (m, 1H), 1.59 (m, 1H), 1.58 (s, 3H)

¹³C NMR (125 MHz, CDCl₃) δ : 201.7, 104.4, 63.4, 61.3, 24.1

Preparation of α -Chloroaldehyde **187**



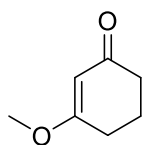
To a cold (0 °C) solution of *N*-chlorosuccinamide (7.34 g, 55.0 mmol) and proline (6.33 g, 55.0 mmol) in CH₂Cl₂ (150 mL, 0.3 M) a crude mixture of aldehyde **186** (50 mmol) was added slowly over 10min. The solution was allowed to reach room temperature and stirred for 1 hr. The mixture was washed with H₂O (2 x 50 mL) and aqueous layers were washed with CH₂Cl₂ (2 x 50mL). The combined organics were dried over MgSO₄, filtered, and concentrated *in vacuo*. The crude material was purified by a short flash chromatography column (1% triethylamine: 10% ethylacetate: 89% pentane). This

procedure resulted in 5.1 g (60% yield over two steps) of pure racemic α -chloroaldehyde **187**.

^1H NMR (400 MHz, CDCl_3) δ : 9.50 (d, $J = 3.3$ Hz, 1H), 4.18 (d, $J = 3.3$ Hz, 1H), 4.08 (m, 4H), 1.47 (s, 3H)

^{13}C NMR (100 MHz, CDCl_3) δ : 202.1, 102.1, 65.5, 63.9, 24.1

Preparation of β -Keto Enol Ether **183**

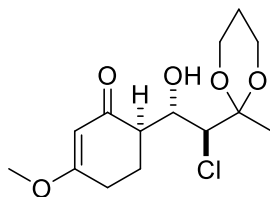


To a solution of 1,3-cyclohexanedione (3.36 g, 30.0 mmol) in methanol (150 mL) at room temperature was added elemental iodine (400 mg) and stirred for 10 min. The reaction mixture was treated with an excess of aqueous sodium thiosuphate ($\text{Na}_2\text{S}_2\text{O}_3$ aq). EtOAc (150 mL) was then added and the organic layer was removed and washed with H_2O (2 x 100 mL). The aqueous phases were washed with EtOAc (2 x 100 mL) and the combined organic layers were washed with brine (100 mL), then dried with MgSO_4 and filtered, and the solvent was removed *in vacuo*. This afforded the β -keto enol ether **183** (3.32 g, 88%) as a thick viscous brown liquid.

^1H NMR (400 MHz, CDCl_3) δ : 5.37 (s, 1H), 3.69 (s, 3H), 2.40 (t, $J = 6.3$ Hz, 2H), 2.34 (t, $J = 6.3$ Hz, 2H), 1.97 (quintet, $J = 6.3$ Hz, 2H)

^{13}C NMR (100 MHz, CDCl_3) δ : 199.2, 178.1, 102.0, 55.3, 36.4, 28.4, 20.9

Preparation of Chlorohydrin **208**



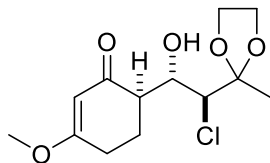
To a cold (-78 °C) flask containing dried THF (300 mL, 0.1M), diisopropylamine (4.36 mL, 31.1 mmol) was syringed, then *n*-butyllithium (12.6 mL, 27.5 mmol) was added dropwise and heated to 0 °C stirred for 15 min. The mixture was cooled to -78 °C and β -keto enol ether **183** (3.01 g, 23.9 mmol) was added slowly as a solution in THF and stirred for 30 min. α -Chloroaldehyde **204** (4.25 g, 23.9 mmol) was added as a solution in THF to the mixture slowly and stirred for 30 min. The reaction was then quenched with a saturated solution of aqueous ammonium chloride and allowed to reach room temperature. The mixture was washed with H₂O (2 x 100 mL), brine (1 x 100 mL) and the aqueous layers washed with ethylacetate (2 x 100mL). The combined organics were dried over anhydrous Na₂SO₄ and the solvent removed *in vacuo*. The crude material was purified by flash chromatography twice in order to completely purify chlorohydrin **208** (4.65 g, 64% yield).

¹H NMR (400 MHz, CDCl₃) δ : 5.33 (d, *J* = 1.3 Hz, 1H), 4.75 (dd, *J* = 1.0, 2.1 Hz, 1H), 4.44 (ddd, *J* = 1.5, 2.1, 8.5 Hz, 1H), 3.99 (m, 2H), 3.95 (bs, 1H), 3.75 (m, 2H), 3.67 (s, 3H), 2.53 (ddd, *J* = 4.7, 8.5, 12.2 Hz, 1H), 2.45 (m, 1H), 2.41 (dd, *J* = 3.9, 5.3 Hz, 1H), 2.06 (m, 1H), 1.91 (m, 1H), 1.69 (m, 1H), 1.64 (s, 3H), 1.47 (dt, *J* = 3.2, 13.4 Hz, 1H)

¹³C NMR (100 MHz, CDCl₃) δ : 202.4, 178.8, 102.4, 100.3, 69.4, 66.4, 60.5, 59.7, 56.1, 48.2, 28.3, 25.4, 23.5, 16.2

HRMS (ESI⁺) calculated for C₁₄H₂₂ClO₅⁺ 305.1150, found 305.1156

Preparation of Chlorohydrin 190

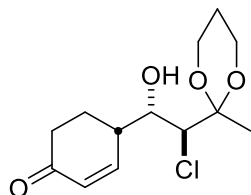


To a cold (-78 °C) flask containing dried THF (300 mL, 0.1M) diisopropylamine (4.86 mL, 34.7 mmol) was syringed, then *n*-butyllithium (14.5 mL, 30.7 mmol) was added dropwise and heated to 0 °C and stirred for 15 min. The mixture was cooled to -78 °C and β -keto enol ether **183** (3.37 g, 26.7 mmol) was added slowly as a solution in THF and stirred for 30 min. α -Chloroaldehyde **187** (4.40 g, 26.7 mmol) was added as a solution in THF to the mixture slowly and stirred for 30 min. The reaction was then quenched with a saturated solution of aqueous ammonium chloride and allowed to reach room temperature. The mixture was washed with H₂O (2 x 100 mL), brine (1 x 100 mL) and the aqueous layers washed with ethylacetate (2 x 100mL). The combined organics were dried over anhydrous Na₂SO₄ and the solvent removed *in vacuo*. The crude material was purified by flash chromatography twice in order to completely purify chlorohydrin **190** 4.9 g (63% yield).

¹H NMR (400 MHz, CDCl₃) δ : 5.39 (d, *J* = 1.3 Hz, 1H), 4.87 (dd, *J* = 1.6, 1.6 Hz, 1H), 4.35 (ddd, *J* = 1.9, 1.9, 8.5 Hz, 1H), 4.03 (m, 4H), 3.87 (bs, 1H), 3.71 (s, 1H), 2.59 (ddd, *J* = 4.9, 8.5, 13.1 Hz, 1H), 2.55 (m, 1H), 2.43 (ddd, *J* = 3.2, 4.9, 17.6 Hz, 1H), 2.08 (m, 1H), 1.68 (ddd, *J* = 4.9, 12.2, 17.6 Hz, 1H), 1.60 (s, 3H)

¹³C NMR (100 MHz, CDCl₃) δ : 199.9, 179.0, 110.4, 102.4, 70.8, 66.0, 65.5, 56.2, 48.0, 28.5, 23.5, 22.1

Preparation of Enone 209

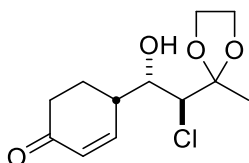


To a cold (0 °C) solution of chlorohydrin **208** (4.65 g, 15.1 mmol) and cerium chloride heptahydrate (5.63 g, 15.1 mmol) in methanol (150 mL, 0.1 M) was added sodium borohydride (640mg, 15.9 mmol) slowly and stirred for 1hr. Acetone (6 mL) was added to the mixture and it was allowed to reach room temperature over 20 min. The mixture was cooled again to 0 °C and H₂O (6 mL) and *p*-toluensulfonic acid monohydrate (2.60 g, 13.6 mmol) was added. After 5 min ethylacetate was added (250 mL) and the mixture was washed with H₂O (2 x 100 mL), brine (1 x 100 mL) and the aqueous layers washed with ethylacetate (2 x 100 mL). The combined organics were dried over anhydrous Na₂SO₄ and the solvent removed *in vacuo*. The crude product was purified by flash chromatography (25-40% EtOAc: pentane) which afforded pure enone **209** (4.9 g, 94%).

¹H NMR (400 MHz, CDCl₃) δ: 7.32 (ddd, *J* = 1.6, 2.3, 10.3 Hz, 1H), 6.08 (dd, *J* = 2.6, 10.3 Hz, 1H), 4.27 (ddd, *J* = 1.3, 1.3, 9.6 Hz, 1H), 4.08 (m, 2H), 3.96 (m, 2H), 3.88 (d, *J* = 1.3 Hz, 1H), 3.80 (bs, 1H), 2.73 (m, 1H), 2.52 (ddd, *J* = 4.5, 4.5, 16.7 Hz, 1H), 2.41 (ddd, *J* = 4.9, 13.1, 16.7 Hz, 1H), 2.06 (m, 2H), 1.67 (s, 3H), 1.63 (m 1H), 1.47 (m, 1H)

¹³C NMR (100 MHz, CDCl₃) δ: 198.9, 149.6, 128.7, 100.5, 68.4, 66.5, 60.2, 59.8, 37.9, 36.7, 25.5, 23.9, 16.6

Preparation of Enone 191



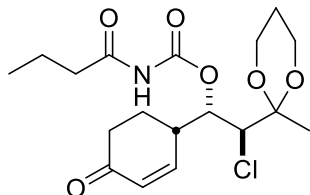
To a cold (0 °C) solution of chlorohydrin **190** (4.90 g, 16.8 mmol) and cerium chloride heptahydrate (6.33 g, 16.8 mmol) in methanol (150 mL, 0.1 M) was added sodium borohydride (675 mg, 17.8 mmol) slowly and stirred for 1hr. Acetone (6.3 mL) was added to the mixture and it was allowed to reach room temperature over 20 min. The mixture was cooled again to 0 °C and H₂O (6 mL) and *p*-toluensulfonic acid monohydrate (2.6 g, 13.6 mmol) was added. After 5 min ethylacetate was added (250 mL) and the mixture was washed with H₂O (2 x 100 mL), brine (1 x 100 mL) and the aqueous layers washed with ethylacetate (2 x 100mL). The combined organics were dried over anhydrous Na₂SO₄ and

the solvent removed *in vacuo*. The crude product was purified by flash chromatography (25-40% EtOAc: pentane) which afforded pure enone **191** (4.09 g, 93%).

^1H NMR (400 MHz, CDCl_3) δ : 7.28 (dt, $J = 2.0, 10.4$ Hz, 1H), 6.09 (dd, $J = 2.5, 10.4$ Hz, 1H), 4.09 (m, 4H), 4.06 (d, $J = 1.0$ Hz, 1H), 3.87 (ddd, $J = 1.0, 3.6, 9.3$ Hz, 1H), 3.34 (d, 3.6 Hz, 1H), 2.74 (m, 1H), 2.53 (dt, $J = 4.2, 16.7$ Hz, 1H), 2.42 (ddd, $J = 5.0, 13.4, 16.7$ Hz, 1H), 1.62 (m, 1H), 1.50 (s, 3H)

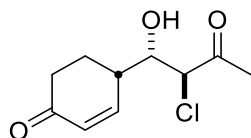
^{13}C NMR (100 MHz, CDCl_3) δ : 197.5, 147.9, 127.9, 101.4, 67.4, 65.5, 63.2, 62.7, 37.9, 32.6, 24.8, 21.9

Preparation of Carbamate **212**



To a solution of butyramide (276 mg, 3.15 mmol) in 1,2-dichloroethane (10 mL) oxalyl chloride (260 μL , 3.15 mmol) was added and the solution refluxed for 1 hr. The mixture was removed from the heating element and enone **209** (290 mg, 1.05 mmol) was added. The mixture was stirred for 30 minutes, then diluted with ethyl acetate (40 mL) and washed with H_2O (2 x 40 mL), brine (1 x 40 mL) and the aqueous layers washed with ethylacetate (2 x 40 mL). The combined organics were dried over anhydrous Na_2SO_4 and the solvent removed *in vacuo*. The crude mixture was purified by flash chromatography (10-33% EtOAc: Pentane) which afforded pure carbamate **212** (225 mg, 55%).

Preparation of Ketone **220**



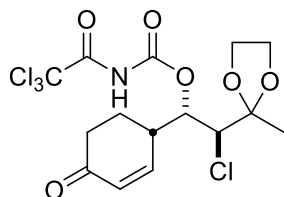
To a solution of enone **209** (60 mg, 0.22 mmol) in acetone (3 mL, 0.1M) trimethylsilyl trifluoromethanesulfonate (45 μL , 0.25 mmol) were added and allowed to stir

for 10 minutes. Ethyl acetate (10 mL) was added to the solution and the solution washed with H₂O (2 x 5 mL), brine (1 x 6 mL) and the aqueous layers washed with ethylacetate (3 x 5 mL). The combined organics were dried over anhydrous Na₂SO₄ and the solvent removed *in vacuo*. This afforded ketone **220** (210 mg, >95%) without the need for further purification.

¹H NMR (400 MHz, CDCl₃) δ: 7.23 (dt, *J* = 1.9, 10.4 Hz, 1H), 6.09 (dd, *J* = 2.5, 10.4 Hz, 1H), 4.40 (d, *J* = 1.9 Hz, 1H), 4.00 (ddd, *J* = 1.9, 6.6, 9.0 Hz, 1H), 2.94 (d, *J* = 6.6 Hz, 1H), 2.72 (m, 1H), 2.54 (dt, *J* = 4.4, 16.9 Hz, 1H), 2.42 (s, 3H), 2.07 (m, 1H), 1.67 (m, 1H)

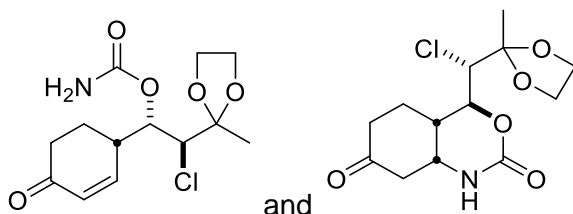
¹³C NMR (100 MHz, CDCl₃) δ: 203.5, 196.9, 144.5, 127.0, 63.5, 59.3, 37.0, 36.6, 29.6, 24.9

Preparation of Carbamate **193**



To a solution of enone **191** (520 mg, 2.00 mmol) in CH₂Cl₂ (20 mL) trichloroacetyl isocyanate (286 μL, 2.4 mmol) was added and the mixture stirred for five minutes. The mixture was washed with H₂O (2 x 10 mL), brine (1 x 10 mL) and the aqueous layers washed with ethylacetate (3 x 10 mL). The combined organics were dried over anhydrous MgSO₄ and the solvent removed *in vacuo*. Carbamate **193** was stored as the crude mixture in the freezer (-4 °C) and only purified just before use due to its affinity for decomposition. Carbamate **193** was purified over a short silica plug and used immediately.

Preparation of Carbamate **230** and Oxazinanone **231**



To a solution of carbamate **193** (180 mg, 0.400 mmol) in methanol (4 mL) potassium carbonate (55 mg, 0.40 mmol) was added and stirred for 3 hours. The mixture was diluted with ethyl acetate (10 mL) and washed with H₂O (2 x 5 mL), brine (1 x 5 mL) and the aqueous layers washed with ethylacetate (3 x 5 mL). The combined organics were dried over anhydrous MgSO₄ and the solvent removed *in vacuo*. The crude material was purified by flash chromatography (20-40% EtOAc: Pentane) which afforded pure carbamate **230** (139 mg, 45%) and oxazinanone **231** (42 mg, 34%)

Oxazinanone **231**:

¹H NMR (400 MHz, CDCl₃) δ: 5.38 (s, 1H), 4.82 (dd, *J* = 1.6, 6.2 Hz, 1H), 4.17 (m, 1H), 4.07 (m, 2H), 4.00 (m, 2H), 3.83 (d, *J* = 1.6 Hz, 1H), 2.67 (dd, *J* = 4.8, 16.6 Hz, 1H), 2.50 (m, 2H), 2.40 (m, 2H), 2.04 (dd, *J* = 6.8, 14.0 Hz, 2H), 1.59 (s, 3H)

¹³C NMR (100 MHz, CDCl₃) δ: 206.3, 152.2, 109.9, 75.6, 65.8, 65.2, 64.7, 49.5, 45.5, 37.9, 33.7, 24.4, 20.7

HRMS (ESI⁺) calculated for C₁₃H₁₉ClNO₅⁺ 304.0946, found 304.0940

References

- (1) David T. Courtwright. *Forces of Habit: Drugs and the Making of the Modern World*; Harward University Press, 2009.
- (2) Newman, D. J.; Cragg, G. M. *J. Nat. Prod.* **2016**, 79 (3), 629–661.
- (3) Guo, Z.; Pharmaceutica Sinica, A. B. *Acta Pharm. Sin. B* **2017**, 7 (2), 119–136.
- (4) Sneader, W. *BMJ* **2000**, 321 (7276), 1591–1594.
- (5) Peach, K. C.; Linington, R. G. *Future Med. Chem.* **2009**, 1 (4), 593–617.
- (6) Conroy, T.; Guo, J. T.; Linington, R. G.; Hunt, N. H.; Payne, R. J. *Chem. - A Eur. J.* **2011**, 17 (48), 13544–13552.
- (7) Mickel, S. J.; Niederer, D.; Daeffler, R.; Osmani, A.; Kuesters, E.; Schmid, E.; Schaer, K.; Gamboni, R.; Chen, W.; Loeser, E.; Kinder, F. R.; Konigsberger, K.; Prasad, K.; Ramsey, T. M.; Repi??, O.; Wang, R.-M. M.; Florence, G.; Lyothier, I.; Paterson, I.; Repič, O.; Wang, R.-M. M.; Florence, G.; Lyothier, I.; Paterson, I. *Org. Process Res. Dev.* **2004**, 8 (1), 122–130.
- (8) Sanderson, R. T. *J. Am. Chem. Soc.* **1983**, 105 (8), 2259–2261.
- (9) Müller, K.; Faeh, C.; Diederich, F. *Science* **2007**, 317 (5846), 1881–1886.
- (10) Pyykkö, P. *Phys. Rev. B* **2012**, 85 (2), 24115.
- (11) Blanksby, S. J.; Ellison, G. B. *Acc. Chem. Res.* **2003**, 36 (4), 255–263.
- (12) Wang, J.; Sánchez-Roselló, M.; Aceña, J. L.; del Pozo, C.; Soroichinsky, A. E.; Fustero, S.; Soloshonok, V. A.; Liu, H. *Chem. Rev.* **2014**, 114 (4), 2432–2506.
- (13) Hagmann, W. K. *J. Med. Chem.* **2008**, 51 (15), 4359–4369.
- (14) Kirk, K. L. *Org. Process Res. Dev.* **2008**, 12 (2), 305–321.
- (15) O'Hagan, D. *J. Fluor. Chem.* **2010**, 131 (11), 1071–1081.
- (16) Fried, J.; Sabo, E. F. *J. Am. Chem. Soc.* **1954**, 76 (5), 1455–1456.
- (17) Duschinsky, R.; Plevin, E.; Heidelberger, C. *J. Am. Chem. Soc.* **1957**, 79 (16), 4559–4560.

- (18) Heidelberger, C.; Chaudhuri, N. K.; Danneberg, P.; Mooren, D.; Griesbach, L.; Duschinsky, R.; Schnitzer, R. J.; Plevin, E.; Scheiner, J. *Nature* **1957**, 179, 663–666.
- (19) Longley, D. B.; Harkin, D. P.; Johnston, P. G. *Nat. Rev. Cancer* **2003**, 3 (5), 330–338.
- (20) Kirk, K. L. *J. Fluor. Chem.* **2006**, 127 (8), 1013–1029.
- (21) Domagala, J. M.; Hanna, L. D.; Heifetz, C. L.; Hutt, M. P.; Mich, T. F.; Sanchez, J. P.; Solomon, M. *J. Med. Chem.* **1986**, 29 (3), 394–404.
- (22) Wise, R.; Andrews, J. M.; Edwards, L. J. *Antimicrob. Agents Chemother.* **1983**, 23 (4), 559–564.
- (23) The Best Selling Drugs Since 1996 - Why AbbVie's Humira Is Set To Eclipse Pfizer's Lipitor - Forbes <http://www.forbes.com/sites/simonking/2013/07/15/the-best-selling-drugs-since-1996-why-abbvies-humira-is-set-to-eclipse-pfizers-lipitor/#216eb2922055> (accessed May 17, 2016).
- (24) Roth, B. D. *Prog. Med. Chem.* **2002**, 40, 1–22.
- (25) Clader, J. W. *J. Med. Chem.* **2004**, 47 (1), 1–9.
- (26) Rosenblum, S. B.; Huynh, T.; Afonso, A.; Davis, H. R.; Yumibe, N.; Clader, J. W.; Burnett, D. A. *J. Med. Chem.* **1998**, 41 (6), 973–980.
- (27) Andrés, J. I.; Alonso, J. M.; Díaz, A.; Fernández, J.; Iturrino, L.; Martínez, P.; Matesanz, E.; Freyne, E. J.; Deroose, F.; Boeckx, G.; Petit, D.; Diels, G.; Megens, A.; Somers, M.; Wauwe, J. Van; Stoppie, P.; Cools, M.; Clerck, F. De; Peeters, D.; de Chaffoy, D. *Bioorg. Med. Chem. Lett.* **2002**, 12 (4), 653–658.
- (28) Thompson, W. J.; Anderson, P. S.; Britcher, S. F.; Lyle, T. A.; Thies, J. E.; Magill, C. A.; Varga, S. L.; Schwering, J. E.; Lyle, P. A. *J. Med. Chem.* **1990**, 33 (2), 789–808.
- (29) Xia, J.-B.; Zhu, C.; Chen, C. *J. Am. Chem. Soc.* **2013**, 135 (46), 17494–17500.
- (30) Huang, X.; Liu, W.; Ren, H.; Neelamegam, R.; Hooker, J. M.; Groves, J. T. *J. Am. Chem. Soc.* **2014**, 136 (19), 6842–6845.
- (31) Amaoka, Y.; Nagatomo, M.; Inoue, M. *Org. Lett.* **2013**, 15 (9), 2160–2163.
- (32) Cantillo, D.; de Frutos, O.; Rincón, J. A.; Mateos, C.; Kappe, C. O. *J. Org. Chem.* **2014**, 79 (17), 8486–8490.

- (33) Bloom, S.; Pitts, C. R.; Woltornist, R.; Griswold, A.; Holl, M. G.; Lectka, T. *Org. Lett.* **2013**, *15* (7), 1722–1724.
- (34) Bloom, S.; McCann, M.; Lectka, T. *Org. Lett.* **2014**, *16* (24), 6338–6341.
- (35) Pitts, C. R.; Ling, B.; Woltornist, R.; Liu, R.; Lectka, T. *J. Org. Chem.* **2014**, *79* (18), 8895–8899.
- (36) Bloom, S.; Sharber, S. A.; Holl, M. G.; Knippel, J. L.; Lectka, T. *J. Org. Chem.* **2013**, *78* (21), 11082–11086.
- (37) Baer, B. R.; DeLisle, R. K.; Allen, A. *Chem. Res. Toxicol.* **2009**, *22* (7), 1298–1309.
- (38) Ametamey, S. M.; Honer, M.; Schubiger, P. A. *Chem. Rev.* **2008**, *108* (5), 1501–1516.
- (39) Miller, P. W.; Long, N. J.; Vilar, R.; Gee, A. D. *Angew. Chem. Int. Ed. Engl.* **2008**, *47* (47), 8998–9033.
- (40) Lee, E.; Kamlet, A. S.; Powers, D. C.; Neumann, C. N.; Boursalian, G. B.; Furuya, T.; Choi, D. C.; Hooker, J. M.; Ritter, T. *Science* **2011**, *334*, 639–642.
- (41) Couturier, O.; Luxen, A.; Chatal, J.-F.; Vuillez, J.-P.; Rigo, P.; Hustinx, R. *Eur. J. Nucl. Med. Mol. Imaging* **2004**, *31* (8), 1182–1206.
- (42) Wahl, L.; Nahmias, C. *J. Nucl. Med.* **1996**, *37* (3), 432–437.
- (43) Gouverneur, V.; Müller, K. *Fluorine in Pharmaceutical and Medicinal Chemistry: From Biophysical Aspects to Clinical Applications*; World Scientific, 2012.
- (44) Campbell, M. G.; Ritter, T. *Chem. Rev.* **2015**, *115* (2), 612–633.
- (45) CDC - The Emergency Response Safety and Health Database: Systemic Agent: Hydrogen Fluoride/ Hydrofluoric Acid - NIOSH http://www.cdc.gov/niosh/ershdb/EmergencyResponseCard_29750030.html.
- (46) CDC - Immediately Dangerous to Life or Health Concentrations (IDLH): Fluorine - NIOSH Publications and Products <http://www.cdc.gov/niosh/idlh/7782414.html> (accessed Jun 1, 2016).
- (47) Champagne, P. A.; Desroches, J.; Hamel, J.-D.; Vandamme, M.; Paquin, J.-F. *Chem. Rev.* **2015**, *115* (17), 9073–9174.
- (48) Wu, J. *Tetrahedron Lett.* **2014**, *55* (31), 4289–4294.
- (49) Nyffeler, P. T.; Durón, S. G.; Burkart, M. D.; Vincent, S. P.; Wong, C.-H. *Angew.*

Chem. Int. Ed. Engl. **2004**, *44* (2), 192–212.

- (50) Campbell, M. G.; Ritter, T. *Org. Process Res. Dev.* **2014**, *18* (4), 474–480.
- (51) Singh, R. P.; Shreeve, J. M. *Synthesis (Stuttg)*. **2002**, *2002* (17), 2561–2578.
- (52) Liang, T.; Neumann, C. N.; Ritter, T. *Angew. Chem. Int. Ed. Engl.* **2013**, *52* (32), 8214–8264.
- (53) Chambers, R. D. *Fluorine in Organic Chemistry*; CRC Press, 2004.
- (54) Zhan, C.-G.; Dixon, D. A. *J. Phys. Chem. A* **2004**, *108* (11), 2020–2029.
- (55) Beaulieu, F.; Beauregard, L.-P.; Courchesne, G.; Couturier, M.; LaFlamme, F.; L'Heureux, A. *Org. Lett.* **2009**, *11* (21), 5050–5053.
- (56) Umemoto, T.; Tomita, K. *Tetrahedron Lett.* **1986**, *27* (28), 3271–3274.
- (57) Umemoto, T.; Kawada, K.; Tomita, K. *Tetrahedron Lett.* **1986**, *27* (37), 4465–4468.
- (58) Differding, E.; Ofner, H. *Synlett* **1991**, *1991* (3), 187–189.
- (59) Banks, R. E. *J. Fluor. Chem.* **1998**, *87* (1), 1–17.
- (60) Rueda-Becerril, M.; Chatalova Sazepin, C.; Leung, J. C. T.; Okbinoglu, T.; Kennepohl, P.; Paquin, J.-F.; Sammis, G. M. *J. Am. Chem. Soc.* **2012**, *134* (9), 4026–4029.
- (61) Neumann, C. N.; Ritter, T. *Angew. Chem. Int. Ed. Engl.* **2015**, *54* (11), 3216–3221.
- (62) Ma, J.-A.; Li, S. *Org. Chem. Front.* **2014**, *1* (6), 712.
- (63) Liu, W.; Huang, X.; Cheng, M.-J.; Nielsen, R. J.; Goddard, W. A.; Groves, J. T. *Science* **2012**, *337*, 1322–1325.
- (64) Bloom, S.; Knippel, J. L.; Lectka, T. *Chem. Sci.* **2014**, *5* (3), 1175.
- (65) Pitts, C. R.; Bloom, S.; Woltornist, R.; Auvenshine, D. J.; Ryzhkov, L. R.; Siegler, M. A.; Lectka, T. *J. Am. Chem. Soc.* **2014**, *136* (27), 9780–9791.
- (66) Bloom, S.; Pitts, C. R.; Miller, D. C.; Haselton, N.; Holl, M. G.; Urheim, E.; Lectka, T. *Angew. Chem. Int. Ed. Engl.* **2012**, *51* (42), 10580–10583.
- (67) López, X.; Carbó, J. J.; Bo, C.; Poblet, J. M. *Chem. Soc. Rev.* **2012**, *41* (22), 7537–7571.

- (68) Tzirakis, M. D.; Lykakis, I. N.; Orfanopoulos, M. *Chem. Soc. Rev.* **2009**, 38 (9), 2609–2621.
- (69) Hill, C. L. *Synlett* **1995**, 1995 (2), 127–132.
- (70) Maldotti, A.; Amadelli, R.; Carassiti, V.; Molinari, A. *Inorganica Chim. Acta* **1997**, 256 (2), 309–312.
- (71) Giannotti, C.; Richter, C. *Int. J. Photoenergy* **1999**, 1 (2), 69–73.
- (72) Giannotti, C.; Richter, C. Aerobic photolysis of saturated C-H bond with decatungstate anion, mechanism and products.
- (73) Renneke, R. F.; Pasquali, M.; Hill, C. L. *J. Am. Chem. Soc.* **1990**, 112 (18), 6585–6594.
- (74) Combs-Walker, L. A.; Hill, C. L. *J. Am. Chem. Soc.* **1992**, 114 (3), 938–946.
- (75) Dondi, D.; Cardarelli, A. M.; Fagnoni, M.; Albini, A. *Tetrahedron* **2006**, 62 (23), 5527–5535.
- (76) Protti, S.; Ravelli, D.; Fagnoni, M.; Albini, A. *Chem. Commun. (Camb)*. **2009**, No. 47, 7351–7353.
- (77) Esposti, S.; Dondi, D.; Fagnoni, M.; Albini, A. *Angew. Chem. Int. Ed. Engl.* **2007**, 46 (14), 2531–2534.
- (78) Angioni, S.; Ravelli, D.; Emma, D.; Dondi, D.; Fagnoni, M.; Albini, A. *Adv. Synth. Catal.* **2008**, 350 (14–15), 2209–2214.
- (79) Halperin, S. D.; Fan, H.; Chang, S.; Martin, R. E.; Britton, R. *Angew. Chem. Int. Ed. Engl.* **2014**, 53 (18), 4690–4693.
- (80) Jen, S. F.; Anderson, A. B.; Hill, C. L. *J. Phys. Chem.* **1992**, 96 (13), 5658–5662.
- (81) Champagne, P. A.; Pomarole, J.; Thérien, M.-È.; Benhassine, Y.; Beaulieu, S.; Legault, C. Y.; Paquin, J.-F. *Org. Lett.* **2013**, 15 (9), 2210–2213.
- (82) Amii, H.; Uneyama, K. *Chem. Rev.* **2009**, 109 (5), 2119–2183.
- (83) Hartman, M.; Svoboda, K.; Pohořelý, M.; Šyc, M. *Ind. Eng. Chem. Res.* **2013**, 52 (31), 10619–10626.
- (84) Ni, Z.; Zhang, Q.; Xiong, T.; Zheng, Y.; Li, Y.; Zhang, H.; Zhang, J.; Liu, Q. *Angew. Chem. Int. Ed. Engl.* **2012**, 51 (5), 1244–1247.

- (85) Knowles, J. P.; Elliott, L. D.; Booker-Milburn, K. I. *Beilstein J. Org. Chem.* **2012**, *8* (1), 2025–2052.
- (86) Nodwell, M. B.; Bagai, A.; Halperin, S. D.; Martin, R. E.; Knust, H.; Britton, R. *Chem. Commun. (Camb)*. **2015**, *51* (59), 11783–11786.
- (87) Horne, G.; Wilson, F. X.; Tinsley, J.; Williams, D. H.; Storer, R. *Drug Discov. Today* **2011**, *16* (3), 107–118.
- (88) Watson, A. A.; Fleet, G. W. J. J.; Asano, N.; Molyneux, R. J.; Nash, R. J. *Phytochemistry* **2001**, *56* (3), 265–295.
- (89) Izquierdo, I.; Plaza, M. T.; Tamayo, J. A.; Sánchez-Cantalejo, F. *Tetrahedron: Asymmetry* **2007**, *18* (18), 2211–2217.
- (90) O'Hagan, D. *Nat. Prod. Rep.* **2000**, *17* (5), 435–446.
- (91) Malik, R. A.; Williamson, S.; Abbott, C.; Carrington, A. L.; Iqbal, J.; Schady, W.; Boulton, A. J. *Lancet* **1998**, *352* (9145), 1978–1981.
- (92) Mancina, G.; Messerli, F.; Bakris, G.; Zhou, Q.; Champion, A.; Pepine, C. J. *Hypertension* **2007**, *50* (2), 299–305.
- (93) Bertelsen, S.; Jørgensen, K. A. *Chem. Soc. Rev.* **2009**, *38* (8), 2178.
- (94) Brochu, M. P.; Brown, S. P.; MacMillan, D. W. C. *J. Am. Chem. Soc.* **2004**, *126* (13), 4108–4109.
- (95) Halland, N.; Braunton, A.; Bachmann, S.; Marigo, M.; Jørgensen, K. A. *J. Am. Chem. Soc.* **2004**, *126* (15), 4790–4791.
- (96) Halland, N.; Alstrup Lie, M.; Kjærsgaard, A.; Marigo, M.; Schiøtt, B.; Jørgensen, K. A. *Chem. - A Eur. J.* **2005**, *11* (23), 7083–7090.
- (97) Draper, J. A.; Britton, R. *Org. Lett.* **2010**, *12* (18), 4034–4037.
- (98) Basler, B.; Brandes, S.; Spiegel, A.; Bach, T. *Topics in Current Chemistry*. 2005, pp 1–42.
- (99) Davis, F. A.; Zhang, J.; Qiu, H.; Wu, Y. *Org. Lett.* **2008**, *10* (7), 1433–1436.
- (100) Gogoi, N.; Boruwa, J.; Barua, N. C. *European J. Org. Chem.* **2006**, *2006* (7), 1722–1725.
- (101) Bertrand, M. B.; Wolfe, J. P. *Org. Lett.* **2006**, *8* (11), 2353–2356.

- (102) Okue, M.; Watanabe, H.; Kasahara, K.; Yoshida, M.; Horinouchi, S.; Kitahara, T. *Biosci. Biotechnol. Biochem.* **2002**, 66 (5), 1093–1096.
- (103) Canova, S.; Bellosta, V.; Cossy, J. *Synlett* **2004**, 2004 (10), 1811–1813.
- (104) Davis, F. A.; Deng, J. *Tetrahedron* **2004**, 60 (23), 5111–5115.
- (105) Reddy, L. R.; Saravanan, P.; Corey, E. J. *J. Am. Chem. Soc.* **2004**, 126 (20), 6230–6231.
- (106) Williams, P. G.; Buchanan, G. O.; Feling, R. H.; Kauffman, C. A.; Jensen, P. R.; Fenical, W.; Philip G. Williams; Greg O. Buchanan; Robert H. Feling; Christopher A. Kauffman; Paul R. Jensen, and; Fenical*, W. *J. Org. Chem.* **2005**, 70 (16), 6196–6203.
- (107) Fenical, W.; Jensen, P. R.; Palladino, M. A.; Lam, K. S.; Lloyd, G. K.; Potts, B. C. *Bioorg. Med. Chem.* **2009**, 17 (6), 2175–2180.
- (108) Chauhan, D.; Catley, L.; Li, G.; Podar, K.; Hideshima, T.; Velankar, M.; Mitsiades, C.; Mitsiades, N.; Yasui, H.; Letai, A.; Ova, H.; Berkers, C.; Nicholson, B.; Chao, T.-H.; Neuteboom, S. T. C.; Richardson, P.; Palladino, M. A.; Anderson, K. C. *Cancer Cell* **2005**, 8 (5), 407–419.
- (109) Ma, G.; Nguyen, H.; Romo, D. *Org. Lett.* **2007**, 9 (11), 2143–2146.
- (110) Endo, A.; Danishefsky, S. J. *J. Am. Chem. Soc.* **2005**, 127 (23), 8298–8299.
- (111) Ling, T.; Macherla, V. R.; Manam, R. R.; McArthur, K. A.; Potts, B. C. M. *Org. Lett.* **2007**, 9 (12), 2289–2292.
- (112) Takahashi, K.; Midori, M.; Kawano, K.; Ishihara, J.; Hatakeyama, S. *Angew. Chemie - Int. Ed.* **2008**, 47 (33), 6244–6246.
- (113) Fukuda, T.; Sugiyama, K.; Arima, S.; Harigaya, Y.; Nagamitsu, T.; Ōmura, S. *Org. Lett.* **2008**, 10 (19), 4239–4242.
- (114) Mulholland, N. P.; Pattenden, G.; Walters, I. A. S. *Org. Biomol. Chem.* **2006**, 4 (15), 2845–2846.
- (115) Mulholland, N. P.; Pattenden, G.; Walters, I. A. S. *Org. Biomol. Chem.* **2008**, 6 (15), 2782–2789.
- (116) Heathcock, C. H.; Buse, C. T.; Kleschick, W. A.; Pirrung, M. C.; Sohn, J. E.; Lampe, J. *J. Org. Chem.* **1980**, 45 (6), 1066–1081.
- (117) Smith, S. W.; Newmana, M. S. *J. Am. Chem. Soc.* **1967**, 2 (10), 1249–1253.

(118) Sardarian, A. R. *RSC Adv.* **2015**, 5 (93), 76626–76641.